POLYETHYLENE OXIDE-INDUCED FLOCCULATION OF DOLOMITE/CLAY/BORAX-CONTAINING SUSPENSIONS

A THESIS SUBMITTED TO
THE GRADUATE SCHOOL OF NATURAL AND APPLIED SCIENCES
OF
MIDDLE EAST TECHNICAL UNIVERSITY

BY

MUSTAFA ÇIRAK

IN PARTIAL FULLFILMENT OF THE REQUIREMENTS
FOR
THE DEGREE OF DOCTOR OF PHILOSOPHY
IN
MINING ENGINEERING

JULY 2014

Approval of the thesis:

POLYETHYLENE OXIDE-INDUCED FLOCCULATION OF DOLOMITE/CLAY/BORAX-CONTAINING SUSPENSIONS

submitted by **MUSTAFA ÇIRAK** in partial fulfillment of the requirements for the degree of **Doctor of Philosophy in Mining Engineering Department, Middle East Technical University** by,

Prof. Dr. Canan Özgen
Dean, Graduate School of **Natural and Applied Science** _____

Prof. Dr. Ali İhsan Arol
Head of Department, **Mining Engineering** _____

Prof. Dr. Çetin Hoşten
Supervisor, **Mining Engineering Dept., METU** _____

Examining Committee Members:

Prof. Dr. Ali İhsan Arol
Mining Engineering Dept., METU _____

Prof. Dr. Çetin Hoşten
Mining Engineering Dept., METU _____

Prof. Dr. Mustafa Ümit Atalay
Mining Engineering Dept., METU _____

Prof. Dr. Asuman Türkmenoğlu
Geological Engineering Dept., METU _____

Prof. Dr. Zafir Ekmekçi
Mining Engineering Dept., HU _____

Date: 04.07.2014

I hereby declare that all information in this document has been obtained and presented in accordance with academic rules and ethical conduct. I also declare that, as required by these rules and conduct, I have fully cited and referenced all material and results that are not original to this work.

Name, Last Name: Mustafa Çırak

Signature:

ABSTRACT

POLYETHYLENE OXIDE-INDUCED FLOCCULATION OF DOLOMITE/CLAY/BORAX-CONTAINING SUSPENSIONS

Çırak, Mustafa

Ph.D., Department of Mining Engineering

Supervisor: Prof. Dr. Çetin Hoşten

July 2014, 182 Pages

Kırka borax formation in Turkey is the largest borate deposit in the world. However, this important boron mineral is associated with significant amount of dolomite and clay gangue. When the run-of-mine ore is processed via simple crushing/washing/scrubbing methods, these gangues are discharged from the concentrator in the form of a stable colloidal suspension. The resultant dolomite/clay/borax-containing tailing creates a critical bottleneck threatening safe and sustainable borax production. To analyze this problem under controlled conditions, dolomite/clay/borax-containing suspensions were prepared in the lab and subjected to polyethylene oxide (PEO)-induced flocculation. Colloidal behavior of these suspensions was elucidated with the characterization studies: $d_{80} \leq 7 \mu m$, $\zeta \leq -76.4 mV$. Also, the challenge in the flocculation was linked to H-bonding incapability of the minerals' surfaces. To overcome the challenges, the effects of different physical and chemical parameters on the PEO-induced flocculation were experimented. During these experiments, intense mixing at 108-306s^{-1} proved beneficial due to increased collision probability between particles and polymers. pH

adjustment and preconditioning with Ca/Mn coagulants played a significant role in the removal of supernatant turbidity, the volume-based reduction of the flocculated sediments and the polymer consumption. This chemical improvement was disclosed with the increased amount of hydrolyzed species $CaOH^+$ and $Mn_2(OH)_3^+$ (actually max. at pH 11.5 and 9.4, respectively) because these species were adsorbed strongly by particle surfaces and served as a cation bridge between particle and polymer. Clinker particles were also used as an unconventional ballast material prior to flocculation and the results suggested that clinker ballasting (hetero-flocculation) can be an esteemed alternative to coagulant pretreatment. On the contrary to these favorable parameters, some undesirable results were obtained. For instance, the performance of PEO was tried to be increased with cationic polyacrylamide preconditioning; however, this anticipation was not substantiated due to excessive interaction between polymer macromolecules. Besides, the flocculation almost completely deteriorated at high temperatures. It was explained with viscosity measurements of PEO that the polymer chains were immoderately sensitive to high temperatures (75°C) although they were durable against intense mixing. In conclusion, it was proved that dolomite/clay/borax-containing colloidal suspensions can be completely flocculated within seconds if the PEO treatment is consolidated with proper physical/chemical parameters.

Keywords: Flocculation, polyethylene oxide, borax, aqueous chemistry, viscosity

ÖZ

DOLOMİT/KİL/BORAKS İÇEREN SÜSPANSİYONLARIN POLİETİLEN OKSİT İLE FLOKÜLASYONU

Çırak, Mustafa

Doktora, Maden Mühendisliği Bölümü

Tez Yöneticisi: Prof. Dr. Çetin Hoşten

July 2014, 182 Sayfa

Türkiye'de bulunan Kırka boraks formasyonu dünyadaki en büyük borat yataklanmalarından biridir. Bu önemli sodyum borat minerali çok yüksek miktarlarda dolomit ve kil mineralleri ile birlikte bulunmaktadır. Tüvenan cevher basit kırma/yıkama/mekanik dağıtma metodu ile zenginleştirilirken, bu gang mineralleri güçlü süspansiyonlar halinde konsantratörden atık havuzlarına gönderilir. Bu işlem esnasında ortaya çıkan dolomit/kil/boraks içerikli atıklar güvenli ve sürdürülebilir boraks üretimini tehdit ederek kritik bir dar boğaza sebep olmaktadır. Bu sorunu kontollü koşullarda analiz edebilmek adına, laboratuar ortaminda dolomit/kil/boraks içerikli süspansiyonlar hazırlanmış ve bu süspansiyonlar polietilen oksit yardımı ile flokülasyona tabi tutulmuştur. Bu süspansiyonların kolloidal davranışları, karakterizasyon çalışmaları ($d_{80} \leq 7\mu m$, $\zeta \leq -76.4mV$) ile açıklanmıştır. Ayrıca, flokülasyonda yaşanan güçlükler mineral yüzeylerinin hidrojen bağı kurma kabiliyetlerinin yetersiz olması ile açıklanmıştır. Bu problemlerin üstesinden gelebilmek için, çeşitli fiziksel ve kimyasal parametrelerin polietilen oksit flokülasyonuna etkileri test edilmiştir. Deneyler

esnasında, mekanik karıştırma hızının parçacık-polimer etkileşimini arttırması sebebiyle yararlı olduğu görülmüştür. pH düzenlemeleri ve Ca/Mn tipi koagülantlarının ilavesinin de bulanıklık giderimi, çökelti hacmi ve polimer tüketiminde anahtar role sahip olduğu gözlemlenmiştir. Bu kimyasal geliştirmeler, $CaOH^+$ and $Mn_2(OH)_3^+$ gibi hidroliz ürünlerindeki artış (pH 11.5 ve 9.4'te maksimum) ile açıklanmıştır. Çünkü bu hidroliz ürünleri parçacık yüzeylerine çok güçlü bir şekilde adsorplanarak parçacık-polimer arasında bir bağlayıcı köprü görevi görmektedirler. Daha sonra, konvansiyonel olarak nitelendirilemeyen clinker parçacıkları balast malzemesi olarak flokülasyon öncesinde süspansiyona eklenmiş ve sonuçlar klinker ballastlama (hetero-flokülasyon) metodunun koagülasyon önkoşullandırma prosedürüne alternatif olarak kullanılabilecek nitelikte olduğunu kanıtlamıştır. Bu olumlu verilerin yanında, bazı öngörülemeyen olumsuz etkilerde gözlemlenmiştir. Örnek olarak, katyonik poliakrilamid yardımı ile polietilen oksit flokülasyonunun performansı arttırılmaya çalışılmış fakat polimer makromolekülleri arasındaki aşırı etkileşimden dolayı bu beklenti gerçekleşmemiştir. Ayrıca, yüksek sıcaklıklarda flokülasyon performansının neredeyse tamamen bozulmaya uğradığı gözlemlenmiştir. Bu durum polietilen oksit için yapılan vizkozite ölçümleri ile desteklenmiş ve polimer zincirlerinin mekanik karıştırmaya dayanıklı olmalarına rağmen yüksek sıcaklık değerlerine (75°C) karşı aşırı hassas olmaları ile açıklanmıştır. Sonuç olarak polietilen oksit uygulaması doğru fiziksel/kimyasal parametrelerle güçlendirildiği takdirde, dolomit/clay/boraks içeren kolloidal süspansiyonların saniyeler içerisinde çöktürülebileceği görülmüştür.

Anahtar Kelimler: Flokülasyon, polietilen oksit, boraks, su kimyası, viskozite

To My Family

ACKNOWLEDGEMENTS

I would like to express my deep and sincere gratitude to my supervisor, Prof. Dr. Çetin Hoşten.

I warmly thank to Zafer Kaplan, Caner Baytar, Tahsin Işıksal for their help during the laboratory work.

I am particularly indebted to my friends, especially Neşe Sevim, Onur Gölbaşı, Mahmut Camalan for their invaluable encouragement and support.

I owe my loving thanks to my family. Without their encouragement and understanding it would have been impossible for me to finish this thesis.

This study was supported by BAP - 03 - 05 - 2012 – 002 of the Middle East Technical University.

TABLE OF CONTENTS

LIST OF TABLES

TABLES

LIST OF FIGURES

FIGURES

CHAPTER 1

INTRODUCTION

1.1. Statement of the Problem

The colloidal mineral particles in the wastewater stream of mineral industries cause significant bottleneck problems. The presence of such stable particles brings about challenges in solid/liquid separation, water recovery for reuse, handling and management of tailings. A real life example for the tailings management problem is the Kırka tincal concentrator in Eskişehir/Turkey. This plant experiences the tailings problem more vigorously with increasing boron production. Clay and dolomite particles are the most abundant mineral phases in the Kırka tincal concentrator tailings and they form very stable suspensions. Furthermore, the presence of dissolved borate ions in the solution leads to a buffer zone around pH 9.40. The buffering capacity of the boron mineral makes the management of stable clay and dolomite particles more difficult by hindering the pH adjustment as a means of destabilizing the colloidal tailings.

There are two most common physicochemical methods to destabilize such colloidal particles in mineral tailing. First one is coagulation and second one is flocculation process. Destabilization with coagulation is achieved with coagulants, simple electrolytes having an opposite charge to the particles. These electrolytes cause charge neutralization and force particles to come into contact resulting in an agglomerated system called as coagula. On the other hand, destabilization with flocculation is achieved with flocculants, complex long chain polymeric reagents. The tail and/or loops of these polymers adsorb on particles and attach particles into larger agglomerating system via the bridging mechanism. The resultant form is

called as a floc in this case. In the mineral industry, flocculation process is generally preferred instead of coagulation for destabilization of the colloidal systems because coagulation is much more sensitive to pH of the solution and produces very weak fragile structures. Conversely, flocculants lead to denser, stronger flocs with faster settling rates. Unfortunately, none of these two physicochemical methods can be implemented in the destabilization of colloidal clay and dolomite minerals in the Kırka tincal concentrator tailings owing to the lack of technical and practical information. Currently, this problematic tailing suspension is not treated and directly sent to the tailing ponds without any technical intervention. Due to the lack of data in the literature considering the actual flocculation mechanism of dolomite/clay/borax-containing systems, the problem could not be solved in either laboratory-scale or industrial scale. The gap in the literature can be summarized as follows:

I. Proper characterization of the dolomite/clay-containing samples of Kırka.
II. Introducing velocity gradient as a controlled parameter to the flocculation process to increase collision probability between polymer and particle.
III. Determining a proper coagulant as flocculant aid to enhance destabilization performance.
IV. Aqueous chemistry of dolomite/clay/borax-containing systems and buffering effect of borax.
V. The viscometric behavior of polymer solutions.
VI. No flocculation process optimization for dolomite/clay/borax-containing suspensions to reduce polymer consumption.

As a summary, previous studies mainly focused only on the effect of the flocculant type, charge and molecular weight on dolomite/clay/borax-containing suspensions. These studies can be considered as general tests that aim only flocculation performance. However, they could not explain the underlying flocculation mechanism of these stable suspensions, and the need for successful flocculation of such systems is ambiguous. For this reason, these studies required extortionate amount of polymer consumptions (1500-2500 g/t-solid) to flocculate dolomite-clay-

borax-containing suspensions. In conclusion, filling this missing information in the literature was attempted with comprehensive flocculation experiments under controlled conditions using dolomite/clay/borax-containing suspensions.

1.2. Aim and Scope of the Thesis

The aim of this study was to reveal polyethylene oxide (PEO)-induced flocculation mechanism of two different dolomite/clay-containing samples from Kırka Tincal Mine in the presence of dissolved borax and necessary parameters for enhanced destabilization and turbidity removal. The results of the flocculation experiments were tried to be supported with characterization studies, conceptual aqueous chemistry calculations and viscometric analyses. In conclusion, the flocculation behavior of the problematic colloidal suspensions was ascertained and an effective flocculation technique for these specific suspensions was determined by optimizing certain parameters. For this purpose, the following steps were implemented sequentially in the scope of this thesis:

1. Detailed qualitative and quantitative characterization of the two different samples (containing mainly dolomite and smectite) from the Kırka borax deposit.
2. Preparation of two different dolomite/clay/borax-containing colloidal suspensions for lab-scale flocculation experiments.
3. Effect of the mixing intensity on the flocculation performance of these two suspensions in borax-buffered solutions.
4. Identification of non-flocculatable mineral phase in the supernatant after PEO-induced flocculation procedure at high velocity gradient.
5. Effect of pH adjustment on the PEO-induced flocculation performance at 108 and 306 s^{-1} velocity gradients.
6. Effect of high solution temperature on the PEO-induced flocculation performance at 108 and 306 s^{-1} velocity gradients.

7. Effect of conditioning with various coagulants prior to PEO-induced flocculation at high velocity gradient.
8. Effect of dual-polymer (Cationic polyacrylamide and non-ionic PEO) treatment at 108 and 306 s^{-1} velocity gradients.
9. Effect of the unconventional ballasting technique on the PEO-induced flocculation at 108 and 306 s^{-1} velocity gradients.
10. Aqueous chemistry calculations for dolomite/clay/borax-containing solutions and coagulant solutions. Determination of favorable hydrolyzed aqueous species and unfavorable metal oxides precipitates as a function of pH for improved PEO-induced flocculation.
11. Comparative viscometric studies.
12. Statistical optimization of the prominent flocculation parameters for these dolomite/clay/borax-containing suspensions with the help of Response Surface Methodology.

CHAPTER 2

LITERATURE REVIEW

2.1. Background Theory

2.1.1. Colloidal Suspension

A colloidal particle is characterized with a dimension less than 2 μm. This phenomenon is controversial depending on research and application areas. Especially, upper limit of the defined particle size is surpassed and sometimes reaches several hundreds of micrometers (Ghosh, 2009). In spite of the scientific debate on the subject, natural particles in a colloidal suspension like clay minerals in soil or turbid water are considered as stable systems because very fine particles carry a high surface free energy. The stability term of such aquatic system has two distinct meanings. Firstly, it refers that there is no sign of phase-separation over a period of time. If colloids sediment over a period of time, it is called unstable. Second meaning refers to the suspension with no tendency of aggregation. So, “colloidal stability” is used for particles which don’t aggregate whereas “mechanical stability” is preferred for particles which don’t sediment (Shaw, 1992). In general, such stable suspensions are constituted of a dispersed phase and a dispersion medium. Both the dispersion medium and the dispersed phase can be liquid, gas and solid. According to these phases, colloidal system is named as emulsion, sol or suspension. In mineral waste water systems, the dispersion medium and the dispersed phase are mostly liquid and solid, respectively.

2.1.2. Particles in Water

Colloidal particles have limited or no attractive force between them in an aquatic environment. Electrostatic repulsion, principally stemmed from crystal and surface charges, prevents particles to interact and agglomerate. These charges on colloid are significant because strength of particle-particle repulsion define stability or instability of the system. The charging mechanism of particles can be summarized as the following:

1-) Ionization of surface groups
2-) Differential solution of ions from the surface of a sparingly soluble crystal
3-) Isomorphous substitution
4-) Specific ion adsorption

If surface of particle have acidic groups, dissociation of these groups promote negatively charged particle surface as in the case of most mineral phases. For this case, the surface charge is essentially interrelated with the initial acidic or basic strengths of the active groups. The charge can be governed easily with pH of the solution. By adjusting pH, it can be increased or decreased and even it can be neutralized (Figure 1). As a result, ionization of such surface groups becomes dominant mechanism for charging of particles in aqueous environment.

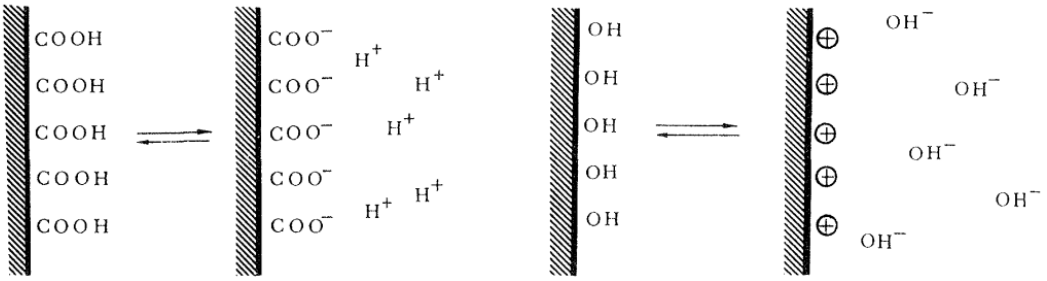

Figure 1. Ionization of surface groups (Everett , 1988)

Differential solution of ions from particle surfaces also gives rise surface charge. Well-known example for this case is silver iodide particles. If the particle is placed in water, silver or iodide ions can be preferentially dissolved (Figure 2) by leaving the surface negatively charged or positively charged, respectively. Depending on the situation, Ag^{+} and I^{-} ions concentration on the surface define net charge.

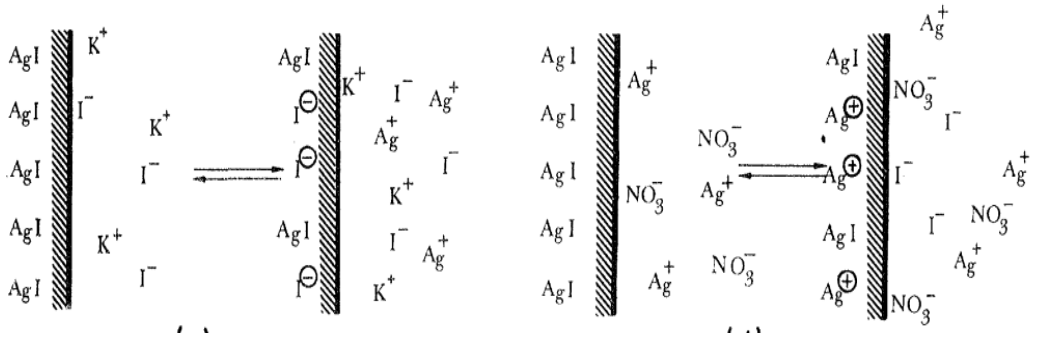

Figure 2. Differential solution of ions from the surface of a sparingly soluble crystal (Everett , 1988)

Isomorphous substitution is another mechanism that is very dominant for clay minerals. The clay crystal can exchange structural ion with another one leaving the surface negatively charged. For example, Al^{+3} can be exchanged with Si^{+4} in tetrahedral sheet or Mg^{+2} with Al^{+3} in octahedral sheet. Due to the differences in valency number of these ions, the resultant surface charge becomes negative. Furthermore, clay crystals can be structurally broken or have lattice imperfections by revealing differently charged surfaces as in the case of edge exposure containing AlOH groups. The Isomorphous substitution can also be combined with ionization of surface groups and charged crystal surface (Figure 3). These three mechanisms determine overall particle charge especially for clay particles.

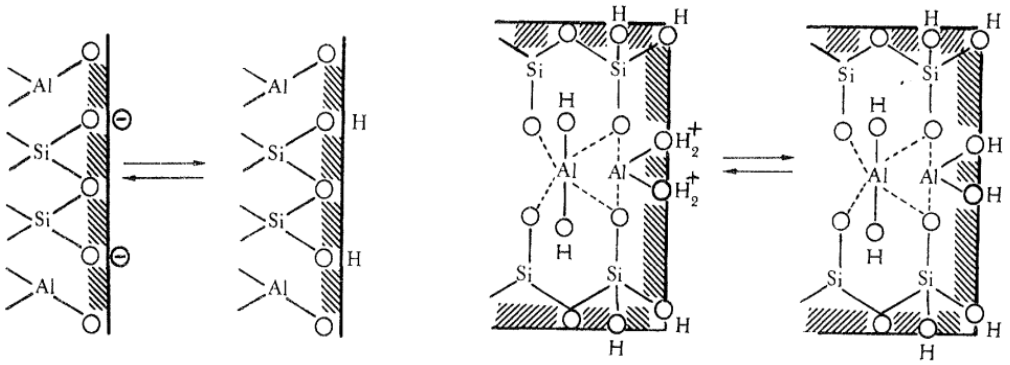

Figure 3. Isomorphous substitution (Everett , 1988)

A final and important charging mechanism is the specific ion adsorption. The attractive force between particle surface and cations in solution, which are superior to simple electrostatic force, can be referred to specific adsorption. Ions initially held around Stern layer can be preferentially exchanged with other ions in diffuse layer (Figure 4). The adsorption strength of these specific ions is greater so it is very important for surface related studies.

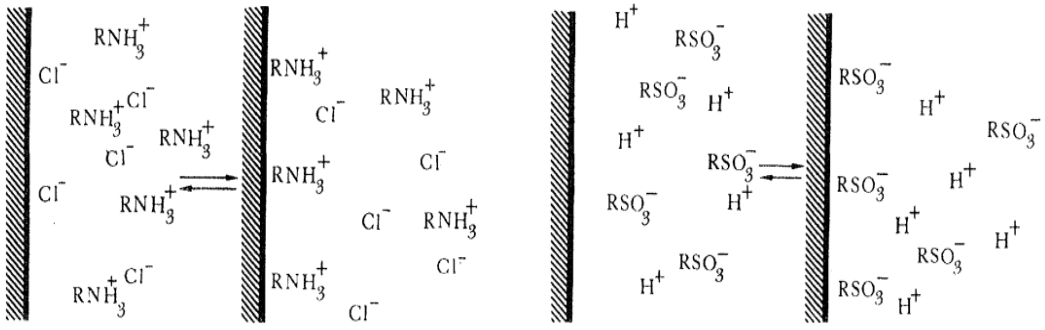

Figure 4. Specific ion adsorption (Everett , 1988)

As mentioned previously, surface charges at the interface between colloid and water promotes stability of a colloidal suspension. In addition to this, it was found (Pashley, 1982) that hydration of particle surfaces contributes the stability concept. Adsorbed water molecules on the surface form a liquid physical barrier which prevents particle-particle collision and interaction. Water molecules have a unique dipolar structure that results in locally unsatisfied negative and positive charges associated with the oxygen atom and hydrogen atoms. Due to this dipolar character, water molecules in contact with charged surfaces and cations tend to be oriented. In the case of adsorbed cation, six water molecules in a spherical envelope also take places on the particle surface together with the cation. This hydrated cation is called as aquacomplex. When aquacomplex of a cation is present in water, its actual form is represented as $Me(H_2O)_6^{+n}$ instead of Me^{+n}. Forming hydrated ions releases large amount of energy and it is called hydration energy of cation. The hydration energy depends on the charge and radius of cation. This explanation is very important regarding suspension stability. For example, Ca has 1Å radius and -1592kJ/mol hydration energy; Mg has 0.72Å radius and -1922 kJ/mol hydration energy (Langmuir, 1997). So, Mg holds water molecules more tightly than Ca and all other cations with +2 valency. This property of adsorbed Mg-aquacomplex on particle surface leads to stable suspension. Adsorbed Mg-aquacomplex presents itself as a drawback in some studies. For example, the stability due to adsorbed Mg-aquacomplex leads to erosion in soil science (Dontsova & Norton, 1999), decrease in flotation recovery ((Haselhuhn et al., 2012; Cheng et al., 2010) and increase in turbidity in flocculation (Çırak, 2010). Orientation of water molecules on particle surface, aquacomplex of cation and related surface blockage in a stable suspension can be seen in Figure 5.

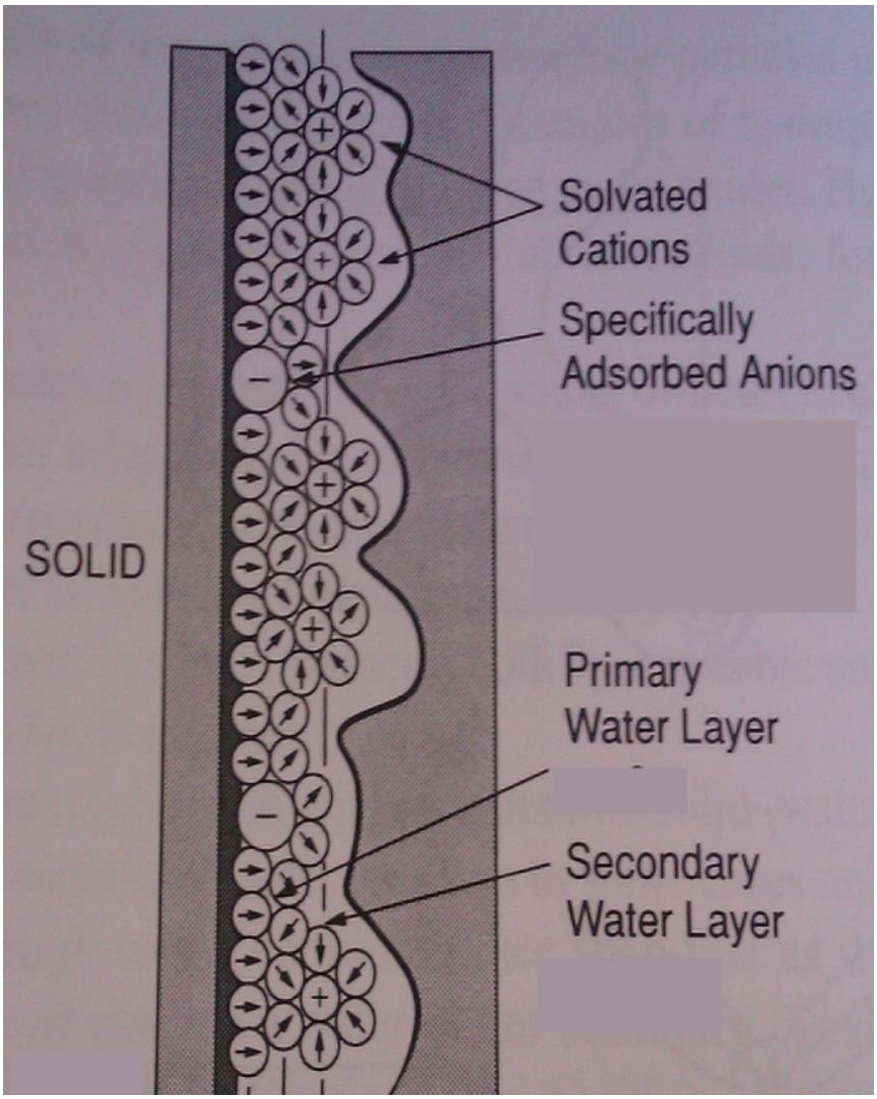

Figure 5. Orientation of water molecules on particle surface

As explained previously, particles carry a net electrical charge depending on their origin. Oppositely charged ions in an electrolytic solution are attracted to the surface of a charged particle on the other hand co-ions are repelled. Due to this reason, some ions are associated with the surface while the others are distributed into the solution according to particle surface character. Two forces promote this movement, namely electrostatic attraction and ionic diffusion. These two forces are opposite of each other and create a diffuse ionic cloud around particle in water. Ultimately, co-

existence of charged particle surface together with counter ions on this surface and co-ions scattered in a diffuse area is called as electrical double layer. Due to the ionic cloud unique distribution surrounding particle, an electrical potential is emerged in this double layer. Based on distribution of charge and electrical potential, Gouy and Chapman tried to model the double layer at the beginning of twentieth century. Their model simplified the system and made some basic assumptions. They assume particle surface is infinitely flat and impenetrable; ion in solution has no volume but only point charges; the water is uniform solvent that is not changing depending on distance from particle surface. According to these initial assumptions, electrical potential changes with distance from particle surface. Whereas highest potential is near charged surface, the lowest potential is obtained at distance from the surface. The drawback of Gouy-Chapman assumption is that the ions are identified as point charges. In reality, they have defined size and volumes. This is very significant because effective distance of closest approach to a charged surface is limited especially when ions are hydrated. Allowing for the finite size of ions gives a region close to the surface which is inaccessible to counterion charge. Otto Stern corrected this false point charge assumptions of ions in 1924. After him, this region is called as the Stern layer. The Stern layer has a certain proportion of the counterion charge and the remaining is distributed through diffuse part of the double layer. This region is called as diffuse layer. These two layers can be seen in Figure 6. The figure shows the decreasing electric potential with distance from the surface toward the bulk solution. The decrease is very sharp up to the Stern plane at a certain distance. From the Stern plane through the diffuse layer, the potential changes exponentially down to zero. Although the Stern layer thickness is very small (around 0.3 nm depending on the radius of hydrated ion), it is very significant in terms of electrical double layer characteristics and suspension stability. Another significant concept related to both the Stern layer and the diffuse layer constituting the double layer is Debye length. The Debye length refers to the thickness of the double layer. This thickness is known as $1/\kappa$ depending on the below formulas:

$$\kappa^2 = \frac{1000F^2}{\varepsilon RT}\sum(c_i z_i^2)$$ (Debye-Hückel Parameter) ;

$$I = \frac{1}{2}\sum(c_i z_i^2)$$ (Ionic Strength)

κ-value can be calculated by known values of ionic strength, I; concentration, c_i; valence, z_i; universal gas constant, R; temperature, T; Faraday's constant, F; permittivity, ε. As it can be seen from the equations, Debye-Hückel Parameter and also the thickness of double layer are function of the ionic strength of solution. When ionic concentration or valence increases, the Debye-Hückel Parameter increases and the thickness of double layers decreases. For instance, the typical value of the double layer thickness in deionized water is 960 nm. The thickness is compressed down to 30 nm in 10^{-4} M NaCl and down to 18 nm in 10^{-4} M $CaCl_2$ (Svarovsky, 2000). The greater is the ionic strength as in sea water, the smaller the thickness approaching to zero, and particle-particle interaction may increase resulting in destabilization of the system. Beside concentration, If Na^+ becomes predominant in the solution instead of Ca^{+2}, the double layer thickness increases due to its monovalent property, relatively. In this case, the decrease in particle-particle interaction may become influential on the system by promoting the stability. Conclusively, the thickness of the double layer also plays an important role regarding the stability of colloidal systems.

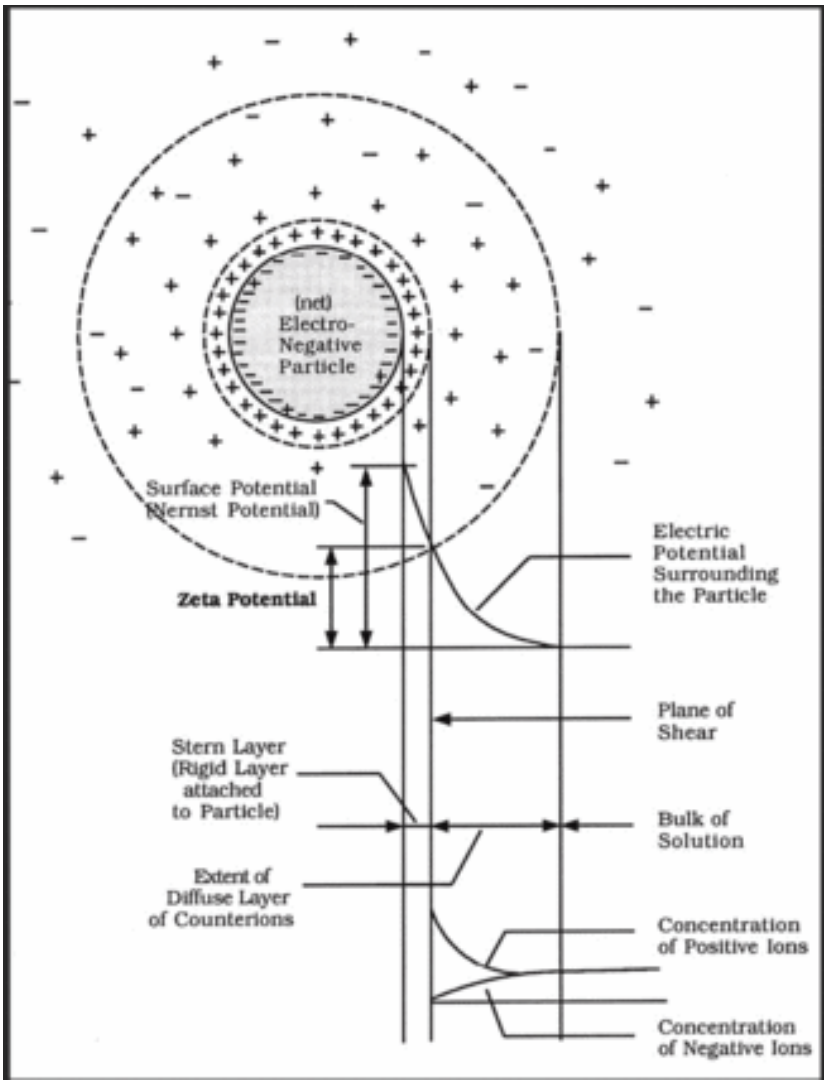

Figure 6. Electrical double layer (Ravina & Moramarco, 1993)

2.1.3. Polymer-Induced Flocculation

Particles in a dispersed system can be aggregated into larger aggregates. The aggregation based on reducing interparticle electrostatic repulsion is classified as coagulation and the aggregates are known as coagula. However, polymer bridging method can also be used for aggregation. This process is called as flocculation and the polymer-induced particle enlargement is known as flocs instead of coagula.

Especially in water treatment, metal salts are commonly used to aid flocculant. There are two main mechanisms of metal salts as flocculant aid. One of them is charge neutralization which reduces particle-particle repulsion. Second mechanism is sweeping which forms metal coagulant precipitates and this type of destabilization is called as sweep flocculation in which particles are agglomerated/swept down with the help of metal hydroxide species (For example: in the case of hydrolysable alum treatment). On the other hand, bridging is predominant mechanism in polymer-induced flocculation. Bridging flocculation is stemmed from adsorption of individual, mostly linear, polymer molecules on several particles simultaneously, and as a result dispersed particles are entrapped in a floc structure. If the polymer macromolecules have a branched three dimensional chemical structure or interacted linear polymer chains are formed, the particles in water rendered into a floc-gel which is termed as network flocculation. Even with linear polymers, meticulous management of polymer addition which is combined with appropriate mixing intensity can produce compact and very strong pellet-like flocs. This particle enlargement process is named as pelleting flocculation. Cationic polymer adsorption on negatively charged particles can be somewhat similar to the coagulation process. In this case, charge neutralization becomes the predominant mechanism over polymer bridging. This phenomenon is described as electrostatic patch flocculation model. Flocculation by incapability of adsorption of polymers on particle surfaces is defined as depletion flocculation. This situation is substantiated in the presence of highly concentrated polymer solutions (For example: 1000 – 10000 mg/l). In depletion flocculation process, the distance between approaching particles is smaller than the size of polymer molecules, and none of these molecules can enter the region between these particles, which is constituted of only the solvent. Polymer concentration outside this interacted particle system remains steady. This concentration exerts an inward force due to the osmotic pressure. Such a force leads to particle flocculation. According to the depletion flocculation theory, polymers have a strong, rigid conformation and they are considered as semi-permeable membranes. However, free non-adsorbing polymers may also create repulsion between suspended particles in some cases. For example, microreservoirs constituted

of solvent, namely water, increases the total free energy of the system. In this case, the phenomenon is called as depletion stabilization. Depletion mechanism is still vaguely defined in the literature. Although significant scientific debates are present on the subject, many researchers claim that polymer bridging is likely the main reason for flocculation.

2.1.4. Polyethylene Oxides

Flocculants are available as natural or synthetic products. Both of these polymer types are water soluble, high molecular weight, macromolecular structures and capable of destabilizing constituents of aqueous suspensions. These polymeric macromolecules are originated from a series of duplicative simple chemical units. The simple chemical structures are attached to each other with strong covalent bonds resulting in very long polymer chains. If the repeating units are made of the same molecular structures, flocculant is called as homopolymeric; if the flocculant is formed from more than one repeating unit, it is called as copolymer. The individual units in polymeric structures are named as monomer. The molecular weight of the polymer is the sum of the molecular weights of these individual monomers. The total number in the polymeric structure refers to the degree of polymerization of flocculant. Preferably, those polymers containing certain functional groups along with its ionizable polymer chains are called as polyelectrolytes. Those ionizable groups can be disassociated and then the remaining molecules become negatively or positively charged based on the specific functional groups. Thus, they are called anionic or cationic polyelectrolytes, respectively. If the functional groups are non-ionizable, they are termed as non-ionic flocculants. The polyelectrolytes may have hydrophilic and/or hydrophobic parts in their chemical structures. Their molecular weights change between 10^4 and 10^7. However, they can be dissolved in water due to hydration of functional groups.

Generally, flocculants are grouped under two categories as natural and synthetic. Natural flocculants are also divided into three according to their ionic character.

Starch, guar gum, tannin and dextrin are examples of non-ionic flocculants, carboxyl methyl cellulose is of anionic flocculant and cationized starch and chitosan are of cationic flocculants. However, synthetic flocculants are much more advantageous than the natural ones, especially in mineral processing. Because, they have superior solid-liquid separation capability, much lower biodegradability and well-defined molecular weight distribution than natural products. So, the synthetic flocculants are emphasized instead of the natural flocculants in most applications and scientific studies. Origin of the polar groups defines the class of the synthetic flocculant, just like in natural flocculants. Polyethylene amide $–CONH_2$, polyethylene oxide –O–, polyethylene alcohol –OH type functional groups are grouped under non-ionic flocculants. Polyacrylate –COOH , and polyethylene sulphonate $–SO_3H$ are grouped into anionic flocculants and polyamides $–NH_2$, polydialkylaminoethylmethacrylate –NH, polydimethyldiactyl-4-ammonium salt are grouped into cationic flocculants. Most common flocculants can be seen in Figure 7 with the related monomer and the functional groups. Polyacrylamide – PAM and polyethylene oxide – PEO type flocculants are widely utilized in wastewater treatment and mineral processing. In general, PAMs are preferred instead of PEOs due to their lower cost. However, PEOs are proved to be more effective, especially for very fine clayey suspensions (Mpofu et al., 2004).

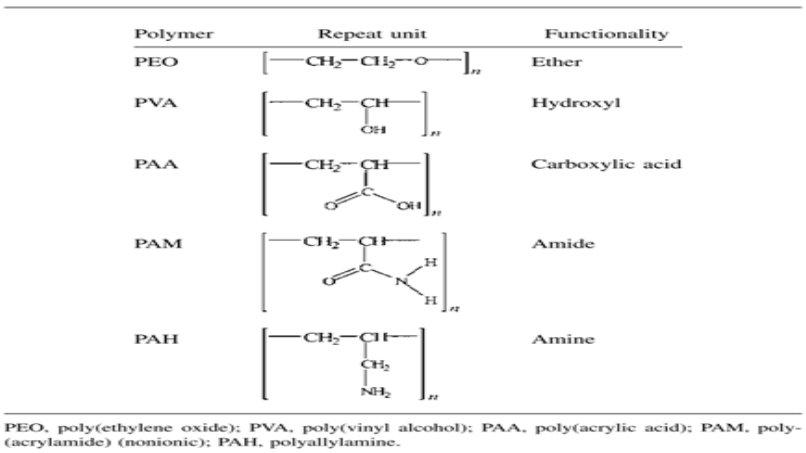

Figure 7. Common synthetic flocculants (Mittal & Shah, 2002)

In this study, PEO will be used as a flocculant and the properties of this polymer will be explained. PEO is a commercial flocculant which is produced by polymerization of ethylene glycol monomer. Depending on the polymerization, its molecular weight can increase from 200 to 10^7. The obtained chemicals after polymerization are called as polyethylene glycols if their molecular weights are less than 25.000. If the molecular weight is greater than 25.000, they are called as PEOs. PEO is dry, free-flowing, white powder. They easily dissolve in water. The rate of the polymer degradation is increased by strong acids, UV light, heat and certain metals like Fe^{3+}. The major role of this macromolecule includes adhesive, textile, lubricants, hydrodynamic drag reducing, medical and pharmaceutical industries but most commonly used as solid-liquid separation reagent in the wastewater treatment industry.

PEO adsorption on mineral surfaces, especially SiO_2 surface is studied systematically by different researchers (Scheiner & Wilemon, 1987; Rubio & Kitchener, 1976; Cheng Y. C., 1985; Mathur & Moudgil, 1997). These previous studies explained the main mechanisms of PEO adsorption on mineral surfaces as the following:

1-) Hydrogen bonding
2-) Hydrophobic interaction
3-) Electrostatic interaction
4-) Cation Bridge

1-) Hydrogen Bonding

PEO is proved useful to flocculate silica particles (Rubio & Kitchener, 1976). They concluded that the isolated silanol groups on mineral surfaces act as main adsorption sites for PEO. The interaction between polymer – mineral believed to be through a strong hydrogen bonding mechanism that includes ether oxygen of PEO and isolated

surface hydroxyls of mineral surfaces. This bonding mechanism is supported with the help of infrared studies that clearly identify the role of isolated groups on mineral surfaces. In relation to the subject of this thesis, early studies (Behl & Moudgil, 1993; Moudgil & Behl, 1993) suggested that dolomite surfaces also interact with the polymer in the above manner. However, later studies (Moudgil et al., 1995) showed that this is not the case. The bands attributed to free hydroxyls on dolomite actually belong to clay coating present on dolomite surfaces but not dolomite itself. By considering this, the flocculation of the dolomite particles can be enhanced by increasing amount of clay content that provides the system with extra isolated (free) hydroxyl groups.

2-) Hydrophobic interaction

PEO contains hydrophilic segments and a very long hydrophobic hydrocarbon chain. The hydrophobic backbone ($CH_3 - CH_2$) of the polymer is attracted to the hydrophobic surfaces because they have a tendency to avoid water molecules. Interaction of siloxane surfaces (Si – O – Si) with PEO is an example of hydrophobic interaction. In some studies, the term is called as hydrophobic bonding however, it is a vague concept and it may be much proper to name interaction instead of bonding. When it is compared to hydrogen bonding, it is found that hydrogen bonding mechanism is more influential than hydrophobic interaction. It is considered as an assistive mechanism of hydrogen bonding.

3-) Electrostatic Interaction

PEO type polymers are classified as non-ionic flocculants. Actually, their nature is very slightly anionic. PEOs can be subjected to unavoidable hydrolysis throughout the production cycle and as a result, this slightly anionic character can be pronounced (Kanungo, 2005). The slightly charged PEO can be attracted to the charged mineral surfaces under proper conditions. When they interact together, a weak floc structure is formed similar to coagula. This mechanism depends only on ineffectual

electrostatic attractive force and it is considered to be weaker than hydrogen bonding in the case of PEO.

4-) Cation Bridge

Polyvalent cations can attached themselves on negatively charged mineral surfaces, firmly. PEO can be adsorbed on to this anchor points on mineral surfaces. These anchor points depends on the solution character and they can be Al^{3+}, Ca^{2+}, Fe^{3+}, Cd^{2+}, Cu^{+2} etc. Especially, when the cations on the surface are hydrolyzed, they interact with PEO potently. Although it is not certain, it is thought that hydrogen bonding (or covalent bonding) takes places in the case of strong floc formation and mere electrostatic attraction in the case of weak floc formation through cation bridge mechanism.

Of the above mechanisms, the most robust one is considered as hydrogen bonding for PEO adsorption on mineral surfaces. Hydrogen bonding on the mineral surfaces involves ether oxygen of PEO which with two lone pair of electrons can be considered to be an electron donor, Lewis base. This explains that the surface hydroxyls playing predominant role in adsorption can exhibit an acidic behavior to lead acid-base type of interaction and promote flocculation. Su and Shen (2009) agreed with this but they took a step forward. They claimed that PEO can establish a hydrogen bond not only on the surface of mineral but also inside the crystal structure. A case study includes smectite-PEO interaction as an example. Su and Shen (2009) explained this example with Figure 8 and suggested that the ether oxygen of PEO can reach and bond even with the structural hydroxyl in the octahedral sheet of the clay mineral. However, it seems a disputable subject. It may be physically and chemically troublesome. The hexagonal cavity of the clay mineral cannot take even simple-large hydrated cations. Considering the complex chemistry of the polyelectrolyte, it may be physically much more formidable. Furthermore, the structural hydroxyls in the octahedral sheet are not active groups as free isolated hydroxyls on the surface so it may be chemically formidable too. In conclusion,

surface free-isolated hydroxyl groups should be considered as functional hydrogen bonding sites for PEO type flocculants excluding structural hydroxyls.

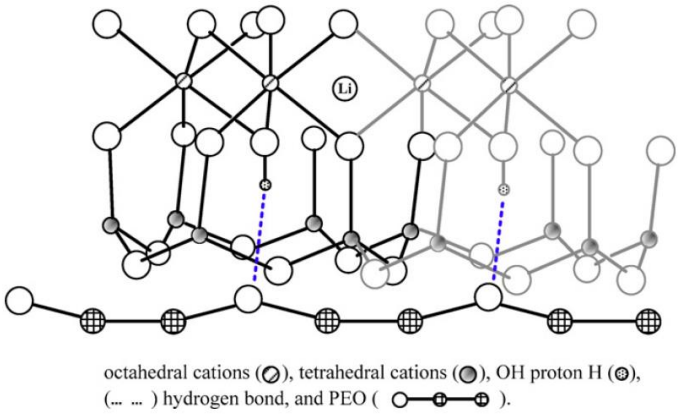

Figure 8. PEO interaction with structural hydroxyls in the octahedral sheet of clay mineral according to Su and Chen (2009),

2.1.5. Importance of Isolated Hydroxyl Groups on Mineral Surface as Anchor Points for PEOs

It is well known that PEOs can attach themselves on mineral surfaces via hydrogen bonds as mentioned previously. The isolated hydroxyl groups on mineral surfaces are of vital importance to accomplish this interaction. However, the isolated hydroxyl is not the only hydroxyl species on the surface. Actually, the hydroxyls are grouped into three broad categories (Zhuravlev, 2000). The most in-depth scientific studies have been carried on silica surfaces, and in the literature most examples are related to SiO_2-surfaces. First and most important one for flocculation studies is the isolated free (single) hydroxyls which, is exemplified as free silanol, –SiOH in Figure 9. The free isolated hydroxyl groups look like dangling anchor points for PEO. Geminal hydroxyls take places under the second group. They are shown as $–Si(OH)_2$ and also named as geminal silanols or silanediols. The third group is the vicinal hydroxyls.

They are hydroxyl groups that bound through hydrogen bonding mechanism so they are sometimes named as hydrogen bonded single silanols. The vicinal hydroxyls can be considered as unimportant for flocculation since these hydroxyls are already attached to each other via hydrogen bonds instead of PEOs. On silica surfaces, siloxane surfaces are also formed, –Si-O-Si–. In this case, Si – atoms are bridged with oxygens and losing hydrogen bonding capability with PEOs.

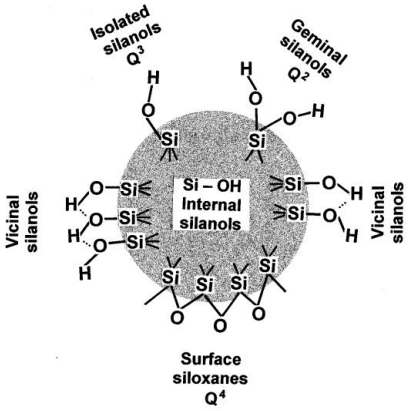

Figure 9. Hydroxyl groups on mineral surface (Zhuravlev, 2000)

Another study (Lu et al., 2005) explains the relation with free isolated hydroxyl groups and PEO. To manipulate the hydroxyl groups on mineral surface, heat is used as a pretreatment method. It is found that surface hydroxyl groups vary with increasing temperature. The study starts with a silica surface fully covered with a layer of silanol groups. The mineral is subjected to dehydration by heating up to 400 ˚C. This dehydration is completely reversible on cooling. However, there is a conversion to hydrogen bonded silanol groups above 400 ˚C. More importantly, the concentration of isolated free hydroxyls (silanol – SiOH) increases with increasing temperature up to 700 ˚C. PEO adsorption appears to be enhanced through the interaction with the increased amount of isolated free hydroxyls. On heating to higher temperatures, the concentration of siloxane groups also increases. It is

observed that both adsorption and flocculation with PEO deteriorates when the proportion of these siloxane groups increases. The pretreatment at temperatures above 1000 ˚C completely eliminates isolated free hydroxyl groups on mineral surface by resulting in negligible adsorption and flocculation with PEO. The flocculation study of heat treated silica with PEO is summarized in Figure 10. A correlation between the adsorption of PEO on the silica and the flocculation performance shows a maximum at 700 ˚C corresponding to the maximum number of isolated free hydroxyl groups on the mineral surface.

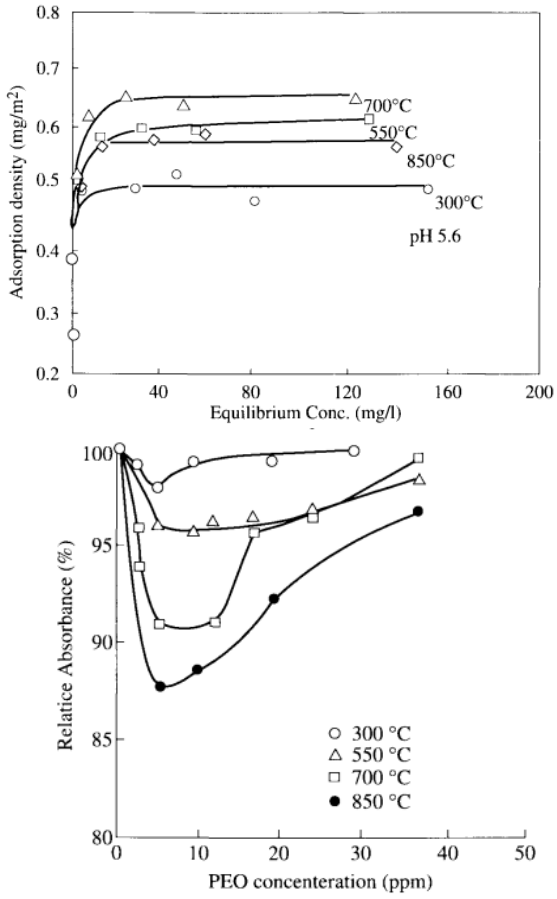

Figure 10. Relation between free isolated hydroxyl groups and PEO (Lu et al., 2005)

2.1.6. Parameters of Flocculation

The parameters are divided into two broad categories as physical and chemical factors. First of all, particle properties in suspension are an important physical parameter. The initial particle size, the surface charge and pulp density define the stability of colloidal system. In some treatment applications, they are tried to be manipulated within the limits. Secondly, the conditioning is significant in polymer-induced water treatment. The type of shear and its intensity may enhance the floc formation. However, the agitation time is the controlling key parameter in the conditioning because if the optimum agitation time is exceeded, the flocs start to disintegrate and the firm structure is broken into fines. Thirdly, polymer dosage is another principal parameter. The amount of the polymer in solution and their adsorption efficiency on mineral surfaces results in the water recovery, the solid-liquid separation and the robustness of floc structure. The rate of flocculant addition is as significant as the amount. If it is fed very fast, polymers are distributed non-uniformly into the colloidal suspension by resulting in decrease in particle-polymer interaction. The slower and controlled rate of addition should be preferred.

The chemical factors are related with the flocculant itself and the water chemistry of suspension. Firstly, the type of the polymer and its functional groups relation with the colloidal particle should be carefully examined for the best performance. Then, depending on the charge of the particle surface, ionic character of the polymer should be determined, anionic, cationic or non-ionic etc. The structure of the polymer and its molecular weight depending on the chain length may determine the settling rate and particle entrapment into the floc so it is another important parameter to be studied. Regarding the solution, most important parameter is the water chemistry. The ions in the solution can be adsorbed by mineral surfaces and behave like a bridge between polymer and particle. The value of pH can activate the mineral surface and/or polymer functional groups for effective adsorption. Furthermore, polymer conformation can change according to the solution pH. For example, the cationic flocculants are highly ionized at acidic pH values and their chains are in the

expanded form. By increasing pH, the cationic flocculants become coiled up. The anionic flocculants behave conversely. They are expanded at higher pH values and coiled up at low pH values. In the case of non-ionic flocculants, pH of the solution is not as important as for the cationic and anionic flocculants because non-ionic flocculants are much less sensitive to pH variations. The insensitivity of non-ionic flocculants takes its source from their negligible residual anionicity. The non-ionic polymer can be subjected to hydrolysis reaction at higher pH values by leading to repulsive forces between its own segments (Besra et al., 2004). This repulsion expands the polymer chain in the longitudinal direction (Figure 11). As a result, non-ionic flocculants have the stretched conformation which enhance the thickness of adsorbed polymer layer, consolidate interaction with more particles and make bridging mechanism dominant over electrostatic forces in alkaline solutions.

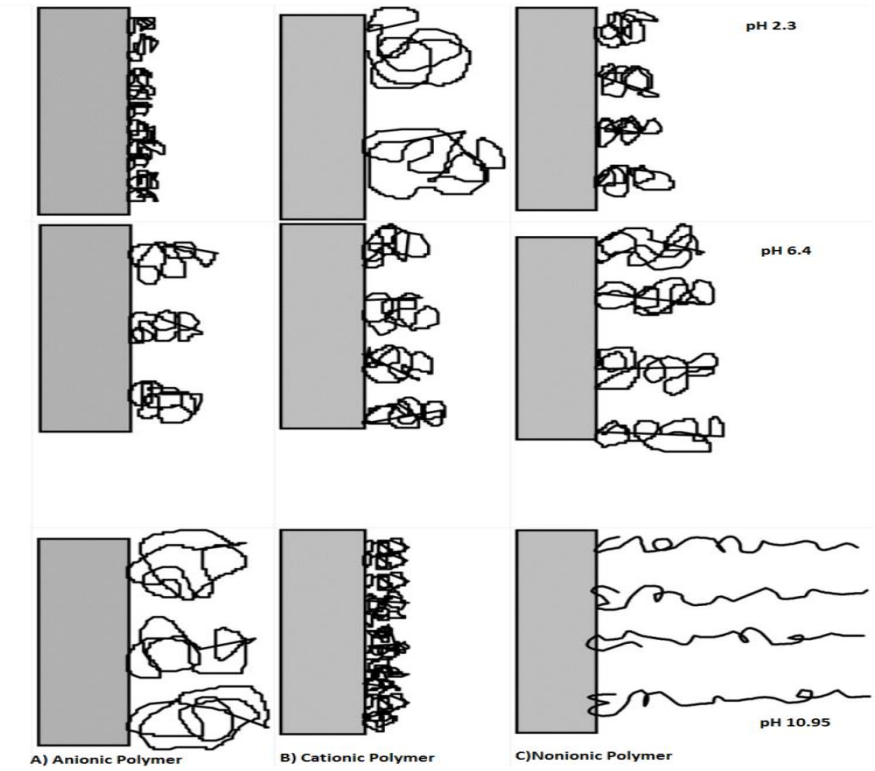

Figure 11. Conformational state of polymers according to their anionicity (Besra et al., 2004)

Table 1 summarizes the factors affecting the flocculation process. All of these physical and chemical parameters can improve flocculation performance significantly when they are optimized.

Table 1. Parameters of flocculation studies

Physical Factors	**1. State of particle dispersion** **2. Initial particle size** **3. Intensity of shear** **4. Type of shear** **5. Time of agitation** **6. Rate of polymer addition** **7. Polymer dosage** **8. Pulp density**	**Chemical Factors**	**1. Type of charge on the polymer** **2. Charge density of the polymer** **3. Structure of the polymer** **4. Molecular weight of the polymer** **5. pH of the suspension** **6. Water chemistry and the species in the solution**

2.1.7. Application of Polymeric Flocculants

Polymeric flocculants are industrially used in a very wide range of practical implementations. Main industrial applications can be grouped into these major fields of studies: drinking water treatment, sludge dewatering, mineral processing, papermaking and biotechnology. In these industrial sectors, PAM type flocculants are frequently preferred due to their high performance and low cost. However, different type of polymer usage can be sometimes required depending on the suspension stability. Due to this reason, generally a range of flocculants are tested for individual systems to find out the most efficient treatment.

In industrial drinking water treatment, mostly low-molecular weight, highly charged, cationic polyelectrolytes are preferred. They serve as a neutralizing agent for anionic impurities in water. The reason for this can be explained with very low particle concentration of suspension and also cationic polyelectrolytes make capture of particles easier. This procedure can be enhanced by applying hydrolysable metal hydroxides prior to polymer addition. In sludge dewatering, medium charged high-molecular-weight cationic polyelectrolytes are used considering pH values of the domestic wastewaters. They proved themselves very efficient in terms of strong floc formation, ease in decantability and filterability. In biotechnology, cationic polyelectrolytes are extensively used to remove microbial cells from medium to recover valuable products. Papermaking industry prefers cationic polymers as well. The purpose is related to the retention of filler particles in the formed paper sheet and binding cellulose fibers in the sheet. In mineral beneficiation, solid-liquid separation has a vital role in the whole system because the wastewater stream of a plant is generally a bottleneck for the production cycle and water recovery. To overcome this, several types of polymeric flocculants are used individually or in combination depending on the stability of mineral suspension. Nevertheless, there is a strong tendency in this sector to use high-molecular-weight anionic and nonionic polymers for flocculation of inorganic mineral suspensions instead of cationic polymers (Records & Sutherland, 2001). The reason of this can be explained that nonionic and anionic flocculants have higher molecular weights up to 20 million whereas cationic flocculants, which sometimes considered as coagulants, have lower molecular weight less than 1 million (Skuse, 2002). Moreover, these flocculants can be used not only for solid-liquid separation but also separate mineral phases in mixed suspensions by selectively flocculating particles in mineral industries.

2.2. General Information about Borax Production

The world's greatest borax deposit is in 250 km west of the capital city of Turkey, Ankara. This deposit is called as Kırka borax formation which dates back the upper Tertiary period. The tincal formation is in a 400 m sequence of various lake

sediments and volcanic tuff. Borax layer has a substantial thickness (Yalçın & Baysal , 1991). The ancient lake type environment of the Kırka formation had very long shores and a central deep zone. This playa lake geometry led evaporation of water and precipitation of several solid phases including boron, calcium, magnesium etc. elements in an arid environment. In 1960, first boron phase was discovered as an outcrop and identified as colemanite in Kırka. However, the detailed geological analysis proved that the deposition contain primarily borax ($Na_2B_4O_7.10H_2O$) but not colemanite. The greatest borax concentrations took places in the central area of the ore (Figure 12). Colemanite ($Ca(B_3O_4(OH)_3.H_2O)$) and ulexite ($NaCa(B_5O_6(OH)_6).5H_2O$) minerals were found of only secondary importance. Then, mineralogical analyses showed (Garrett, 1998) that minor amounts of other boron phases were detected as a result of mineralogical analysis; for example, hydroboracite ($CaMgB_6O_{11}.6H_2O$), inderite ($Mg_2B_6O_{11}.15H_2O$), inyoite ($Ca_2B_6O_{11}.13H_2O$), kurnakovite ($Mg_2B_6O_{11}.15H_2O$), meyerhofferite ($Ca_2B_6O_{11}.7H_2O$), tincalconite ($Na_2B_4O_7.5H_2O$) and tunnelite ($SrB_6O_{10}.4H_2O$).

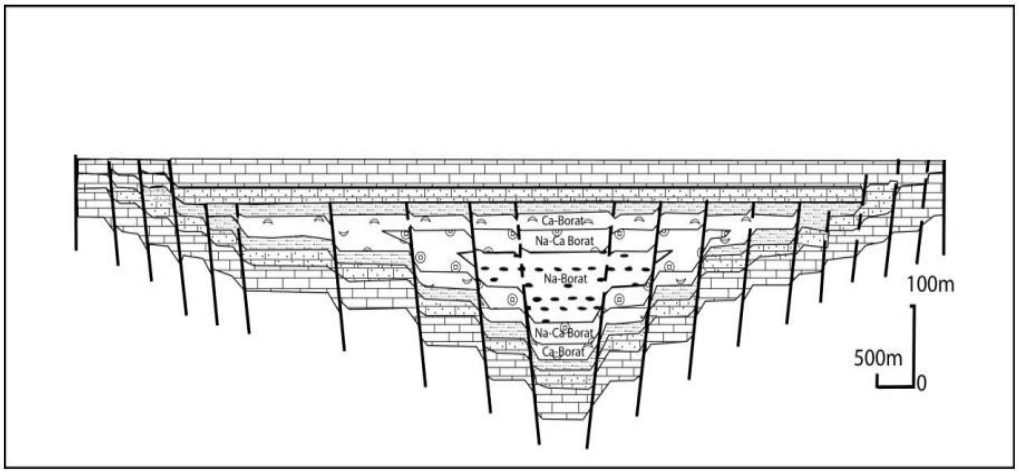

Figure 12. Generalized borate sequence in Kırka borax deposit (Yalçın & Baysal , 1991).

The layer of deposited borax is protected and sealed up with the help of upper clay and tuff layer originated from volcanic activities and calcium and magnesium precipitates in the form of carbonate. However, these clay and carbonate minerals are not only present in the upper lake sediments but also present within the borax layer as gangue minerals (Kistler & Helvaci, 1994). These impurities are mostly smectite type swelling clay and dolomite minerals (Çolak, 1995). The lesser amount of clay minerals (illite and chlorite) and non-clay minerals (quartz, K-feldspar, plagioclase, strontianite, magnesite etc.) are associated together with the dominant mineralogical phases.

The borax production was started in an open pit mine in the northwest of the deposit near an old mine shaft where the ore grade was greatest. The stripping ratio was calculated as 1.3/1 for this open pit mine. The ore have a specific gravity of 1.92 with a B_2O_3 grade of 25.4%. The reserve of Kırka borax formation comparison to other playa lake depositions in Turkey can be seen in Table 2 (Karaömerlioğlu, 2011) :

Table 2. Reserve values of boron formations in Turkey

The reserve values in Turkey		
Kırka	Borax	750 620 000 ton
Bigadiç	Colemanite – Ulexite	623 459 000 ton
Emet	Colemanite	1 682 562 000 ton
Kestelek	Colemanite	7 000 000 ton
Total		3 063 641 000 ton

The ore is constituted of 70.4% borax and the rest is principally smectite and dolomite. The borax bed dipped from 2 to 150m and the overburden thickness was 70 m. The borax mine covered 5.2 km^2 area. The benches of the open pit mine were 8 m in height and 15 - 25 m in width. At the end of the 90s, the open pit mine

became 400 m x 500 m in size, 60 m deep and 16-25˚ slope (Garrett, 1998). This ore formation is fragmented by drilling, blasting and then loaded to dump trucks and hauled to the concentration plant. The mined ore below 40 cm in size was first stocked onto a 3000 ton stockpile in 1972 and then a run-of-mine ore silo has been constructed for continuous uniform feeding in 1974. The material in this silo is first conveyed to a series of crushers working in closed circuit with screens. First crusher is an impact crusher and it reduces the size of the run-of-mine ore below 10 cm. Secondary crusher is a hammer type crusher and it produces material with a particle size below 2.5 cm. The product of the two-staged crushing unit is conveyed to a stockpile with a capacity of 10 000 ton (Figure 13).

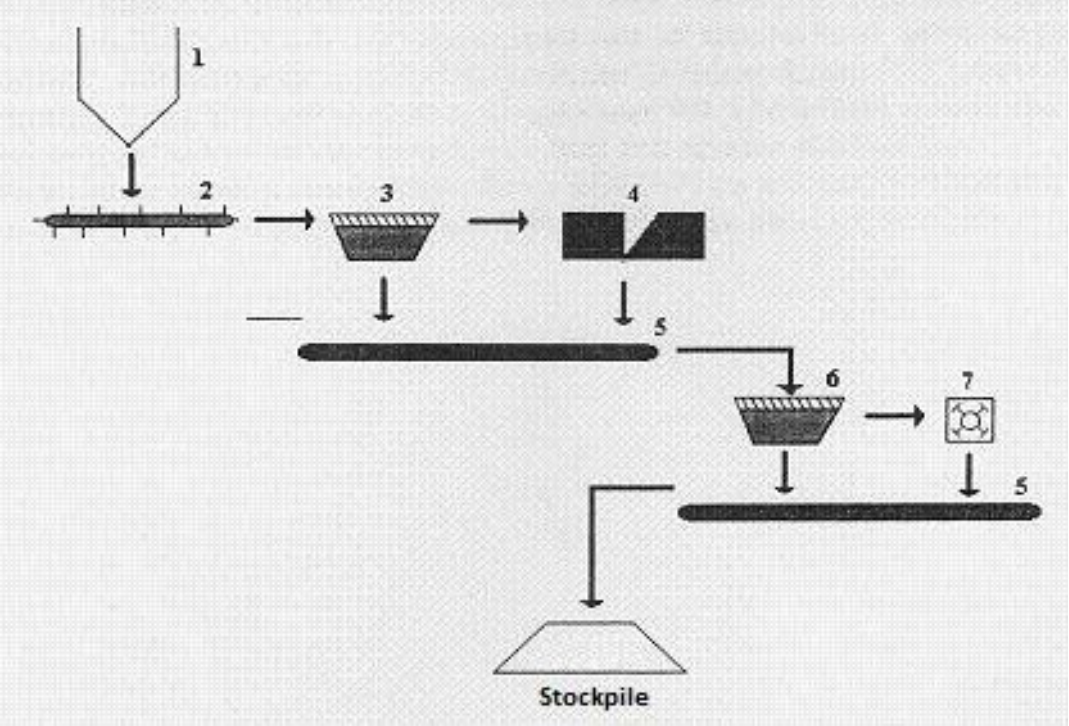

Figure 13. Size reduction stage of Kırka borax concentrator
1-) R.O.M. silo 2-) Feeder 3-) Sieve (-10 cm) 4-) Impact Crusher 5-) Conveyor (-2.5 cm) 6-) Vibratory Screen 7-) Hammer Crusher

In the later stage of processing, - 2.5 cm material is continuously fed from the stockpile at a capacity of 70 – 100 ton per hour. This material is further crushed below – 6 mm with tertiary crushers (Figure 14). Clayey material in the paste form due to the tertiary roll crusher is eliminated at the 15 mm clay screen. The rest of the material is mixed with saturated borax solution with a ratio of 1:1. This pulp is vigorously agitated in 6.5 m^3 attrition scrubbers, which are connected in series. The scrubbing leads to clayey material dispersion helping separation of valuable mineral from gangue minerals. The agitated pulp is sent to 1 mm screen. + 1 mm material is separated from the system and called coarse concentrate which covers 60-70% of the dispersed pulp. The undersize material of the 1 mm screen is pumped to a 2-staged hydrocyclone group. The underflow of the hydrocyclones is sent to spiral classifiers. The overflow of hydrocyclones and spiral classifiers are directly discharged to the tailing pond without any treatment including coagulation or flocculation to manage solid/liquid separation. The underflow product of spiral classifiers is mixed with coarse concentrate and the water content of the mixture is decreased down to 9% by dewatering centrifuges. As a result borax concentrate is obtained with a grade of 32-34% B_2O_3 and collected in the product stock area. The borax production is around 2500 ton/day in the Kırka concentrator.

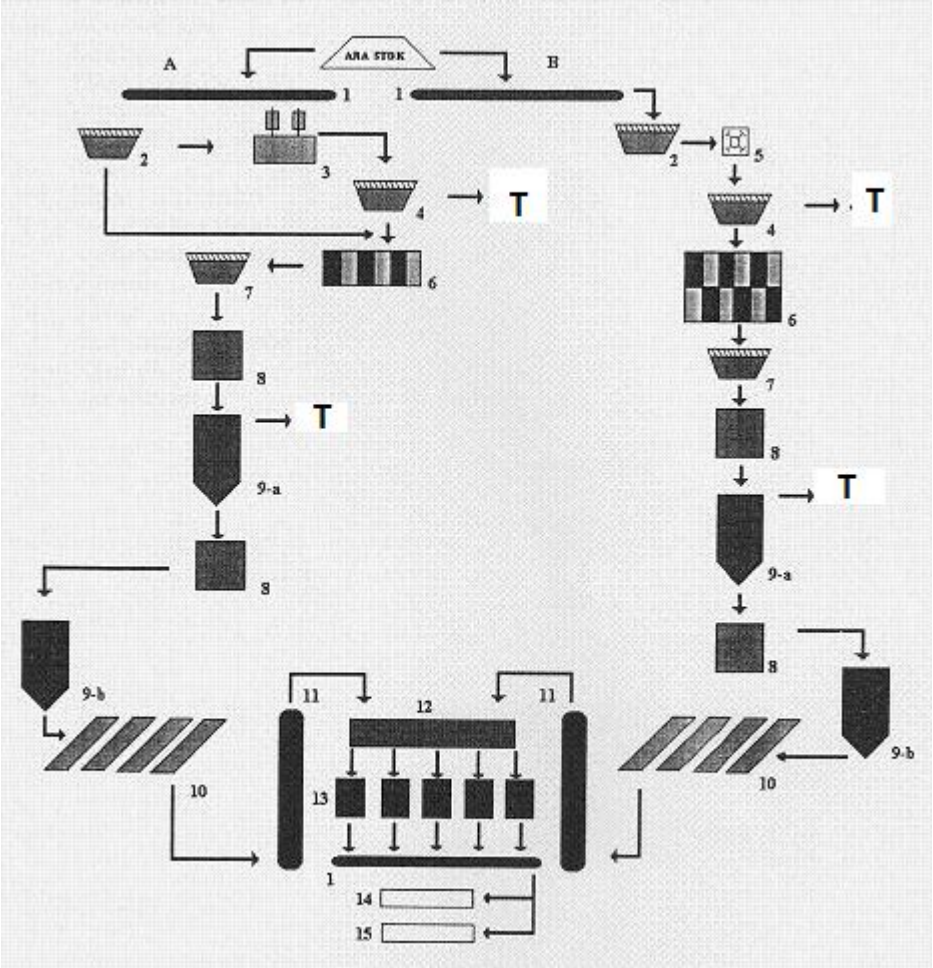

Figure 14. Dispersion and washing stage of the Kırka borax concentrator

1-) Conveyor belt 2-) Vibratory screen – 6 mm 3-) Roll crusher 4-) Clay screen 5-) Hammer crusher 6-) Attrition scrubber 7-) Vibratory screen – 1 mm 8-) Bunker 9-a) Primary hydrocyclone 9-b) Secondary hydrocyclone 10-) Spiral classifiers 11-) Elevator 12-) Raklet 13-) Dewatering centrifuges 14-) Concentrate 15 -) Boron derivatives T-) Tailing

This concentrator is the largest borax plant that unceasingly works and produces to meet world's ever-growing demand for boron. However, significant waste material is also discharged from the plant in conjunction with the vast amount of product. The tailing of the plant is pumped directly to 13 000 000 m^3 capacity tailing ponds without being subjected to any solid/liquid separation like coagulation, flocculation,

thickening etc. So, more than 12 000 000 m^3 tailing filled up these tailing ponds (Kökkılıç et al., 2005). In Kırka, 400 000 ton clay material is discharged per year on dry basis according to Sönmez & Yorulmaz (1995). 75% of the discharged material comes from the concentrator and only 25% from the boron derivative plant. Considering this ratio, the most challenging problem experienced in the management of the tailing is related to the borax concentrator. The previous analysis (Table 3) showed that the tailing of the borax processing plant includes mostly dolomite and clay as gangue minerals (23.09% and 27.16% respectively) together with significant amount of borax (Garrett, 1998). As known from the previous studies related (Taspinar & Çalışan, n.d.) and unrelated (Swartzen-Allen & Matijevic, 1976) to boron industry, clay minerals form very stable colloidal suspensions. Such clay suspensions lead to a formidable challenge in mineral industries as well as in the Kırka case. However, other dominant gangue mineral of Kırka borax formation, dolomite may also exist in a very stable colloidal form (Akdeniz et al., 2003).

Table 3. Quantitative mineralogical analysis of the Kırka borax ore, the concentrate and the tailing (Garrett, 1998)

Mineral Name	Ore	Concentrate	Tailing
Borax	69.11%	88.43%	41.44
Dolomite	13.76%	4.35%	23.09%
Clay	11.14%	2.60%	27.16%
Other	5.99%	4.62%	8.31%
TOTAL	100.00%	100.00%	100.00%

The clayey tailings of the concentrator contain around 97% water by weight. The high water content requires great volumes for tailing storage, and the shortage of the tailing ponds creates a significant trouble for continuous productivity of the plant and environmental safety. The tailing ponds can be easily located with enormous

projected area that can be compared to the mine site's area in Figure 15. It reveals that the tailing ponds are strictly surrounded by Kırka county and the farmlands. The tailing ponds are also very close to these surroundings and threaten them with a possible dam wall leakage or failure, water and/or soil pollution (Sakarya Newspaper G.A.C., 2013). Furthermore, additional tailing pond needs make itself evident with increasing boron demand and each tailing pond costs the company 10 million $. In 2012-2013, the company has started building another costly tailing pond with a tender number of 2012/96063 to solve the problem, temporarily.

Figure 15. Kırka borax mine and the tailing ponds which surrounded by the county and the farmlands.

2.3. Previous Studies Related to Destabilization of Dolomite/Clay/Borax-Containing Suspensions

Flocculation of the clay size particles in the discharge stream of the Kırka borax concentrator is a major technical problem and some laboratory researches were carried out to find out an alternative solution to this problem. Because, if Kırka concentrator tailings are not treated with a proper dewatering technique, it takes seven to ten days for sufficient sedimentation (Khan, 1980). This long period for sedimentation is not acceptable for a continuously working plant. Disposal of the process effluents from the plant is gradually filling up the tailings ponds with insufficient solid/liquid ratio. The capacity of the tailings ponds can be increased by raising the height of the dikes surrounding ponds. Another solution can be to construct a new tailings dam. However these two options are temporary solutions to the problem. (Çebi et al., 1994).

To find out a permanent solution, firstly mechanical dewatering systems like successive thickeners system and centrifugal decanters were studied but it showed that efficient polymer-induced flocculation was certainly needed for the mechanical dewatering equipment even in the centrifuge decanter used to enhance solid/liquid separation (Çebi et al., 1994).

Prior to the flocculant trial, laboratory-scale coagulation test were also carried out with different type electrolytes; however, the results of these studies were involving some unknown parameters and associated uncertainties. For instance, the most critical point is pH adjustment in the treatment of borax solutions and this significant parameter was ignored in the some studies. Generally, Al and Fe type coagulants gave optimum results at pH = 5–6. Borax presence in the tailings can make pH adjustment (down to pH=5-6) difficult due to its strong buffering capacity. Based on this fact, the flocculants were generally preferred and suggested instead of the coagulants in the wastewater treatment of the boron industry (Garrett, 1998).

PEO and PAM type flocculants are very important for both dewatering purposes and recovery of the boron products. So, a comparative study between PAM and PEO was done on dolomite/clay/borax-containing suspensions. As explained previously, the plant tailings include mostly dolomite and clay. Flocculation behavior of these minerals is different from each other. It was claimed (Gür et al., 1996) that PAM was favorable in flocculation of montmorillonite-rich clay suspension whereas PEO was favorable in flocculation of dolomite-rich clay suspension. In spite of this comparison, the great amount of polymer consumption was reported by Sabah and Yesilkaya (2000) (between 1 and 2 kg polymer consumption per ton). Although high amount of polymer was used (both PAM and PEO), the turbidity values were still high and settling time was very long.

CHAPTER 3

MATERIAL AND METHODS

3.1. Material Characterization

3.1.1 Dolomite/Clay-Containing Samples

The samples used in the experiments were collected from two different zones in Kırka borax mine. Considering the colors of these formations, one of the samples was called as the green sample and the other as the white sample in the literature (Helvaci et al., 2003; Yalçın & Baysal, 1991). These green and white materials were considered as good model samples that represent the gangue minerals of the borax ore and they have been preferred for controlled laboratory experiments instead of the actual plant tailing in previous similar studies (Gür et al., 1994; Taspinar & Çalışan, n.d.; Gür et al., 1996). In this study, these samples collected from the borax mine were used to form stable suspensions buffered by dissolved borax, and then the suspensions were subjected to polymer-induced flocculation to test destabilization behavior of these clayey samples.

3.1.2 Chemical and Mineralogical Analysis of the Collected Samples

Chemical analysis of the sample was performed using Spectro IQ X-ray Fluorescence (XRF) spectrometer in the Mineral Processing Laboratory of METU - Mining Engineering Department. The pellet method was preferred in this study due to the high amount of carbonate presence. The pellets were prepared by mixing 6.25 g of –38 micron clayey sample with 1.40 g of wax material and then the mixture was subjected to pressure under a press for the purpose of producing disk-shaped pellets

which were suitable for the sample holder. Finally, the X-ray spectra was analyzed with the help of the equipment software and presented as elemental percentages.

X-ray diffraction studies were carried out by a Rigaku X-ray diffractometer in the Clay Mineralogy Laboratory of METU – Geological Engineering Department, operating at 40 kV and 20 mA using CuKα radiation at a scanning speed of 2°/min (0.2°/min for the identification of octahedral character). Bulk mineralogy of the whole sample was determined with randomly ordered mounts of the powdered sample (-38 micron), and both qualitative and quantitative analysis were conducted on the spectra obtained from the random powder mount's readings. The actual qualitative clay content analysis had been previously performed by using detailed techniques on the oriented samples (Çırak, 2010) regarding the suggestion in the literature (Moore & Reynolds, 1997). The result of these previous studies showed that the dominant clay mineral with an ability to swell up to 1.8 times of its original crystal size was a smectite group mineral (Çırak, 2010). So, the random powder mounts' qualitative and quantitative analysis was covered but not the oriented mounts in the scope of this study.

Quantitative mineralogical analyses of the samples were accomplished using the Rietveld method via the computer program MAUD - Material Analysis Using Diffraction (Lutterotti et al., 1999). The Rietveld method, which is known as whole-pattern fitting structure refinement, uses all intensity data in the XRD pattern rather than a few of the most intense peaks. In the Rietveld analysis, refinement was done by minimizing the sum of the weighted squared differences between observed and calculated intensities in the XRD pattern. The calculated intensity at a given step (y_{ic}) was determined by summing the contributions from background and all neighboring Bragg reflections (k) for all phases (p). Hence, the Rietveld method can be considered as an iterative computation technique as summarized by Bish and Post (1993) with a given formula:

$$y_{ic} = \sum_p S_p \sum_k p_k L_k |F_k|^2 G(\Delta\theta_{ik}) P_k + y_{ib}(c)$$

where S is the scale factor; L_k is the Lorentz and polarization factors for the k-th Bragg reflection; F_k is the structure factor; p_k is the multiplicity factor; P_k is the preferred orientation function; θ_{ik} is the Bragg reflection angle for the kth reflection; $G(\Delta\theta_{ik})$ is the reflection profile function; and $y_{ib}(c)$ is the refined background.

3.1.3. Analysis of the Particle Size and Surfaces

The particle size analyses of the representative samples were carried out in suspension after the suspension was agitated and sonicated for the purpose of complete dispersion. Then, the particle size distribution was determined by Malvern Mastersizer 2000 in METU – Central Laboratory utilizing the light scattering technique with the help of a laser beam. BET analysis was carried out with Quantachrome Corporation–Autosorb 6 surface characterization equipment. The sample was prepared to eliminate surface water and moisture by applying heat treatment. Then, the sample was weighed (0.23 g) and placed on the holders. The powder was measured at a pressure of P/P_0=0.31 by using nitrogen gas for the purpose of determination of the surface areas.

Zeta potential measurements gave significant information about the surface properties of the colloidal particles. In this study, Malvern Zetasizer Nano-Z meter in the Mineral Processing Laboratory of METU – Mining Engineering Department was used to carry out required measurements with the help of laser doppler micro-electrophoresis method. However, it should be noted that the surface analysis regarding electrokinetic measurements were very challenging in this study as in the case of most of the real life samples. First of all, the prepared suspensions had a very high total dissolved solid (TDS) values. When borax was added into the distilled water, it was dissolved immediately and created a saline environment for the colloidal particles. The salinity resulted in unacceptable conductivity values out of the applicable range of Zetasizer Nano-Z. Moreover, the movement of the

concentrated conductive ions in solution could cause the electrode polarization and degradation. So, the capillary cells became dysfunctional producing misleading results. The solid clayey samples were also problematic because they were neither monodisperse in size nor monophase. Another problem was related to the particle concentration in the prepared suspensions. Due to very high solid concentrations, the excessive absorbance decreased the intensity of the scattered light and crowded particles lead to multiple scattering. As a result, the data quality/reliability was lost and even the measurement might become impossible. Considering these problems, the zeta potential measurements could not be carried out at actual concentrations. Instead of that, 10 mg green and white samples were added in per 100 ml of distilled water and mechanically dispersed at 1000 rpm. The measurements were taken for these diluted dispersions both at the beginning and at the end of the 24 – hour aging period to observe the variation in surface charges of the particles depending on the time. In addition to the time dependency, pH of the solution was studied as a parameter of the surface charge. 0.1 M HCl and 0.1 M NaOH solutions were dosed into the dilute dispersion to adjust the pH to the aimed values. The prepared diluted dispersions were injected into the standard disposable capillary cell – DTS1060 (Figure 16). After the capillary cell was sealed with two stoppers, it was placed into the Zetasizer and the required information was collected via Malvern Software.

Figure 16. Disposable capillary cell – DTS1060 for zeta potential measurements

In addition to the zeta potential measurements of the mechanically dispersed suspensions, the suspensions were subjected to ultra-sonication to observe the effect of sonic waves on the zeta potential of the dolomite/clay-containing samples, specifically at pH 9.40. Vibra Cell product of Sonics & Materials Inc., which had a tip type standard probe, was used for this sonication process (Figure 17). The suspensions were ultra-sonicated for 10 minutes at 100% amplitude with a power output of 200 watts and then the zeta potential measurements were carried out on these ultra-sonicated samples. The resultant zeta potential findings were reported as a function of the ultra-sonication time.

Figure 17. The ultra-sonic processor

To make further surface identification in addition to the zeta potential, the infrared spectra were generated with Bruker Fourier Transform Infrared Spectrometer. The

mid-infrared and far-infrared spectral regions were covered by this instrument (Figure 18). For the mineral-containing samples, the mid-infrared region between 400 and 4000 cm^{-1} is generally very helpful for the identification of the functional groups as well as solid phases. However, the more specific wavelength region between 3000 and 4000 cm^{-1} was analyzed to focus isolated hydroxyl groups on the green and the white samples particles in the scope of this thesis because these active groups had a spectral peaks around 3600 cm^{-1}. This method required no detailed sample preparation. The powdered samples (100% < 37 micron) were directly used for this measurement. The samples in the spectrometer were purged with dry air to remove water vapour and carbon dioxide at room temperature due to their unfavorable infrared absorbing properties. Then, the measurements were carried out with the standard spectral resolution at 4 cm^{-1} and the specifically narrowed resultant spectra were examined for the isolated hydroxyl groups detection.

Figure 18. Bruker Fourier Transform Infrared Spectrometer

3.2. Preparation of the Colloidal Suspensions and the Flocculant Solution

3.2.1. Preparation of Suspension Samples

The two collected samples, called as green and white based on the original colors, were used to obtain two different colloidal suspensions. The required amounts of these solid samples and borax were weighed and put into distilled water. It was vigorously stirred at 1000 rpm for three minutes for the purpose of complete dispersion of solid particles and complete dissolution of borax. The equipment shown in Figure 19 was used for this procedure. The resultant colloidal suspension buffered by dissolved borax around pH 9.30-9.40 had a content of 3% (w/w) solid and 3% (w/w) borax. The prepared suspensions were aged 24 hour. The reason of the aging process was to analyze changing flocculation behavior of the suspensions at the end of 24th hour. Prior to the polymer addition, the aged suspensions were mildly mixed again just for reassurance of the dispersion. Then, suspensions were placed in the jar test equipment.

Figure 19. The mixing equipment used to disperse solid particles

3.2.2. Polymeric Flocculant - Polyethylene Oxide (PEO)

Widely used flocculants in mineral industries are PAMs and PEOs. A comparison of these common polymers on the flocculation performance of clayey suspensions showed that PEO has greater settling efficiency and higher turbidity removal (Scheiner & Wilemon, 1987; Mpofu et al., 2003). Furthermore, PEO treatment of the clayey suspensions yielded more stable and stronger flocs. Especially under mild mixing conditions, for instance at 250 rpm, ultra-fine colloidal clay particles can be coalesced into a single mass forming a very large floc structure with the help of PEO (Mpofu et al., 2004). Regarding these previous findings and its superiority on the flocculation performance of Kırka clayey suspensions, PEO was preferred over PAM in the scope of this thesis.

PEO used in this study was supplied by ECS Kimya. It is a water-soluble chemical which is in the form of a free-flowing white powder (100% < 1000 μm). The flocculant is actually a nonionic homo-polymer with the repeating unit $[-CH_2-CH_2-O-]_n$. This monomer repetition results in a very long linear polymer chain. Due to the high degree of polymerization, PEO used in this study has a very high molecular weight of 8 000 000 M_W. It is also classified as non-ionic flocculant considering its neutral charge density. The density of the polymer is 1.15 – 1.25 g/cm^3 where as its bulk density is 0.15 – 0.35 g/cm^3.

To prepare feed solution for flocculation experiments, 0.5 g PEO in solid form was added into 999.5 g distilled water and they were mixed in 1000 mL beaker with the help of the magnetic stirrer for one-hour. At the end of the one-hour mixing period, the polymer had been completely dissolved by forming very clear 0.05% (w/w) feed solution. The original pH of this feed polymer solution was measured around neutral pH value of 7. During the preliminary flocculation tests, it was observed that the feed solution performances significantly decreased, most probably due to the degradation of polymer chains, if it was used after 24-hour aging period. Considering this problem, each flocculant solution was prepared freshly on a daily basis.

Figure 20. PEO in free-flowing powder form

3.3. Flocculation Procedure

3.3.1. Jar Test Apparatus

The basic apparatus generally preferred for assessing flocculation performance is the jar test apparatus. It consists essentially of a rack of stirrers driven by one motor. RPM values of the stirrers that are connected to the motor can be adjusted between 0 – 300 rpm. To study the effect of the mixing intensity on the flocculation performance, the suspensions were conditioned at 10 rpm, 100 rpm and 200 rpm. In general, the beakers with a capacity of 600 – 1000 ml are arranged in jar test apparatus. In the scope of this thesis, 800 ml - standard beakers were used for flocculation tests. The jar test has six stations for these standard beakers (Figure 21). With the help of this property, different dosage treatments can be applied at the same time. The aimed polymer dosages added to the beakers at the outermost point from the vortex center at a rate of 1 ml PEO solution per second. The polymer-injected suspensions were mixed by adjusting automatic timing unit to 120 s at a pre-defined stirrer speed.

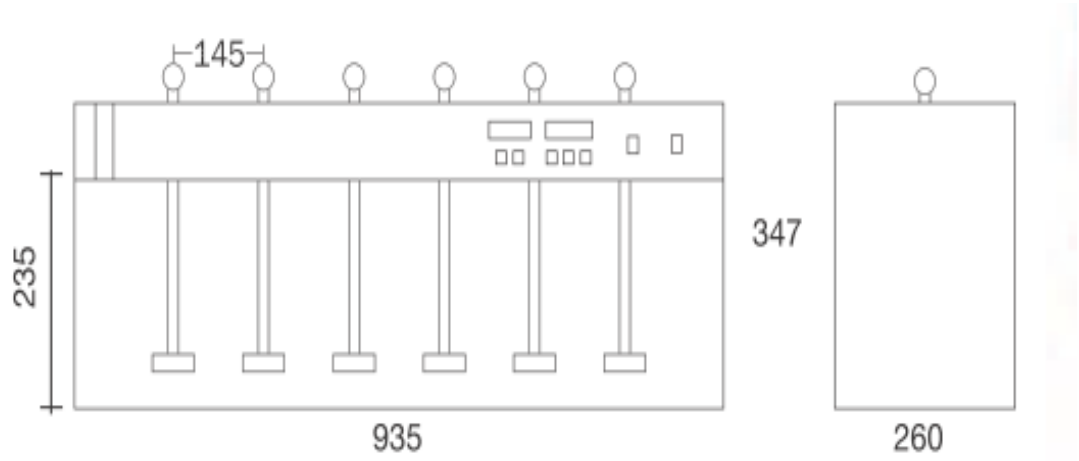

Figure 21. Jar test apparatus – dimensions in mm.

The most effective way in which appreciable contact between particles can be achieved is to induce shear motion with the help of a jar test apparatus. In this case, particles interact with each other and also polymer molecules by movement with the surrounding liquid environment. The process of floc aggregation by inducing such velocity gradient is termed orthokinetic flocculation. For orthokinetic flocculation studies in literature, the term velocity gradient is preferred instead of rpm values of rotating impellers to represent mixing conditions. However, calculation of velocity gradient is a complicated subject due to its obscurity in turbulent regimes. Due to this reason, the researchers renovated the velocity gradient term by a measurable average value, root mean square velocity gradient – G (Camp, 1946, 1955, 1969) as follows:

$$G = \sqrt{\frac{W}{\mu}} \quad s^{-1}$$

where

μ = absolute viscosity – Ns/m^2 and

W = dissipation function – N/m^2s.

In most of the studies, frequently used velocity gradient term actually refers to this root mean square velocity gradient with the symbol of G. In a similar way, G value was found considering the size and shape of standard beakers and mixing impellers of the jar test apparatus with the help of a calculation of dissipation function which is given by (Leentvaar & Ywema, 1980):

$$W = \frac{\emptyset \cdot \rho \cdot n^3 \cdot D^5}{V}$$

where

$\emptyset$ = dimensionless power number

ρ = liquid density – kg/m^3

n = mixer rotational speed - rpm

D = diameter of mixer impeller – m

V = volume of suspension in tank – m^3

The resultant G values used in this study are shown in Figure 22 together with the dissipation function.

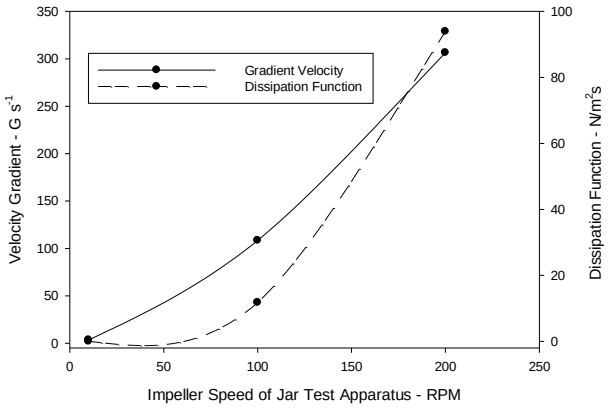

Figure 22. Velocity gradient and RPM relation for the standard jar test apparatus

In addition to the polymer dosing, another parameter was studied. The original pH of the suspensions was increased from 9.3 – 9.4 to 11.5. The pH adjustment was done

with the help of 1 M NaOH addition prior to the polymer dosing. When pH of the suspension was fixed to 11.5, the flocculant was syringed and the suspensions were mixed for 120 s as mentioned previously.

Temperature of the suspensions was studied for any possible favorable or adverse effect on the PEO-induced flocculation. The flocculation of the standard green and white sample suspensions was carried out at room temperature. For this set of experiments, the temperature of the suspensions was increased from 25 °C to 75 °C with the help of a hot plate of magnetic stirrers. When the temperature of the suspension was fixed at 75 °C, the required amount of PEO was added and the polymer-treated system was mixed for 120 s.

Aluminum, iron, copper, calcium and manganese coagulants were also tested as flocculant aids. The pre-defined amounts of coagulants were syringed into the suspension and mixed for 10 min. conditioning time. At the end of this 10 min. period, the polymer solution was dosed into the conditioned system. Then, the mixing procedure was continued for 120 s.

Dual-flocculant effect on the suspensions was also tested as a parameter. Cationic polyacrylamide (PAM: Low charge density, 10% and high molecular weight, 6 000 000 MW) was firstly injected into the suspensions and this PAM preconditioned systems was mixed for 120 s. Following this, non-ionic high molecular weight PEO was injected and mixed for another 120 s.

Ballasted flocculation was also experimented on the green and the white sample suspensions. However, clinker was used as ballast material instead of the conventional micro-sand ballast. The chemical and mineralogical content of this unconventional ballast material was given in Table 4. 10 g of clinker material (100% < 75 μm) was added for per liter of the green and the white sample suspension. These ballasted suspensions were mixed for 10 min for obtaining homogenously distributed clinker particles throughout the colloidal suspension. The mixing was an

important part of the ballasting because clinker particles had a strong tendency for rapid sedimentation. To prevent this sedimentation, the clinker ballasted colloidal systems should be mixed completely prior to the PEO treatment for the purpose of efficient hetero-flocculation. Once the polymer was injected, the mixing was continued for additional 120 s.

Table 4. Chemical and mineralogical properties of clinker ballast (100 % < 75µm)

Chemical Content		Mineralogical Content	
Ca	45.99 %	C3S - Tricalcium silicate	69.91 %
Si	8.96 %	C2S – Dicalcium silicate	2.29 %
Fe	2.54 %	C3A – Tricalcium aluminate	8.59 %
Al	2.94 %	C4AF – Tetracalcium aluminoferrite	11.84 %
Mg	1.42 %		

3.3.2. Turbidity Measurements:

At the end of the standard mixing perdiod of 120 s following the polymer addition, the stirrers were switched off and the suspensions were rested for 20 minutes. After 20 minutes of settling period, the samples were drawn at a fix depth of 20 mm from the top level of the suspensions. These samples which had volume of 20 ml were collected from each beaker with the help of a graduated pipette. Then, the samples were analyzed with infrared light source of Aqualytic AL450T-IR Turbidimeter (Figure 23) to assess the flocculation performance. Each sample placed in the clean sample vial was measured 45 times and the average value of these measurements was shown on the instrument digital display. The turbidity values of the supernatants

were expressed in terms of the nephelometric turbidity unit – NTU with a sensitivity of 0.01 NTU. The turbidimeter calibration was carried out weekly with the standard solutions of 0.1 NTU, 20 NTU, 200 NTU and 800 NTU to obtain reliable results.

Figure 23. Aqualytic AL450T-IR Turbidimeter

3.4. Aqueous Chemistry Calculation with PHREEQC

To gain generalized/conceptual information about the aqueous chemistry of the suspension of the green and the white samples in borax solution, PHREEQC version 2.18 was used to calculate required data. PHREEQC is an open-source computer program written in C/C++ languages and developed by U.S. Geological Survey Department. The purpose of the program is to perform wide variety of practical aqueous geochemical/chemical calculations in governmental and academic studies. The most useful module of the program for this study is based on equilibrium chemistry of aqueous solutions interacting with solid mineral phases. The mineral phase's database is very comprehensive as well as aqueous ions database. More

importantly, all the mineral phases, which were present in the green and the white samples, were covered in the program database in addition to borax mineral. So, the qualitative and quantitative mineralogical information obtained in X-ray diffraction analysis was entered into the program as input data. The solid mineral phases were dissolved in pure water (Figure 24) in the software environment, and then the aimed speciation and aqueous chemistry calculations were carried out.

```
Pure water
----------------------------Description of solution----------------
-------

                                       pH  =   7.000
                                       pe  =   4.000
                         Activity of water  =   1.000
                        Mass of water (kg)  =  1.000e+000
                       Temperature (deg C)  =  25.000
 Percent error, 100*(Cat-|An|)/(Cat+|An|)  =   0
```

Figure 24. Pure water properties used in the PHREEQC calculations

One gram of the white sample (including 0.76 g of dolomite and 0.24 g tri-octahedral Mg-clay) and one gram of the green sample (including 0.457 g of dolomite, 0.315 g of tri-octahedral Mg-clay, 0.193 g of K-feldspar and 0.035 g of illite) was dissolved individually in 1 L pure water (Figure 24) together with 1 g of readily soluble borax in PHREEQC software. For the chemical equilibration, "llnl.dat" database file was used and the required solid phases were equilibrated with solutions according to the reactions shown in Table 5.

Table 5. Dissolution reactions

Dolomite-(Ordered/ideal)$_{Solid}$ +2.00 H^+ ⇌ 1.00 Ca^{++} + 1.00 Mg^{++} + 2.00 HCO_3^-
Trioctahedral Mg-Clay$_{Solid}$ + 7.32 H^+ ⇌ 0.33 Al^{+++} + 3.16 Mg^{++} + 3.67 SiO_2 + 4.66 H_2O
Illite$_{Solid}$ + 8.0000 H^+ ⇌ 0.25 Mg^{++} + 0.60 K^+ + 2.30 Al^{+++} + 3.50 SiO_2 + 5.00 H_2O
K-Feldspar$_{Solid}$ + 4.00 H^+ ⇌ 1.00 Al^{+++} + 1.00 K^+ + 2.00 H_2O + 3.00 SiO_2
Borax$_{Solid}$ +2.00 H^+ ⇒ 2.00 Na^+ + 4.00 $B(OH)_3$ + 5.00 H_2O

The low solid concentration was introduced into the PHREEQC calculation instead of the actual solid concentration studied in flocculation experiments due to several reasons. These reasons were as follows:

1-) The quantities of substances are represented as activities (a_i) for the mass-action law but not concentrations (c_i).

$$a_i = f_i \cdot c_i$$

The activity coefficient – f_i is an ion-specific correction factor defining how interactions among charged ions influence each other. Since the activity coefficient is a non-linear function of ionic strength, there is also a non-linear relationship between the activity and the concentration (Merkel & Planer-Friedrich, 2005). The activity decreases with increasing ionic strength and is always lower than the concentration due to the ions interaction in a solution. The interaction between the ions in solution approaches to zero in an infinitely dilute solution and the activity coefficient becomes 1. In this ideal case, the activities equal the concentration. Due to this reason, the interpretation of the diluted system becomes easier than highly concentrated systems.

2-) The ionic strength is also important for the mass-action law. It equals one-half the sum of the product of the moles of the species involved, m_i and their charge numbers z_i.

$$I = 0.5 \cdot \sum m_i \cdot z_i^2$$

With the help of this ionic strength calculation, the activity coefficients can be obtained. Several different equations are available for this type of calculation. Although all of them are based on the Debye-Hückel equation, they differ in the applicable upper limit of the ionic strength. The equations and the related ionic strength limits are as follows:

DEBYE-HÜCKEL equation (Debye & Hückel 1923)

$$\log(f_i) = -A \cdot z_i^2 \cdot \sqrt{I} \qquad I < 0.005 \text{ mol/kg}$$

extended DEBYE-HÜCKEL equation

$$\log(f_i) = \frac{-A \cdot z_i^2 \cdot \sqrt{I}}{1 + B \cdot a_i \cdot \sqrt{I}} \qquad I < 0.1 \text{ mol/kg}$$

GÜNTELBERG equation (Güntelberg 1926)

$$\log(f_i) = -0.5 z_i^2 \frac{\sqrt{I}}{1 + 1.4\sqrt{I}} \qquad I < 0.1 \text{ mol/kg}$$

DAVIES equation (Davies 1962, 1938)

$$\log(f_i) = -A \cdot z_i^2 \left(\frac{\sqrt{I}}{1 + \sqrt{I}} - 0.3 \cdot I\right) \qquad I < 0.5 \text{ mol/kg}$$

In conclusion, such calculations are very successful at defined ionic strength limits and depending on that, mass-action computations are reliable within these ranges. Especially in salty waters, the upper limits of these equations are exceeded. Considering the flocculation tests carried out in this study, these limits were also exceeded due to the presence of dissolved borax. So, the aquatic chemistry calculations were simplified in the form of a low concentrate system (1000 ppm

borax solution) to produce reliable, interpretable results instead of the actual concentration as in the flocculation test.

3-) Solid concentration of the white and the green sample in PHREEQC calculations was similarly simplified into the diluted system (1 g/L of solid concentration). Due to the prevention of exceeding the ionic strength limit, solid concentration was kept at such a low value. In addition to that, the main reason of the dilution in the PHREEQC calculations was to eliminate surface reactions and to focus on the dissolved species, especially aqua-complexes of calcium. The surface reactions were mainly a function of surface area and active sites density (which is also a function of the area) of the mineral phases in the green and the white sample. However, it was a real challenge to find out actual surface area of the phases. High amount of dolomite lead to carbonate cementation due to the nature of the sedimented samples, and fluctuate the results of the measurements and decreased the total surface area by agglomerating particle mixtures. Furthermore, the carbonate cementation makes differentiation of the individual surface area of the mineral phase impossible. In conclusion, any acceptable data could not be obtained to assign surface reactions to related mineral phase. So, the surface reactions were tried to be minimized/eliminated by diluting the system, and the required interpretation was carried out on the dissolved aquatic species.

4-) The presence of trioctahedral clay both in the green sample and in the white sample complicates the aquatic chemistry calculations owing to the different characteristics of basal-edge surface reactions and also unique interlayer space behavior. This was a well-known challenge for computer-based calculations due to the complex nature of these minerals, especially in the case of additional different mineral phases' presence. The interlayer complexity was observed considering the swelling property of these clay minerals and this was proved (Çırak, 2010) that the crystal size of these minerals in the green and the white samples increased due to the intercalation of excessive amount of dissolved aqua-complexes. To quantify this specific reaction, which leads to swelling, is much harder than the quantification of

basal surface reaction of the clays. Wersin (2003) concluded his studies on this specific subject that significant uncertainties were associated with the results of the chemical calculations because of the effects of swelling and physico-chemical properties of the clays. So, the surface reactions and interlayer reactions related to such clay minerals were ignored due to the thermodynamic inconsistency and scarcity (Gaucher et al., 2004), especially in concentrated and/or saline solutions (Wersin et al., 2004; Lucia, et al., 2012). For this reason, PHREEQC calculations with low solid concentration helped to delimitate the effect of these complexities down to negligible levels in this study.

In conclusion, the dilution improved the reliability and interpretability of the calculation to gain generalized/conceptual information about the aqueous chemistry of the suspension of the green and the white samples in borax solution.

3.5. Viscosity Measurements

3.5.1. Viscosity Measurements of the Polymer Solution

Brookfield RVDV-II+Pro type viscometer (Figure 25-a) was used for the viscosity measurements of 0.05% PEO solution. The readily prepared 0.05% PEO solution was placed in a low form standard Griffin beaker with a capacity of 600 ml. For this part of the study, the standard HB2 series disc spindle (Figure 25-b) was attached to the equipment coupling and inserted into the polymer solution up to the notch on the shaft. The Brookfield Engineering Labs Inc. also suggested this type of spindles for accurate, reproducible viscosity determination for general purpose fluid measurements. Unfortunately, the velocity gradient determination is a mathematically-challenging subject due to the non-uniformity around the flat disk (Steffe & Daubert, 2006). So, a mixer viscometry approach suggested for non-Newtonian fluid properties (Mitschka , 1982) was used. First part of this approach is to find out the flow behavior index (n) which is unique for the studied material.

$$M = (\text{constant}) \times N^n$$

N represents the revolutions per minute (rpm) of the spindle. This value can be directly adjusted by the operator so it was suggested instead of the velocity gradient (Steffe & Daubert, 2006). Similarly, percent torque can be obtained from the instrument and substituted for M in the above equations with no loss of accuracy in finding the flow behavior index. *N and M* values obtained from the instrument were plotted on a graph. Then, regression equations were produced in the form of linear line; y = constant + ax. The slope of this line gave the flow behavior index (n) of the polymer solution. Then, shear rate conversion factor k_γ was calculated with the help of the known flow behavior index (n).

$$k_\gamma = 0.263 \times \left(\frac{1}{n}\right)^{0.771}$$

Then, the spindle speed in rpm was converted to the velocity gradient – G, as follows:

$$G = k_\gamma \times (N)$$

In conclusion, the flow behavior index (n) was used to show the non-Newtonian character of the polymer solution. In addition, the viscosity measurements were interpreted to define the rheological properties of the polymer solution as a function of the spindle speed and temperature.

3.5.2. Viscosity Measurements of the Floc Sediments

Viscous floc sediment is also demanded in tailing management in addition to high turbidity removal. To evaluate such a structural property of the floc, best way is to carry out viscosity measurements. In this study, six sets of flocculation experiment were carried out for each sample under given parameters in Table 6, and then the

sedimented flocs obtained after simple decantation process were subjected to viscosity measurement for the purpose of comparing the floc structures.

Table 6. Different floc sediments used in the viscosity measurements

	Flocculation of the Green Sample Suspension						Flocculation of the White Sample Suspension					
Parameters	**Test1**	**Test2**	**Test3**	**Test4**	**Test5**	**Test6**	**Test7**	**Test8**	**Test9**	**Test10**	**Test11**	**Test12**
PEO dosage	**666 g/ton**	**666 g/ton**	**666 g/ton**	**666 g/ton**	**666 g/ton**	**666 g/ton**	**666 g/ton**	**666 g/ton**	**666 g/ton**	**666 g/ton**	**666 g/ton**	**666 g/ton**
Mixing Intensity	**3 s^{-1}**	**306 s^{-1}**	**306 s^{-1}**	**306 s^{-1}**	**306 s^{-1}**	**306 s^{-1}**	**3 s^{-1}**	**306 s^{-1}**	**306 s^{-1}**	**306 s^{-1}**	**306 s^{-1}**	**306 s^{-1}**
$CaCl_2$ (mg/l)	**0 mg/l**	**500 mg/l**	**0 mg/l**	**0 mg/l**	**0 mg/l**	**0 mg/l**	**0 mg/l**	**500 mg/l**	**0 mg/l**	**0 mg/l**	**0 mg/l**	**0 mg/l**
$MnSO_4$ (mg/l)	**0 mg/l**	**0 mg/l**	**500 mg/l**	**0 mg/l**	**0 mg/l**	**0 mg/l**	**0 mg/l**	**0 mg/l**	**500 mg/l**	**0 mg/l**	**0 mg/l**	**0 mg/l**
pH	**9.4**	**9.4**	**9.4**	**11.5**	**9.4**	**9.4**	**9.4**	**9.4**	**9.4**	**11.5**	**9.4**	**9.4**
Clinker Ballast	**0 g/l**	**0 g/l**	**0 g/l**	**0 g/l**	**10 g/l**	**0 g/l**	**0 g/l**	**0 g/l**	**0 g/l**	**0 g/l**	**10 g/l**	**0 g/l**
Cationic PAM dosage	**0 g/t**	**0 g/t**	**0 g/t**	**0 g/t**	**0 g/t**	**167 g/t**	**0 g/t**	**0 g/t**	**0 g/t**	**0 g/t**	**0 g/t**	**167 g/t**
Obtained floc sediment	**Floc-1**	**Floc-2**	**Floc-3**	**Floc-4**	**Floc-5**	**Floc-6**	**Floc-7**	**Floc-8**	**Floc-9**	**Floc-10**	**Floc-11**	**Floc-12**

The viscosity measurements on the floc samples as a result of flocculation studies are given in Table 6, immediately carried out to prevent time-dependent behavioral

changes. Brookfield RVDV-II+Pro Model rotating type viscometer (Figure 25-a) was used for these experimental studies. The SC4-27 type spindle (Figure 25-c) supported by Brookfield was attached to the RVDV-II+Pro viscometer. The diameter of the standard spindle is 11.76 mm and the length of this spindle is 33.02 mm. According to this spindle type, SC4 Series disposable small sample chamber was selected for the measurements. The diameter and the depth of the disposable sample chamber are 19.05 mm and 64.77 mm, respectively. Sedimented flocs were immediately placed in this chamber and measurements were carried out with this test apparatus arrangement.

In viscosity measurements, there are various ways to obtain information on the behavioral change of flocs, like single point viscosity test, controlled rate ramp test, up-down rate ramp test etc. In this part of the study, up-down rate ramp method was used. The reason of this selection was to analyze time sensitivity and shear sensitivity of the floc structures. In this method, the RPM value of the spindle was increased after every 15 second (10 rpm, 100 rpm and 200 rpm → 15^{th}s, 30^{th}s and 45^{th}s, respectively). This increasing tendency both in shear rate and time represented up-ramp region of the measurement. Upon reaching the maximum rpm value, the direction was reversed and the rpm value was returned back to the starting speed (200 rpm, 100 rpm and 10 rpm → 45^{th}s, 60^{th}s and 75^{th}s, respectively). This decreasing experimental condition created down-ramp region of the measurement. Each reading at a given time was measured in terms of centipoise. The obtained centipoise values were plotted against the spindle rpm at each 15s. The spindle rpm can be also converted to shear rate with the help of a simple formula which is given by the equipment producer as follows:

Shear rate of the SC4-27 spindle = Shear rate constant (SRC: 0.34) x rpm

Non-flowing or slow-flowing samples such as flocs and pastes, creates special problems in viscosity measurements. The rotation of the spindle tend to channel these materials by pushing the material aside of the disposable sample chamber. This channeling phenomenon results in decreasing viscometer reading and misleading the

related interpretations. To overcome this challenge, the time intervals between viscosity measurements were limited to 15s.

a. Brookfield RVDV-II+Pro Visc.

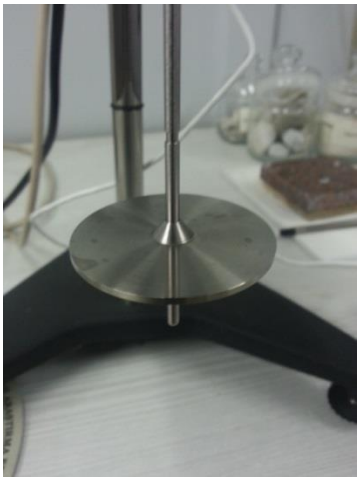

b. HB2 Series Spindle

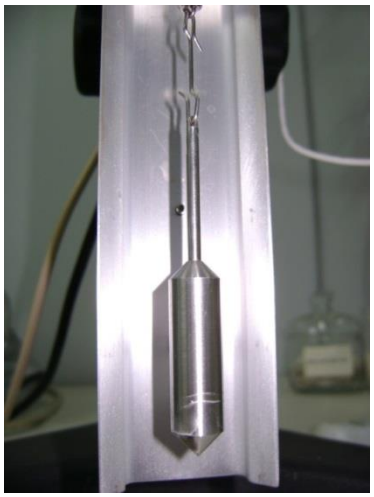

c. SC4 Series Spindle

Figure 25. Brookfield Viscometer

3.6. Optimization of Certain Parameters with Response Surface Methodology – RSM

A simple way of optimization is usually performed by varying a single parameter while keeping others fixed at specific values. However, this simple method is actually incapable of reaching the actual optimum. The main reason behind this fact is ignoring the interactions among the parameters. On the other hand, the response surface methodology offers the interactive influences of parameters in addition to the individual influences (Ghafari et al., 2009). So, more extensive and realistic information can be obtained with the help of response surface methodology. Considering this advantageous effect, the response surface methodology was used in this study as a statistical technique. The applied procedure of the response surface methodology was as follows:

1-) Designing of a series of flocculation experiments for sufficient and practical measurement of the response in terms of nephelometric turbidity unit (NTU) of supernatant.
2-) Developing a representative mathematical/statistical model for the response surface of collected flocculation data set.
3-) Determining the optimum experimental conditions for the improved flocculation performance.
4-) Representing the direct and interactive effects of flocculation parameters graphically through three dimensional plots.

In a general, the resultant response surfaces in this procedure can be expressed with,

$$y = f(x_1, x_2, x_3, \ldots, x_k)$$

Y and X_i represents the response of the data set and the related parameters. In this study, the response was turbidity of supernatant and the variables were (most utilizable/beneficial ones) the dosage of PEO, the velocity gradient of mixing intensity, and the amount of coagulant preconditioning in the form of calcium

chloride. To main purpose of this statistical study was to optimize supernatant turbidity (*Y*) against the experimental variables (X_i). To reach this goal, it was required to find a convenient mathematical approximation for the accurate relationship correlating the variation in response (*Y*) to the variables (X_i). As a general rule, a second-order model was implemented in the response surface methodology as follows:

$$y = \beta_0 + \sum_{i=1}^{k} \beta_i x_i + \sum_{i=1}^{k} \beta_{ii} x_i^2 + \sum_{i=1}^{k-1} \sum_{j=2}^{k} \beta_{ij} x_i x_j + \varepsilon$$

$x_1, x_2, \ldots, x_k$ are the input factors which influence the response (*Y*); β_0, β_{ii} (i = 1,2,. . .,k), β_{ij} (i = 1,2, . . .,k;j = 1,2,. . .,k) are unknown parameters and ε is a random error. The β coefficients were determined in the second order model with the help of least square method. In this study, Box-Behnken experimental design was preferred to define relationship between the response and the variables. Because, the Box-Bhenken Design had advantages over the Central Composite Designs. The first advantage was that three levels for the experimental factors were sufficient and this made data collecting easier and less laborious. Second advantage was that Box-Behnken required less total runs than the Central Composite Design. For example, the three-factor central composite design needs 20 runs whereas the three-factor Box-Behnken needs only 15 runs (Lawson, 2010). Moreover, there is a distinguishing geometrical difference between Box-Behnken and Central Composite Design and this difference can be easily perceptible with the cubic view representation of the designs. In the Box-Behnken design, the treatment combinations were at the midpoints of the cubic representations (Figure 26), on the other hand they were placed at the corners of the cubic representations in the Central Composite Design. It can be claimed that Box-Behnken design may produce more realistic results at the mid-region rather than the corners due to the data concentration locale. The corners represented the boundaries which could be named as extreme flocculation conditions in the scope of this study and these extremes at the corner points had secondary

importance. However, the points in the mid-region had primary importance because the optimum flocculation parameters were anticipated to fall into this region instead of the near extreme corner points. In conclusion, the Box-Behnken design was preferred due to the ease in data collection and success in the mid-region of a cubic representation. The required experimental procedure and optimization study for the flocculation of the green and the white sample suspensions in the presence of borax were carried out via the statistical package program, STATGRAPHICS considering the randomized Box-Behnken design in Table 7. The findings were explained on the spreadsheet and graphics.

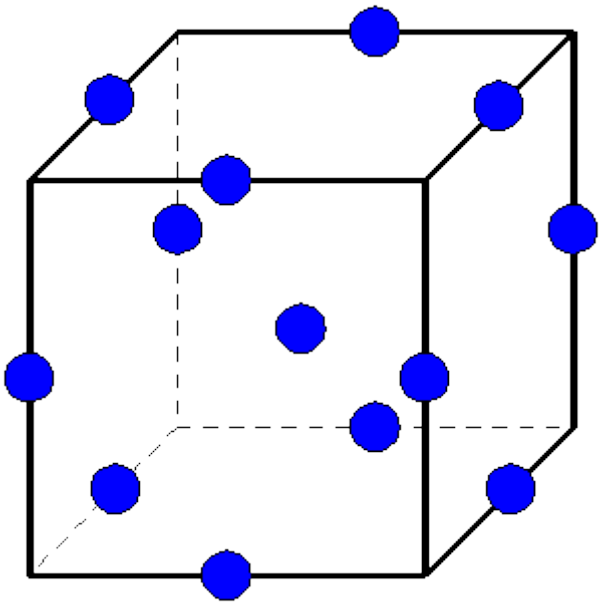

Figure 26. Generalized cubic view of Box-Behnken design

Table 7. Box-Behnken design for the flocculation studies

The Green Sample Flocculation Design				The White Sample Flocculation Design			
Block	PEO Dosage	Calcium Chloride	Velocity Gradient	Block	PEO Dosage	Calcium Chloride	Velocity Gradient
1	0	1	1	1	0	0	0
1	1	0	-1	1	0	-1	1
1	-1	0	-1	1	-1	1	0
1	0	-1	1	1	1	0	-1
1	0	1	-1	1	0	-1	-1
1	0	-1	-1	1	0	0	0
1	-1	1	0	1	0	1	1
1	0	0	0	1	0	0	0
1	0	0	0	1	1	0	1
1	-1	-1	0	1	1	1	0
1	1	0	1	1	0	1	-1
1	-1	0	1	1	-1	0	1
1	1	1	0	1	-1	0	-1
1	0	0	0	1	1	-1	0
1	1	-1	0	1	-1	-1	0

CHAPTER 4

RESULTS AND DISCUSSION

4.1. Characterization Studies

4.1.1. Chemical and Mineralogical Analysis

The results of the chemical analysis both for the white sample and the green sample were presented in Table 8. Considering the loss on ignition values in Table 8, the white sample had a greater volatile content (35.03%) than the green sample (17.85%). These volatile contents were associated with carbonate phase and it was proved with X-ray diffraction analysis. The percentage of SiO_2 of the green sample (26.60%) was greater than the white sample (15.94%) which may indicate silicate rich phase(s) in the green sample. This was also proved later with the help of the mineralogical analysis. When the results of chemical analysis were interpreted, it may be claimed that the green sample was a silicate rich material whereas the white sample was a carbonate rich material. However, exact mineralogical identification was carried out with X-ray diffraction method.

Table 8. Chemical constituents of the white and the green samples used in the flocculation studies

Constituent (Based on weight percentages)	The White Sample %	The Green Sample %
SiO_2	15.94	26.60
Al_2O_3	0.49	4.96
Fe_2O_3	0.22	1.89
MgO	21.36	15.02
CaO	28.57	16.16
Na_2O	0.98	1.60
K_2O	0.29	3.69
*B_2O_3	*0.17	*0.62
LOI	35.03	17.85

*All constituents were analyzed with XRF except B_2O_3, which was determined with the conventional titrimetric (volumetric) chemical analysis.

Mineralogical analyses were carried out for both the white and the green sample following the chemical analyses. The phases in the each sample were identified qualitatively and quantitatively with the help of the X-ray diffraction method. The X-ray patterns were assessed with the software (MAUD – Material Analysis Using Diffraction). These patterns studied on the software screen can be seen in Figure 27 and Figure 28.

In the X-ray diffraction pattern of the green sample (Figure 27), the highest intensity peaks referred to the d-spacings values of 3.69Å, 2.88Å, 2.66Å, 2.40Å, 2.19Å, 2.06Å, 1.84Å, 1.80 Å, 1.78 Å, indicating the presence of a perfect dolomite crystal; in other words, ideal dolomite mineral with ordered chemical structure. Similarly, the sharp peaks in the X-ray diffraction pattern of the white sample (Figure 28) with d-spacings of 3.69 Å, 2.88 Å, 2.67 Å, 2.40 Å, 2.19 Å, 2.01 Å, 1.81 Å and 1.79 Å indicated the same ideal dolomite phase. These ideal dolomite phases in both the green and the white sample had the highest intensity peaks, which were easily interpreted and identified, at d(104) with a d-spacing of 2.88 Å.

The weaker intensity peaks of the green sample's X-ray diffraction pattern at 4.20Å, 3.30Å, 3.28Å, 3.26Å, 3.24Å, 2.99Å, 2.60-2.55Å were easily identified as K-Feldspar (Figure 27). However, the identification of the very broad peak about 12.76Å (7° 2θ) was not as easy as that of the sharp peaks. In the shoulder of the broad peak, a very small peak was also detected at 10.01Å, especially when 2θ values were plotted against logarithmic scale of intensity axis (logarithmic presentation was not shown here) to differentiate between these broad overlapping peaks. As a result of the simple scale based interpretation, the shoulder peak was considered to be the indication of a minor amount of illite presence in the green sample. On the other hand, the peaks belong to K-Feldspar and illite phases of the green sample in Figure 27 were not observed for the white sample's X-ray diffraction pattern in Figure 28.

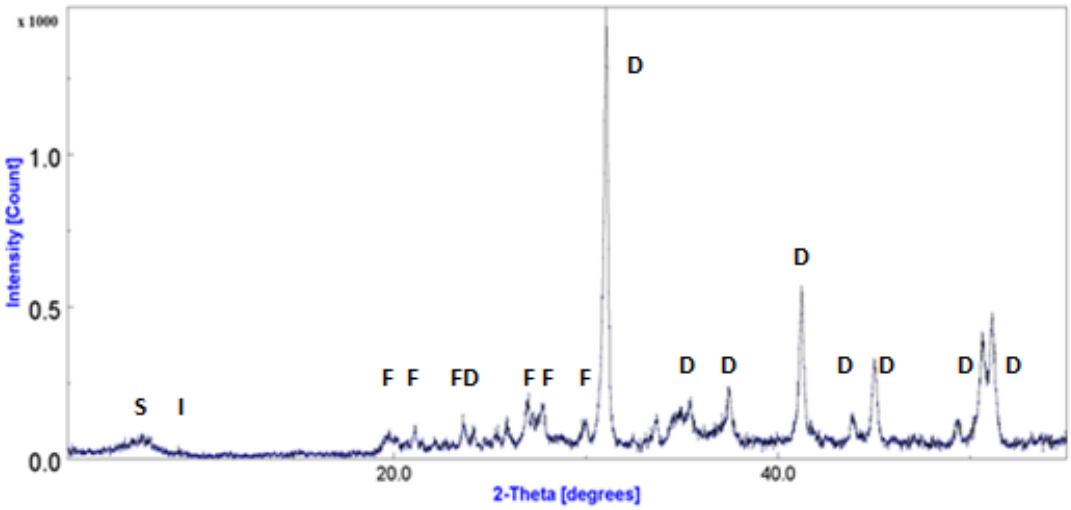

Figure 27. MAUD software's output for the X-ray diffraction pattern of the green sample (S: smectite, I: illite, D: dolomite and F: K-feldspar)

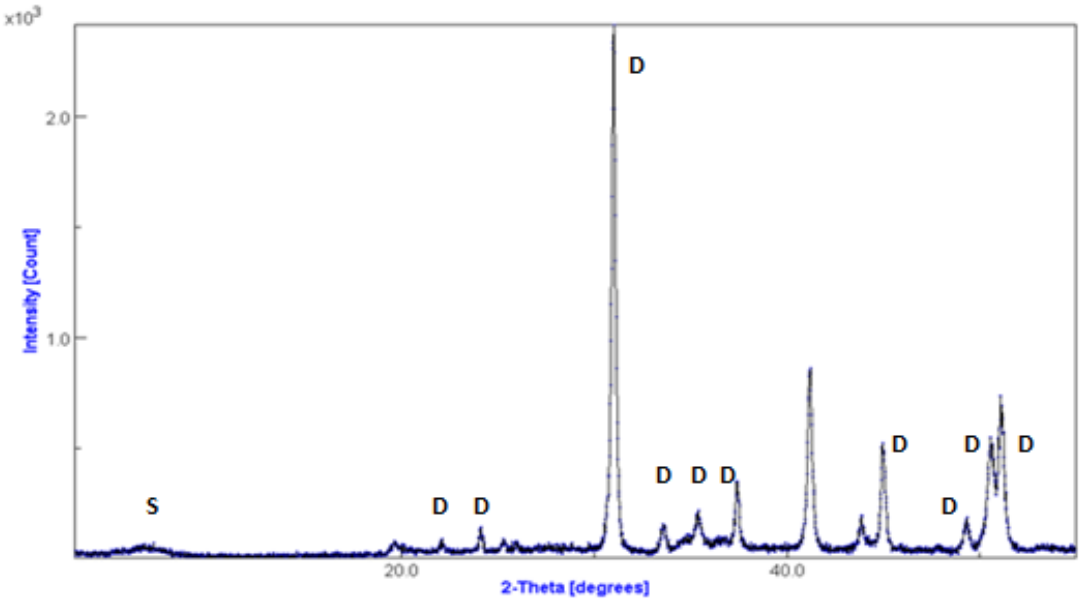

Figure 28. MAUD software's output for the X-ray diffraction pattern of the white sample (S: smectite and D: dolomite)

As mentioned previously, very broad peaks were observed around 6.5-7° 2θ for both samples. These broad peaks in Figure 27 and Figure 28 had d-spacing values of 12.76Å for the green sample and 13.23Å for the white sample. It had been considered that these peaks indicated the presence of clay minerals. To identify such clay peaks was not an easy procedure and it required detailed analysis together with elaborate sample preparation including orientation of clay platelets, carbonate/silicate removal, clay fraction separation, ethylene glycolation and heat treatment at 300°C and 550°C. These detailed analyses of the green and the white samples were carried out in the scope of another study (Çırak, 2010) and they were not repeated in this thesis. However, these clay minerals were previously identified as smectite (Çırak, 2010) because the d-spacing of these broad clay peaks increased up to 17.35 Å for the green sample and 17.47 Å for the white sample after ethylene glycolation procedure revealing the swelling property of the clays in both samples. In addition to these previous findings (Çırak, 2010), the octahedral character of the clay was determined with the additional X-ray diffraction patterns (Figure 29 and Figure 30)

in this study. According to the results of these additional patterns (Figure 29 and Figure 30), *(060)-peaks* of smectites in both of the samples had the same d-spacing at about 1.53Å. This d-spacing value unveiled the octahedral character of the smectite compound of the samples. It meant that three Mg^{2+} ions took places in the octahedral sheet instead of two Al^{3+} cations (Lemons & McAtee, 1983; Moore & Reynolds, 1997). Therefore, all of the three available octahedral sites around each hydroxyl were filled with Mg^{2+}. Based on this inference, smectite clays in both the green and the white sample were identified as Mg-rich trioctahedral clays. This identification was also important in terms of the surface character because this type of octahedral structure formed Mg-surface at the edge of the clay crystal instead of the Al-surface. As a result of the qualitative analyses, it had been shown that two Mg-rich minerals, namely dolomite and trioctahedral smectite, were present in both of the samples. This finding confirmed the low percentages of Al and the high percentages of Mg in the chemical analyses (Table 8). As a summary, the white sample included only dolomite and trioctahedral smectite whereas the green sample included dolomite, trioctahedral smectite, K-feldspar and illite minerals.

Quantitative mineralogical analyses were carried out using Rietveld refinement method with the help of MAUD software following the qualitative analyses. According to these quantitative analyses summarized in Table 9, 45.7 % dolomite and 31.5 % trioctahedral smectite (w/w) were found in the green sample whereas 76.0 % dolomite and 24.0 % trioctahedral smectite (w/w) were found in the white sample. Ultimately, it was ascertained that the green sample had greater amount of silicate material whereas the white sample had greater amount of dolomite (Table 9). This quantitative analysis may also explain the reason of high background noise in Figure 27 than Figure 28. The higher percentages of clay minerals in the green sample gave rise to this higher background noise in the X-ray diffraction pattern due to the amount of randomly orientated clay platelets.

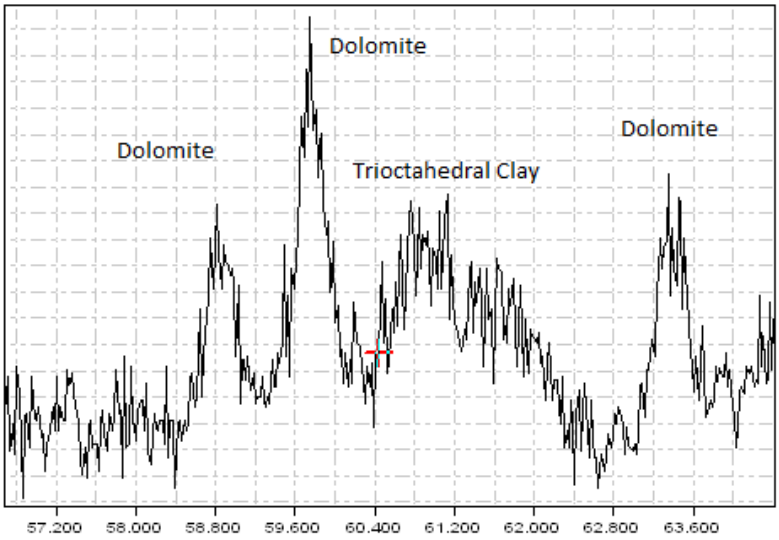

Figure 29. The (*060)*-peak of the smectite in the green sample indicating trioctahedral character

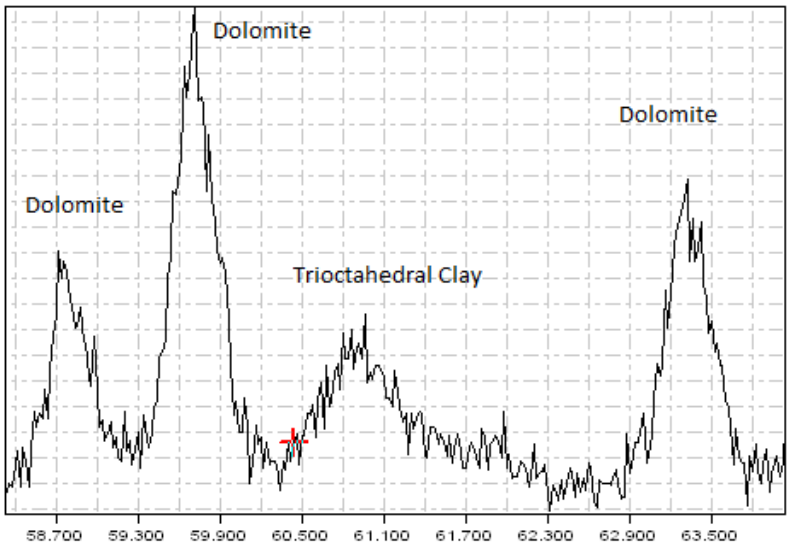

Figure 30. The (*060)*-peak of the smectite in the white sample indicating trioctahedral character

Table 9. The results of quantitative phase analyses via Rietveld refinement method

Mineral Name	Mass Percentages of the Green Sample	Mass Percentage of the White Sample
Dolomite	45.7 %	76.0 %
Trioctahedral Clay	31.5 %	24.0 %
K-Feldspar	19.3 %	-
Illite	3.5 %	-

4.1.2. Particle Size of the Dispersed White and Green Samples Used in the Flocculation Studies

The results of the particle size analysis of the green and the white samples in suspension are presented in Figure 31. The green sample has a slightly finer size distribution than the white sample. d_{80} sizes for the green and the white samples are 5 µm and 7 µm, respectively. However, it should be noted that the particle size analysis in this study relied on light scattering technique which produced volumetric outputs and the clay mineral with swelling capability had variable crystal size and volume. So, the results may be affected from the presence of the swelling type clay mineral which might have produced higher volumetric percentages than the actual upon swelling of the clay particles.

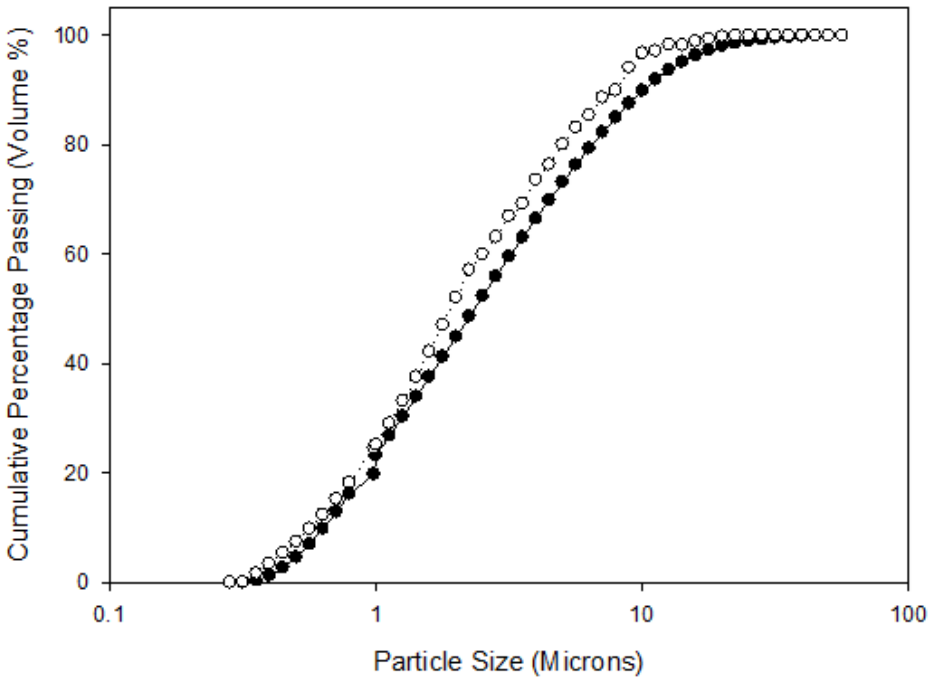

Figure 31. Particle size of the dispersed white and green samples used in the flocculation studies (Black circles: the white sample suspension; White circles: the green sample suspension)

4.1.3. Zeta Potential Measurements

To evaluate zeta potential values consistently, the related standard deviations, and the mobility values were presented together with the conductivities of each measurement. The conductivity was a significant parameter in this part of the study and it affected both zeta potential and the related standard deviation. The similar conductivity curves were obtained as anticipated in Figure 32, Figure 33, Figure 34, Figure 35, and the resemblance between these curves and the standard deviations curves were clear. The conductivities were very close to zero around neutral pH; however, their values increased up to 20 – 25 mS/cm while pH was approaching 2 and 12. The reason of the increase in the conductivity was due to the pH adjustment

with HCl and NaOH as well as soluble mineral phases like carbonate. This increasing tendency in the conductivity resulted in greater standard deviations in zeta potential and mobility measurements around pH 2 and 12 for all cases. As a result, it should be noted that the measurement quality was adversely affected from high conductivity values especially under severe acidic or basic conditions. Considering these high standard deviation findings, the effect of borax presence on zeta potential measurements was not studied because it makes the solutions much more conductive due to its soluble character by increasing standard deviation of the measurements which cause uninterpretable results.

In general, none of the zeta potential values of both the green and the white samples ever reached zero throughout the studied pH range. All of the samples, including freshly dispersed and aged suspensions, had negatively charged mineral surfaces.

Aging effects on zeta potential was also studied and the difference in zeta potential due to the aging can be observed both for the green and the white sample in Figure 32, Figure 33, Figure 34 and Figure 35. These figures clearly showed that the zeta potential curves of freshly prepared dispersions shifted to the lower zeta potential levels for the aged samples. For instance, the zeta potential of the green sample particles at pH 9.40 (borax buffers the solution at pH 9.40 as in the case of all flocculation studies in this study) decreases from -21.2 mV to -18.1 mV upon aging whereas the zeta potential of the white sample particles decreases from -24.3 mV to -13.8 mV at the same pH. This decrease in the negative zeta potential values for both the green and the white samples can be explained with dissolution of the dolomite phase. When dolomite dissolves upon aging, the cations are released into the solution. The cations especially calcium has an affinity for the negatively charged mineral surfaces. This affinity leads to adsorption of cations on the particle surfaces resulting in less negative zeta potential values for both the green and the white sample particles. However, it can be claimed that the extent of decrease in zeta potential to less negative zeta potential values was greater for the white sample particles compared to the green sample particles. Considering the higher amount of

the dolomite phase in the white sample, this should be expected because more cations may be dissolved from dolomite and adsorbed by the particle surfaces. Although this decrease of the zeta potential to less negative values was appreciable, the measured zeta potential for the green and the white samples never reached a positive or neutral value. In summary, 24 – hour aging of the green and white clay dispersions affected the particle surfaces and most probably this led to the variations in the flocculation behavior of these samples.

The flocculation experiments were carried out with the aged suspensions of the green and the white samples. So, their zeta potential measurements were significant for the purpose of interpretation of the flocculation experiments. The zeta potential of these aged suspensions at pH 9.40 were measured as -18.1 mV (std. deviation of 4.2) for particles of the green sample and -13.8 mV (std. deviation of 4.3) for particles of the white sample. These zeta potentials increased to more negative values -33.8 mV (std. deviation of 14.6) for particles of the green sample and -31.1 mV (std. deviation of 13.0) for particles of the white sample when pH increased to about 12 (Figure 33 and Figure 35). When the pH was decreased down to acidic condition around 2, the zeta potential of these aged suspensions were decreased to -10.0 mV (std. deviation of 19.1) for particles of the green sample and -6.8 mV (std. deviation of 19.2) for particles of the white sample. As it can be seen in Figure 33 and Figure 35, the zeta potentials were always in the negative range which indicated strong negative-negative repulsion between particles, especially under alkaline conditions.

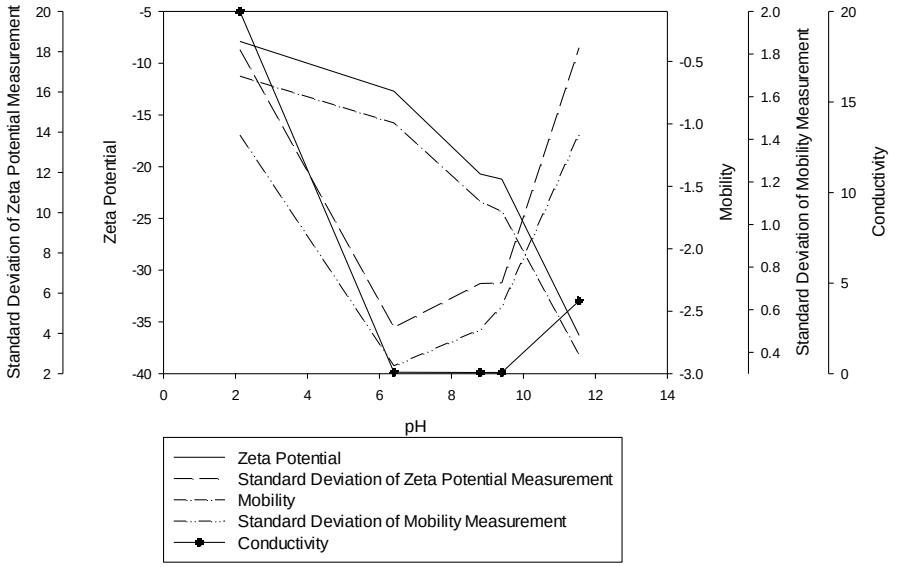

Figure 32. Zeta potential measurements of the freshly dispersed green sample particles

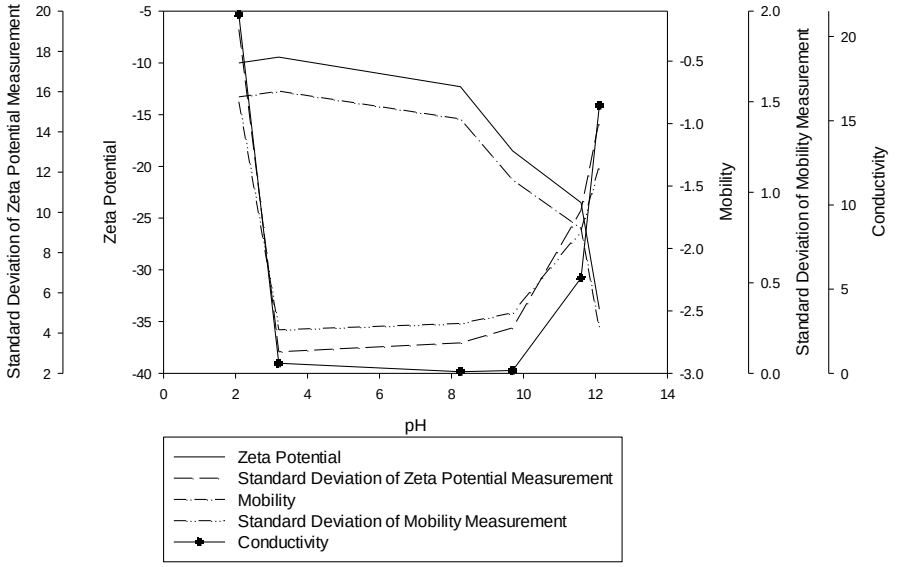

Figure 33. Zeta potential measurements of the green sample particles after 24 hour aging

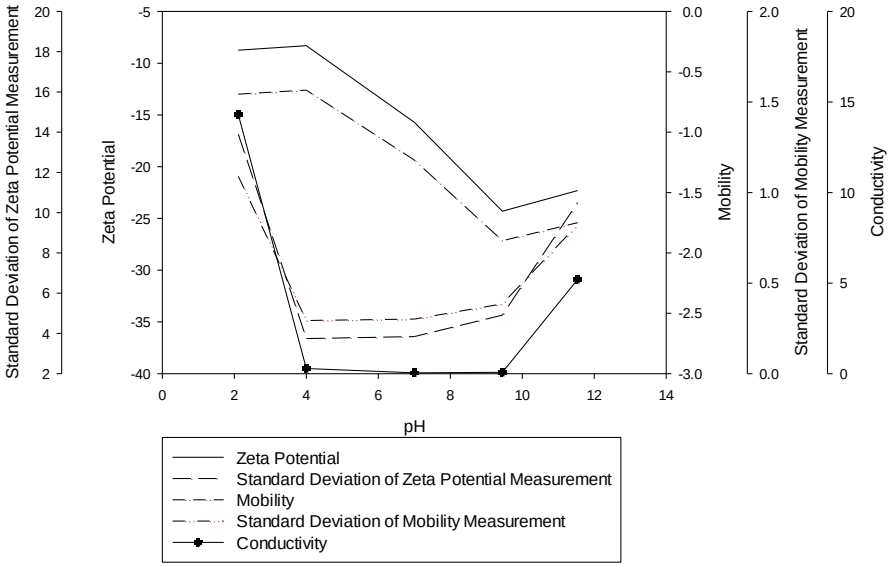

Figure 34. Zeta potential measurements of the freshly dispersed white sample particles

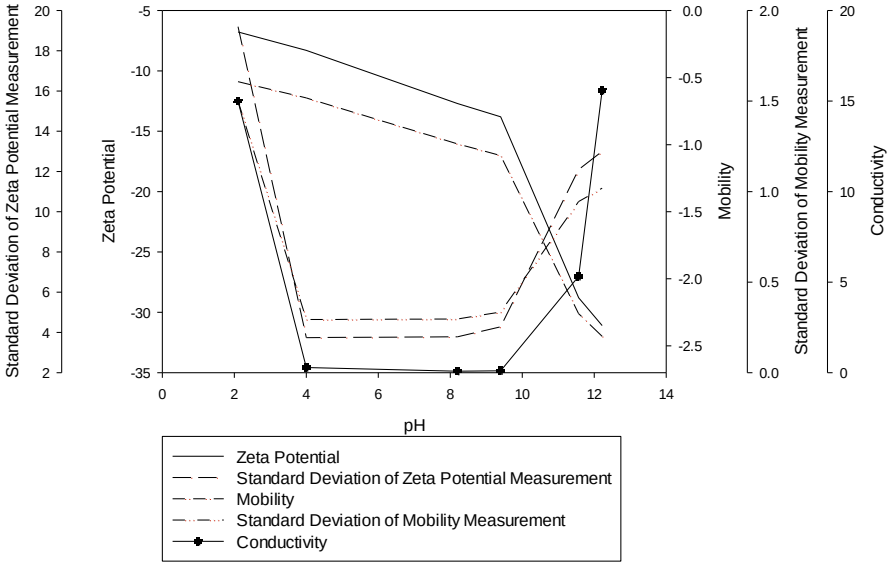

Figure 35. Zeta potential measurements of the white sample particles after 24 hour aging

In addition to the zeta potential analyses of the mechanically agitated samples given above, the green and the white samples were subjected to ultra-sonication prior to the zeta potential measurements, specifically at pH 9.40. The aim was to observe the effect of ultra-sonic waves on the zeta potential values of these natural dolomite-clay mixtures. The results are given in Figure 36 as a function of ultra-sonication time at fix pH. During this period, no significant pH and conductivity changes were observed. The standard deviation of the zeta potential measurements increased from 4 mV to 8 mV with increasing ultra-sonication time. The most interesting trend in Figure 36 was obtained for the zeta potential values of the green and the white samples. At the fifth minutes of the ultra-sonication, the zeta potential values became almost three times more negative (-60.4 mV for the green sample and -48.6 mV for the white sample) than the non-sonicated ones. At the tenth minutes of the ultra-sonication, the zeta potential increased from -60.4 mV to -70.1 mV for the green sample particles and from -48.6 mV to -62.7 mV for the white sample particles. Although many surface characterizations were previously carried out for these samples in the literature, none of them indicated to such high zeta potential values. As a result, the concealed high degree of surface negativity of the natural dolomite-clay mixtures collected from the borax formation was revealed with the help of the ultra-sonication.

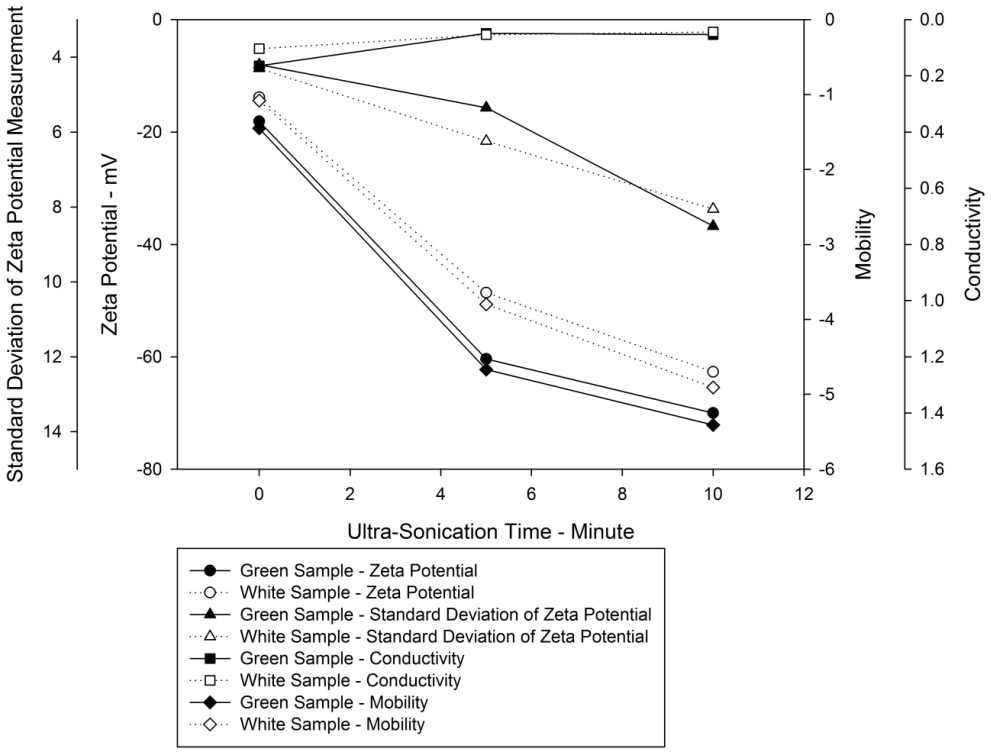

Figure 36. The effect of the ultra-sonication on the zeta potential measurements

4.1.4. Fourier Transform Infrared Spectroscopy

It was proven previously via zeta potential measurements that these particles had negatively charged surfaces throughout the studied pH range. The colloidal character of the samples can be explained with the pronounced negative surface charges which lead to strong particle-particle repulsion. However, zeta potential results could not exactly explain the problem in polymer-particle interactions. For this reason, Fourier transform infrared technique was applied to the green and the white samples to gain a better understanding about this surface-induced problem.

The isolated hydroxyl groups on the mineral surfaces act as free dangling anchor sites for the PEO type flocculants. The ether oxygen of PEO can form strong hydrogen bonding with these hydroxyl groups. So, the presence of the isolated hydroxyls on the particle surfaces is of vital importance for the flocculation process. The infrared study is known as a very useful tool to identify these hydroxyl groups (Pokrovsky et al., 2000; Gunasekaran & Anbalagan, 2007). The infrared intensity peaks around 3600 cm^{-1} and 3700 cm^{-1} indicate the presence of the isolated hydroxyl surfaces on particle surfaces. More specifically, the peaks (Madejova, 2003; Moudgil et al., 1997) at 3621 cm^{-1} and 3679 cm^{-1} refer to the isolated hydroxyl groups of dolomite and trioctahedral clay minerals, respectively. In the previous studies (Moudgil & Behl, 1993), it was shown that if these peaks were available on the infrared pattern, PEO-induced flocculation led to extraordinary turbidity removal performances due to the intense adsorption of the polymer on the particle surfaces. On the other hand, if these peaks of the isolated hydroxyl groups were not visible on the infrared patterns, the polymer adsorption on the particle surface completely failed. In this case, the flocculation performance deteriorated and turbidity removal percentages became zero.

Similar infrared study was carried out for the green and the white samples used in the flocculation studies. The high resolution patterns between 3000 cm^{-1} and 4000 cm^{-1} are given in Figure 37. Previously stated isolated hydroxyl peaks at 3621 cm^{-1} and 3679 cm^{-1} were tried to be determined. Nevertheless, the infrared pattern showed that the isolated hydroxyl region for the samples abnormally suppressed and no definable solid peaks were observed. This means that the samples collected from the Kırka formations had some surface related deficiency. The lack of isolated hydroxyl groups on the samples prevented the hydrogen bonding formation between particle and PEO and it caused insufficient particle-polymer interaction. Most probably, the difficulties in the enrichment of boron and the tailing management originated from this abnormal surface property of dolomite/clay-containing gangue materials. In conclusion, the hydrogen bonding incapability of these gangue mineral surfaces should be taken into consideration for all laboratory scale and industrial scale studies.

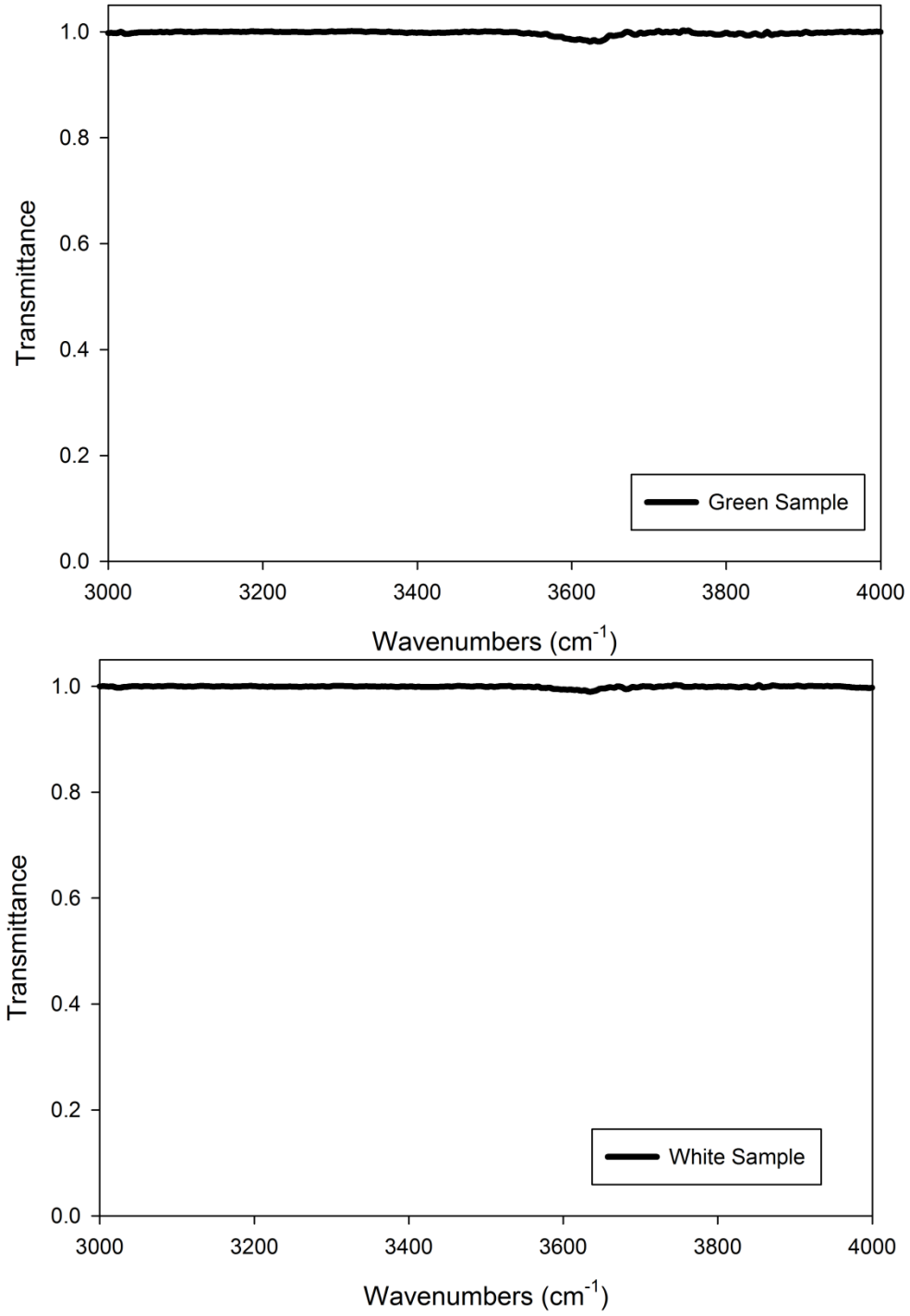

Figure 37. Fourier Transform infrared spectroscopy of the green and the white samples (3000-4000 cm^{-1})

4.2. Flocculation Studies

4.2.1. Flocculation Studies of the Suspensions under Low-Intensity Mixing Conditions

Initial flocculation experiments carried out under low intensity mixing conditions (3 s^{-1}) to compare the flocculation behavior of freshly prepared and aged suspensions. The PEO dosages were tested up to 666 gram per ton of solid. However, the resultant turbidity values were still very high and the expected sharp decrease (Figure 38) due to PEO dosing could not be observed in the turbidity curves of both the green and the white samples in fresh and aged suspensions. It can be deduced that the particles in the green and the white samples had colloidal character with strong particle-particle repulsion and the interaction between these colloidal particles and PEO chains were limited. This ineffective interaction can be stemmed from incapability of the hydrogen bonding between particle and PEO and the insufficient probability of particle-particle and particle-polymer collision in low intensity mixing as suggested in the literature (Laskowski & Ralston, 1992; Tripathy & De, 2006).

The flocculation performance of the green sample suspension improved upon 24 hour aging period of the suspension whereas the flocculation performance of the white sample suspension decreased. For instance, the turbidity of the freshly prepared green sample suspension treated with 333 gram PEO per ton of solid was 4963 NTU. However, in the case of the aged green sample suspension treated with the same polymer dosage, the turbidity decreased down to a lower value of 2873 NTU. As it can be seen in Figure 38, the turbidity curve of the freshly prepared green sample suspension shifted to lower turbidity values when the suspension of the green sample was aged for 24 hour before the flocculation. On the other hand, the flocculation performance of the white sample suspension was adversely affected by aging. For example, the turbidity of the freshly prepared white sample suspension treated with 333 gram PEO per ton of solid was 2569 NTU. When the suspension of

the white sample was aged for 24 hours and treated with the same amount of PEO, a higher turbidity value (4108 NTU) was obtained.

The performance improvement of the green sample suspension upon aging can be understandable. During the aging period, the mineral phases like dolomite may be dissolved and increase the ionic strength of the solution by releasing cations and anions into the solution. The green sample was richer in silicate phases and the silicate surfaces had a great affinity especially for cations. Most probably, higher amount of silicates (Table 9) in the aged green sample suspensions were activated by these cations for more effective particle-polymer interaction and with the help of this property the overall flocculation performance was enhanced. Based on this fact, silicates, especially swelling type clays, are already used as flocculant aids in the dewatering studies to enhance overall flocculation performance (Aygun & Yilmaz , 2010). On the other hand, the adverse effect of aging on the flocculation behavior of the white sample suspension can be explained with the lower amount of silicates and higher amount of dolomite than the green sample suspension. In conclusion, the flocculation behavior difference between the green and the white sample suspensions was related to the differences in silicate and dolomite content (Table 9).

In addition to this time-dependent flocculation behavior, the effect of borax on the flocculation was tested (Figure 38). When the results of flocculation test in the presence (3%) and absence of borax (0%) were compared, the resultant turbidity values significantly differed from each other. As shown in Figure 38, the presence of borax decreased the turbidity to a limited extent; however, the flocculation performances were still poor for both the green and the white sample suspensions. The reason for such a slight improvement was due to high solubility of borax in water. This property led to increase in ionic strength of the solution and the double layer around the colloidal particles was significantly compressed as a function of ionic strength. As a summary, the limited improvement in the flocculation performances were observed in the presence of borax as compared to the absence of

borax, and the greatest turbidity values in this study were observed for those suspensions which did not contain borax.

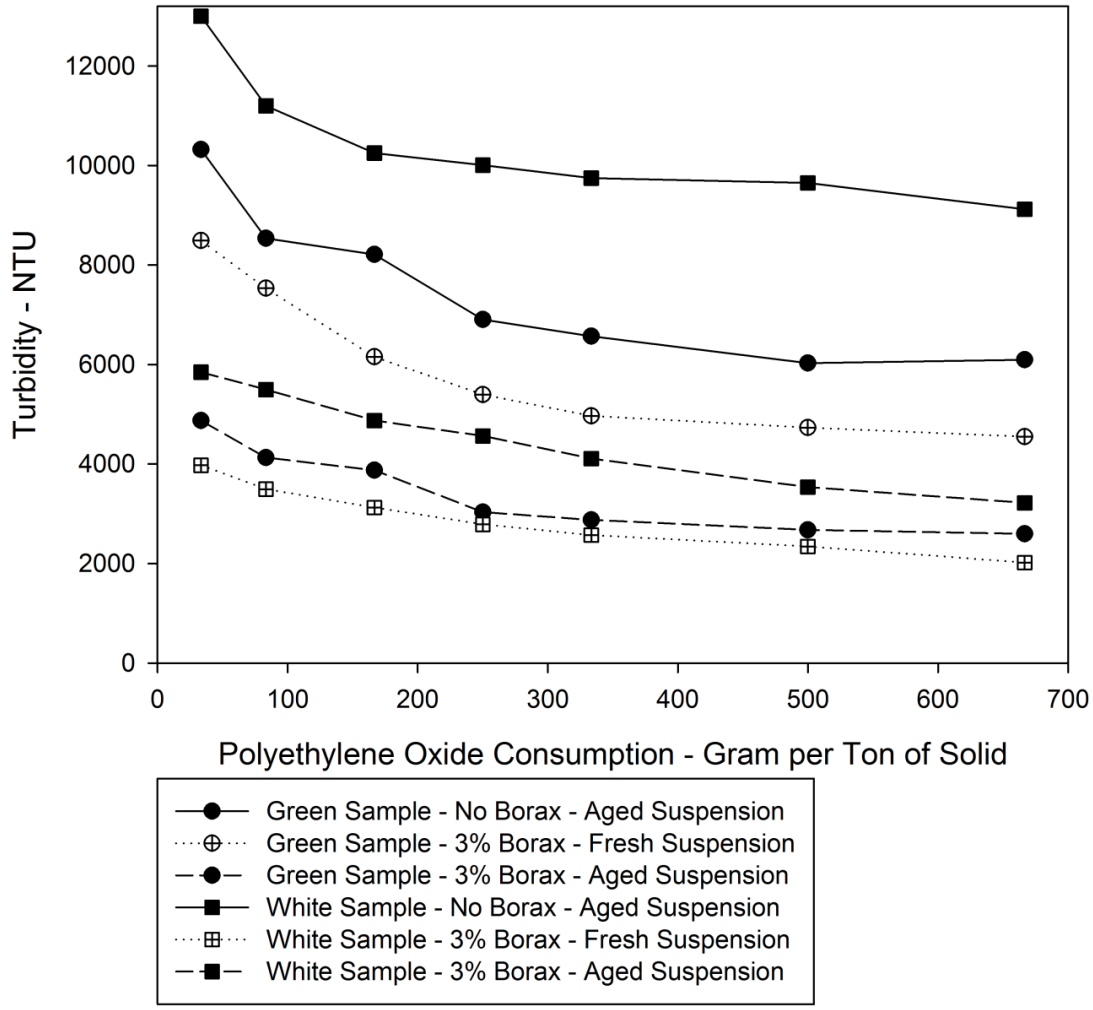

Figure 38. Initial flocculation tests of the suspensions at low-intensity mixing (3% solid, pH=9.40, 3 s^{-1})

As an endnote to the turbidity results of low velocity gradient flocculation studies, it can be claimed that the collision probability between PEO macromolecules and suspended particles was very low (at 3 s^{-1}) due to the colloidal particle swarm and also the flocculants could not efficiently adsorbed on the particle surfaces at pH 9.40.

So, further physical and chemical flocculation parameters were applied and presented under controlled conditions to enhance the supernatant turbidity results in the following sections of this thesis. Besides, it should be noted that the fresh suspensions were used only in this part of the study just for comparison. Flocculation experiments presented in the following sections were always carried out on 24 hour aged suspensions of both green and white samples because the main aim of this study was to analyze flocculation behavior of the green and the white samples in aged suspensions form.

4.2.2. Flocculation Studies of the Suspensions under High-Intensity Mixing Conditions

A low velocity gradient value was tested at 3 s^{-1} and the poor flocculation performances were obtained with very turbid supernatants which was over 2000 NTU in the previous experiment set. So, the intense mixing conditions were tested to enhance the probability of particle-polymer collision. For this purpose, flocculation experiments on both the green and the white sample suspensions were carried out at velocity gradient of 108 and 306 s^{-1} instead of 3 s^{-1}.

The supernatant turbidity values of both the green and the white sample decreased significantly (<2000 NTU) at the higher velocity gradient, 108 s^{-1} (Figure 39) compared to the supernatant turbidity values (>2000 NTU) at the lower velocity gradient, 3 s^{-1} (Figure 38). This finding revealed that the intense mixing conditions had a significant effect on the flocculation performance. The underlying reason of this performance improvement was stimulated by particle-polymer collision and physical and/or chemical entrapment of very fine colloidal particles into the reticular floc structure due to the hydrodynamic movement inside the beakers.

The results of the flocculation experiments are presented in Figure 39. The turbidity of the green sample suspension was sharply decreased down to around 700 NTU when 83 gram PEO per ton solid was added. When this polymer dosage increased up

to 666 gram per ton solid, the turbidity could not be decreased below 597 NTU and the turbidity values formed a straight line parallel to the x-axis. On the other hand, no sharp decrease in turbidity was observed for the flocculation of the white sample suspension. Although 666 gram PEO per ton solid was added into the white sample suspension, the turbidity was hardly decreased down to 883 NTU.

Furthermore, a remarkable difference between the flocculation behavior of the green and the white sample suspension was disclosed. For instance, the supernatant turbidity of the green sample suspension was found as 603 NTU at a velocity gradient of 108 s^{-1} after the PEO treatment with a dosage of 333 gram of per ton of solid. However, the supernatant turbidity of the white sample suspension had a much higher value 1155 NTU than the green sample suspensions at the same velocity gradient and polymer dosage. In conclusion, it was clearly observed in Figure 39 that flocculation of the particles in the supernatant of the white sample suspension was more troublesome than the flocculation of the particles in the supernatant of the green sample suspension.

In addition to the velocity gradient of 108 s^{-1}, a more intense mixing at velocity gradient of 306 s^{-1} was tested to observe its effect on flocculation performance of both the green and the white sample suspension. Very slight improvements in the turbidity results were obtained when the velocity gradient increased from 108 s^{-1} to 306 s^{-1}. In Figure 39, the turbidity lines belong to the velocity gradient of 108 s^{-1} and 306 s^{-1} were found very close to each other. As a summary, increasing the velocity gradient from 3 s^{-1} to 108 s^{-1} significantly contributed to the flocculation performance; however, increasing the velocity gradient from 108 s^{-1} to 306 s^{-1} did not result in the same strong effect at the desired level. In this sense, the increasing velocity gradient helped turbidity removal up to a certain extent. Based on this fact, other parameters were had to be tested to eliminate highly turbid supernatant values in addition to the mixing intensity.

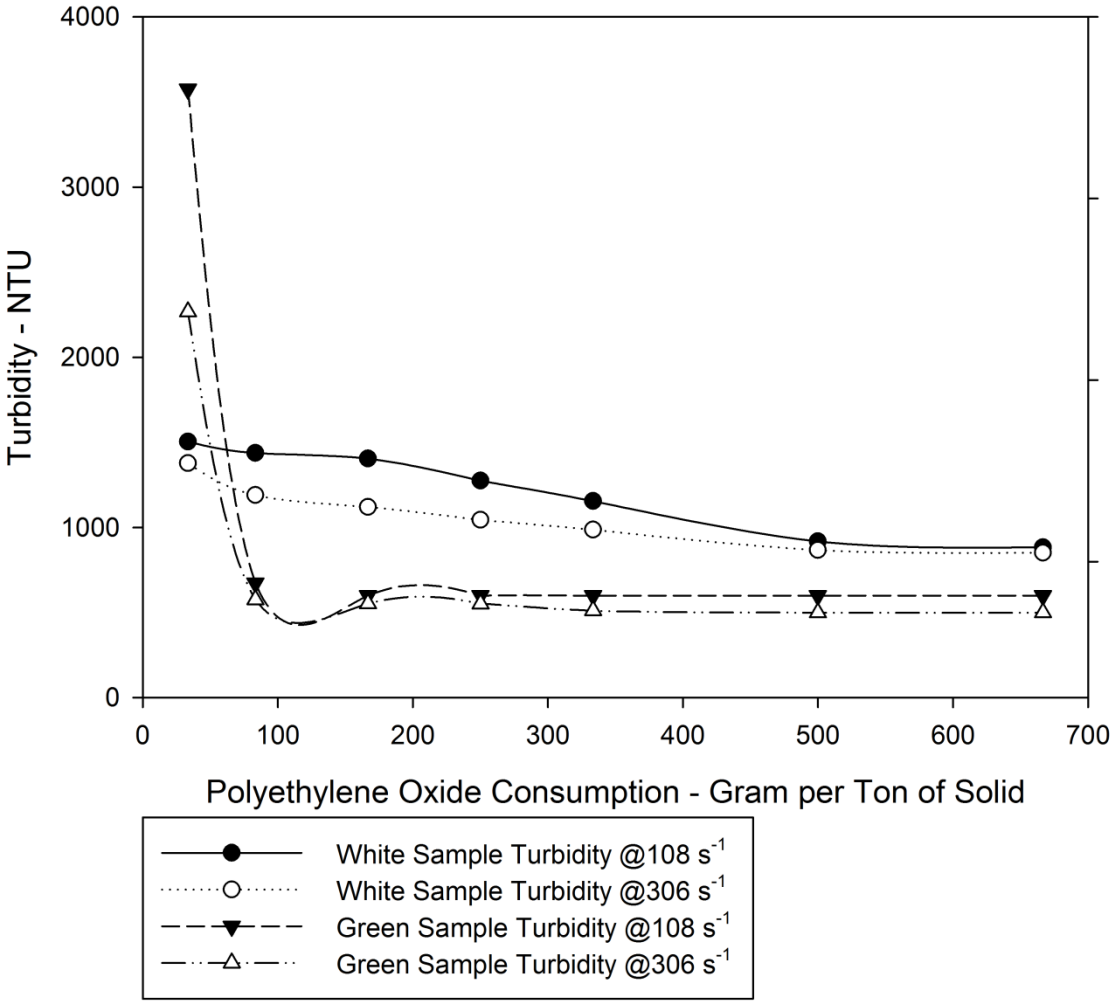

Figure 39. Flocculation results of the green and the white sample suspensions at high-intensity mixing (3% solid, 3%borax, pH=9.40)

The volumetric changes of the flocculated sediment were also taken into consideration (Figure 40). As expected, the volumes of the flocculated sediments were gradually decreased for all cases of the green and the white samples during 20 minute flocculation period. Increasing the velocity gradient from 108 s^{-1} to 306 s^{-1} made the flocculated sediments denser and reduced the final sediment volumes (Figure 40). As it helped turbidity removal, the high-intensity mixing also assisted to the formation of denser floc. Furthermore, the increasing amount of PEO addition into the suspensions significantly contributed to the volume-based reduction of the flocculated sediments. The increased amount of polymer with the help of the mixing intensity enhanced the particle-polymer interactions via stronger bridging formations. As a result, denser floc formation was observed by increasing the polymer dosage and mixing intensity.

The above inferences were valid for the flocculation of both the green and the white sample suspensions. However, there was a significant difference between these two sample suspensions. This distinctness can be seen in Figure 40 at a single glance. The flocculated sediment of the white sample suspension had a much lesser final sediment volume than the flocculated sediment of the green sample suspension. For instance, the flocculated sediment of the white sample had a V_f/V_i ratio of 0.2 whereas the flocculated sediment of the green sample had a V_f/V_i ratio of 0.6 (when 666 g/t PEO and velocity gradient of 306 s^{-1} were implemented). In conclusion, although the turbidity of the green sample suspension was removed easily comparing to the white sample suspension (Figure 39), the settling rate and the final sediment volume of the green sample particles were much more challenging than the white sample particles (Figure 40). Considering the results of the studies thus far, it can be claimed that the green and the white sample suspensions had their own specific complications in terms of flocculation perspective.

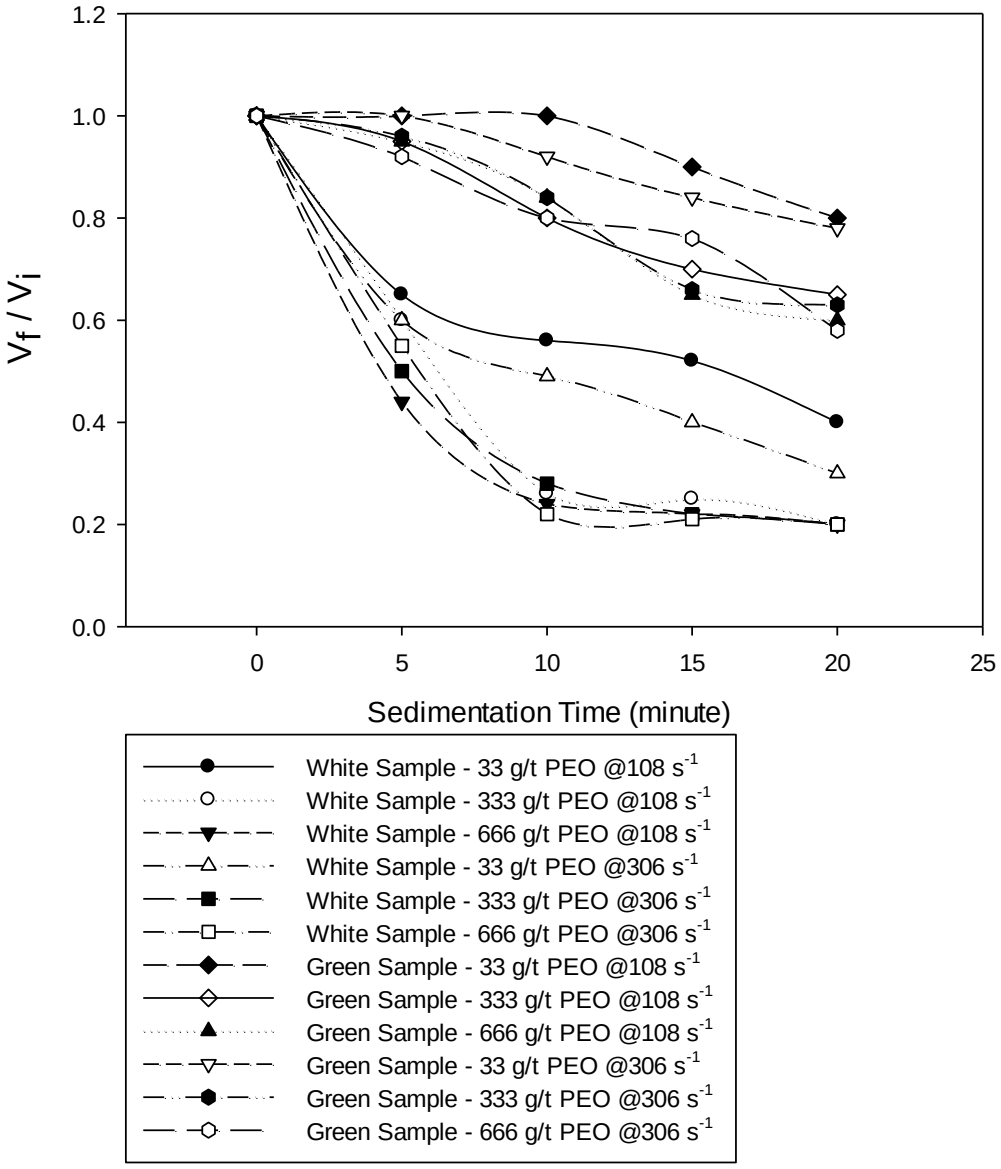

Figure 40. Time-dependent volumetric changes of flocculated sediments (3% solid, 3%borax, pH=9.40).

4.2.2.1. Characterization of Colloidal Particles in the Supernatant after Flocculation

This characterization study was carried out on the supernatants of the green and the white sample suspensions after the flocculation procedure with 333 gram PEO per ton of solid at 108 s^{-1}. The turbidity result of this flocculation study was previously presented in Figure 39 and Figure 40. This experimental flocculation conditions were selected because the resultant colloidal particles in the supernatant showed significant resistance to flocculation and they had a great tendency to remain in the supernatant. Despite the addition of increasing amounts of PEO up to 666 g/t-solid into the suspensions, the supernatant turbidity could not be reduced any further below the significantly high, irreducible turbidity levels shown in Figure 39. The colloidal particles remaining in the supernatants having these irreducible turbidity levels were collected and analyzed to identify the problematic mineral phase and its related properties.

X-ray diffraction results of the particles in the supernatants of the green and the white sample suspensions indicated the same single solid phase. The same peaks can be observed both in Figure 41 and Figure 42. The most intense and identical peaks were detected at 30.94° 2theta with (104) reflection of d-spacing around 2.88 Å. These (104) reflections were characteristic peaks of dolomite phases. In addition to (104) reflections, other minor peaks were analyzed and all of them indicated dolomite presence. All other peaks, which were previously found on the green and the white sample (Figure 27 and Figure 28), were not detected in the X-ray diffraction patterns of the particles in supernatants (Figure 41 and Figure 42). Therefore, the problematic non-flocculatable phases in both supernatants were identified as dolomite. Contrary to expectations, these highly turbid supernatants were clay-free.

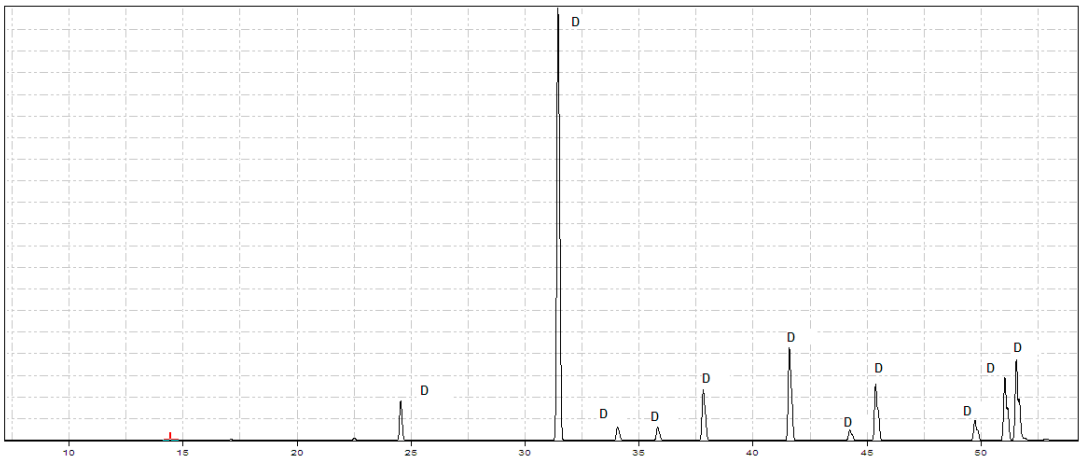

Figure 41. X-ray diffraction pattern of the particles in the supernatant of the green sample suspension after flocculation (D: Dolomite)

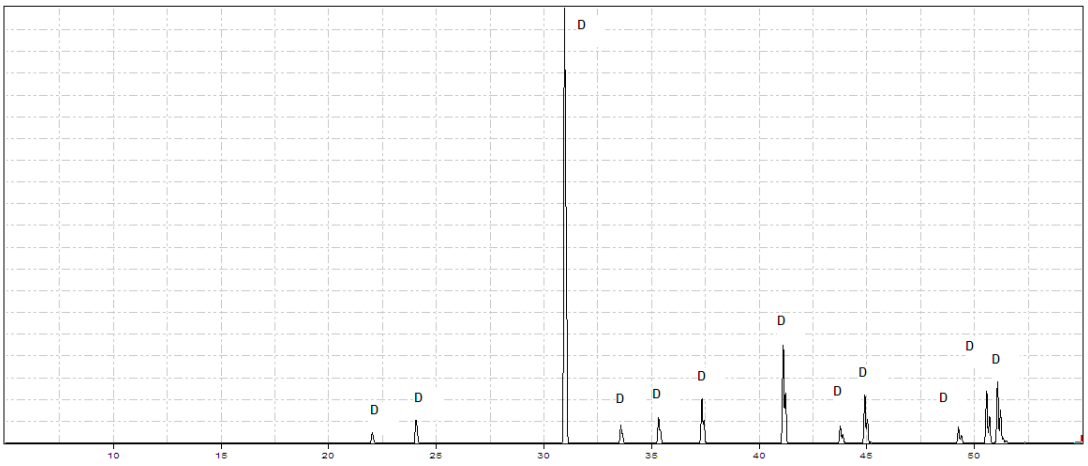

Figure 42. X-ray diffraction pattern of the particles in the supernatant of the white sample suspension after flocculation (D: Dolomite)

Size analyses of the particles suspended in the supernatants were also carried out after flocculation, and the resulting size distributions are presented in Figure 43 and Figure 44. According to these results, the volume-median of the particles in the supernatant of the green sample suspensions was found as 1.84 µm whereas the volume median of the particles in the supernatant of the white sample suspensions was found as 0.59 µm. The colloidal particles were very fine both in green and white supernatants. In general, such fine colloidal materials were associated with clay minerals. However, previous X-ray diffraction results (Figure 41 and Figure 42) proved that these fine materials were not clay minerals but dolomites. The green and the white samples were collected from the playa lake deposit in Kırka/Eskişehir and it was known that the particle size of dolomite formations in such an ancient lake environment can vary from 2 µm to less than 0.2 µm (Counties & Counties , 1965). This characterization study also attested that dolomite can be very fine and very stable as much as colloidal clays. This conclusion suggested that dolomite should also be considered as a problematic material in future studies related to both mineral processing and mineralogy.

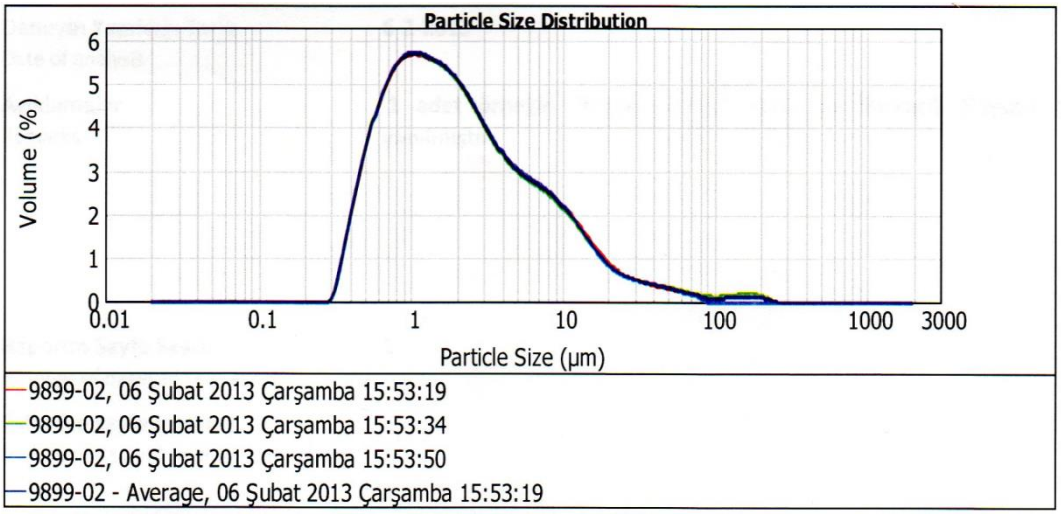

Figure 43. Particle size distribution of the supernatant of the green sample suspension after the flocculation

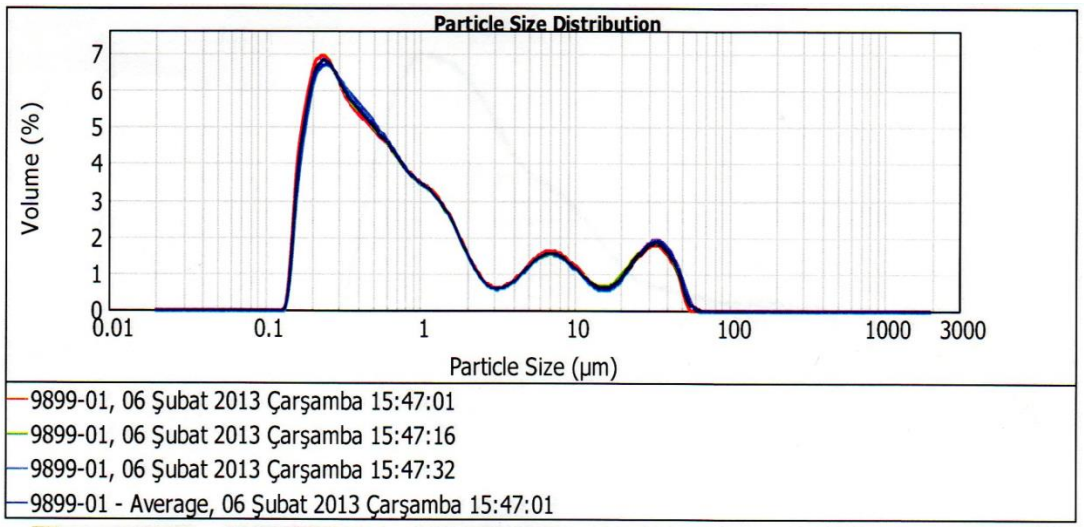

Figure 44. Particle size distribution of the supernatant of the white sample suspension after the flocculation

The colloidal particles in these supernatants were also analyzed in Malvern Zetasizer. The electrophoretic mobility of these particles both in the supernatant of the green and white suspensions resembled each other. The mobility was found as -2.12 µmcm/Vs for the particles in the supernatant of the green sample suspensions and as -1.82 µmcm/Vs for the particles in the supernatant of the white sample suspensions. The standard deviation of the former was 7.37 µmcm/Vs whereas the latter was 1.46 µmcm/Vs. The character of the electrophoretic mobility distribution affected inherently the zeta potential findings. The zeta potentials of the particles remaining in the supernatants were shown in Figure 45 and Figure 46. Only one single broad peak was observed in each figure. 100% of the total peak area was assigned to this peak. The particles in the supernatant of the green sample suspension had a zeta potential of -27.1 mV whereas the particles in the supernatant of the white sample suspension had a zeta potential of -35.1 mV. The zeta potential values were close to each other and indicated similar colloidal stability behavior. Generally, such particles with the zeta potentials around -30.0 mV were considered as stable particles in wastewater treatment industry (Howe et al., 2012). The conductivities were also obtained for the

solutions inside the capillary cell and the results were close (15.1 mS/cm for the measurements in Figure 45 and 11.5 mS/cm for the measurements on Figure 46). These conductivity values were rather high because particles were collected from the saline solution of the flocculation process. In general, sample solutions having conductivities less than 1 mS/cm are often preferred in the zeta potential measurement because the quality of the measurements increases with lower salt concentration. The broadness of the peaks may be most probably stemmed from these high conductivity values. The mere zeta potential findings did not reveal the sample character at such high conductivity values. As a result, the intensity vs. zeta potential curves were given in this part of the study to explain the electrokinetic behavior of the colloidal particles in the supernatants. With the help of Figure 45 and Figure 46, it was observed that the particles within the supernatant had a large zeta potential distribution. However, the generalized information was obtained and it was proved that the supernatant particles had negatively charge particle surfaces which form stable colloidal system due to the repulsion between these particles.

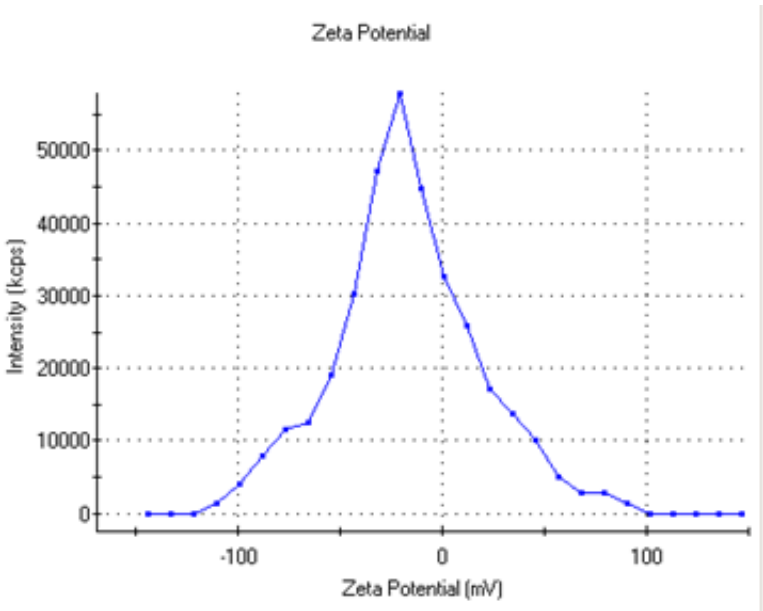

Figure 45. Zeta potential measurement of the particles in the supernatant of the green suspension after the mechanical dispersion

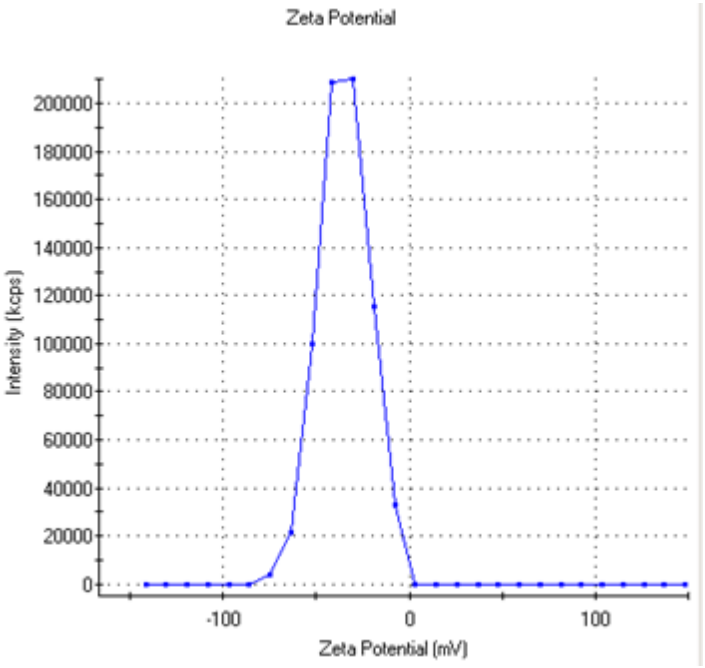

Figure 46. Zeta potential measurement of the particles in the supernatant of the white suspension after the mechanical dispersion

After these supernatants were treated with the ultra-sonication for ten minutes, the zeta potential measurements were repeated and the results were shown in Figure 47 and Figure 48. During this procedure, there was no change observed in the total dissolved solid, the conductivity of the solution and the pH of the suspensions. However, the intensity peaks became narrower and the zeta potential values became more negative following the ultra-sonication process. The zeta potential of the particles in the green supernatant was measured as -76.4 mV and the zeta potential of the particles in the white supernatant was measured as -68.1 mV. The standard deviations of the measurements were also decreased below 18.3 mV for both samples. The large negative surface charges indicated strong particle-particle repulsion and explained the high degree of stability of the supernatants.

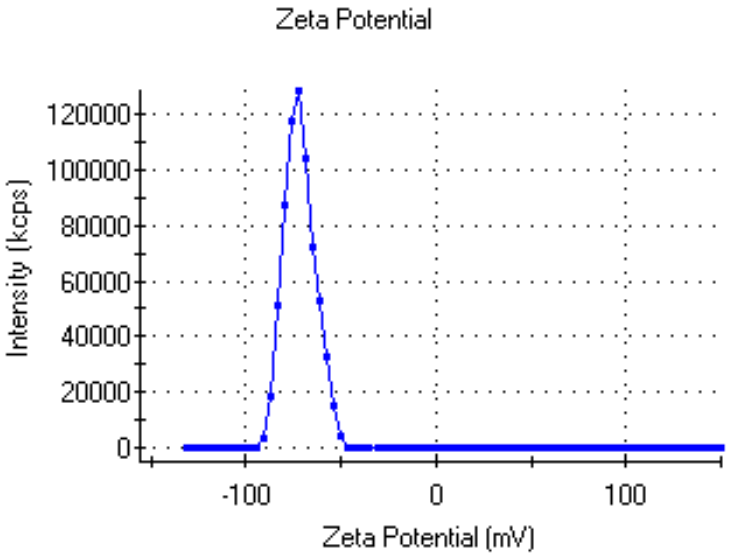

Figure 47. Zeta potential measurement of the particles in the supernatant of the green suspension after the ultra-sonication

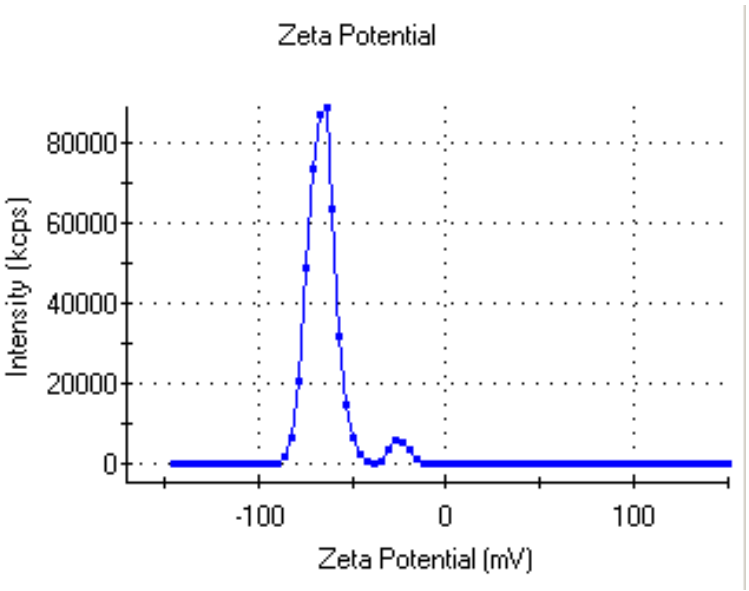

Figure 48. Zeta potential measurement of the particles in the supernatant of the white suspension after the ultra-sonication

4.2.3. Flocculation Studies of the Suspensions at pH 11.50

Previously, the intense mixing conditions proved to be useful for flocculation of the green and the white sample suspensions up to a certain level. In this part of the study, the flocculation performances tried to be enhanced further by using high pH value as an additional parameter together with intense mixing. By increasing pH to 11.50, the proper aqueous chemistry conditions were obtained and this parameter provided a basis for improved flocculation with more effective particle-polymer interaction.

Actually, pH adjustment of a system in equilibrium with boron minerals is not an easy task. Especially, alkali-metal borates have a significant solubility in water. In their aqueous solutions, borates form equilibrium state constituted of two main species, boric acid and metaborate ion which are very important in terms of the water chemistry. In conjunction with this generalization, Kistler and Helvaci (1994) claimed that $Na_2B_4O_7.10H_2O$ has also the same aqueous property and it dissolves in water producing an equilibrium state constitutes of $B(OH)_3$ and $B(OH)_4^{-1}$ which generate a good buffer system at pH 9.40 as follows:

$$Na_2B_4O_7.10H_2O\ (Borax) + H_3O^{+1} + B(OH)_4^{-1} \rightleftharpoons\ + 2H_2O + B(OH)_3$$

In this study, the above reaction governed the water chemistry of the green and the white sample suspensions. When borax dissolved, H_3O^{+1} was immediately consumed resulting increase in pH and the reaction proceeded to the right hand side of the formula forming buffer zone at pH 9.40 as suggested by Kistler and Helvaci (1994). As a consequence of the buffering property of borax, pH adjustment became problematic due to extortionate acid/base requirement. However, the original pH values of 9.40 was increased to 11.50 only to observe the change in flocculation behavior of the green and the white sample suspensions and understand what was needed for the complete flocculation. This may not sound reasonable at a first glance especially considering the previous zeta potential findings (Figure 33 and Figure 35)

that became more negative with increasing pH but the underlying reasons will be explained with the aqueous chemistry calculations.

The turbidity results of the flocculation experiments carried out at pH 11.50 are presented in Figure 49. As in the previous experiments, increasing the velocity gradient from 108 s^{-1} to 306 s^{-1} slightly enhanced the flocculation performance of both the suspensions. Nevertheless, remarkable turbidity results were obtained with the help of pH adjustment to 11.50. For both the green and the white sample suspensions, colloidal particles were successfully flocculated and very clean supernatants were obtained. More importantly, these exceptional turbidity results were achieved with very low PEO dosages. For instance, 333 g/t PEO dosing successfully decreased the turbidity values below 26 NTU both for the green and the white sample suspensions at adjusted pH 11.50. The turbidity of the green sample suspension decreased down to 8 NTU whereas the turbidity of the white sample suspension decreased down to 25 NTU by injecting 333 g/t PEO at velocity gradient of 108 s^{-1} (Figure 49). These values decreased further down to 16 NTU and 2 NTU respectively with the same PEO dosage at increased velocity gradient of 306 s^{-1}. The turbidity removal efficiencies of these suspensions were around 99.99% when 333 g/t PEO dosage was used at pH 11.50. Considering these values, the flocculation performances of both the green and the white sample suspensions were significantly enhanced due to the manipulation of the aqueous chemistry for the best particle-polymer interactions resulting in denser floc structures. Based on this, the macromolecules of PEOs attached themselves on the particle surfaces via stronger chemical bonds (most probably hydrogen bonding) under increased pH 11.50. As a result, very firm, dense solid flocs were obtained. Non-breakable character of these flocs formed at this pH was shown in section 4.3.2. Furthermore, these strong floc formations were obtained at very low PEO dosages. The reason for this stemmed from the physical state of non-ionic PEO chain as well as enhanced particle-polymer interaction. Because, when pH of the solutions was increased, the polymer chains were physically elongated into straight line conformation (Besra et al., 2004) instead of coiled state (Figure 11). Such elongated polymer chains with a head-to-tail

conformation means improved capability of catching more colloidal particles into reticular floc structure. In conclusion, the flocculation performance of the green and the white sample suspension increased dramatically based on the optimized chemical and physical conditions at pH 11.50.

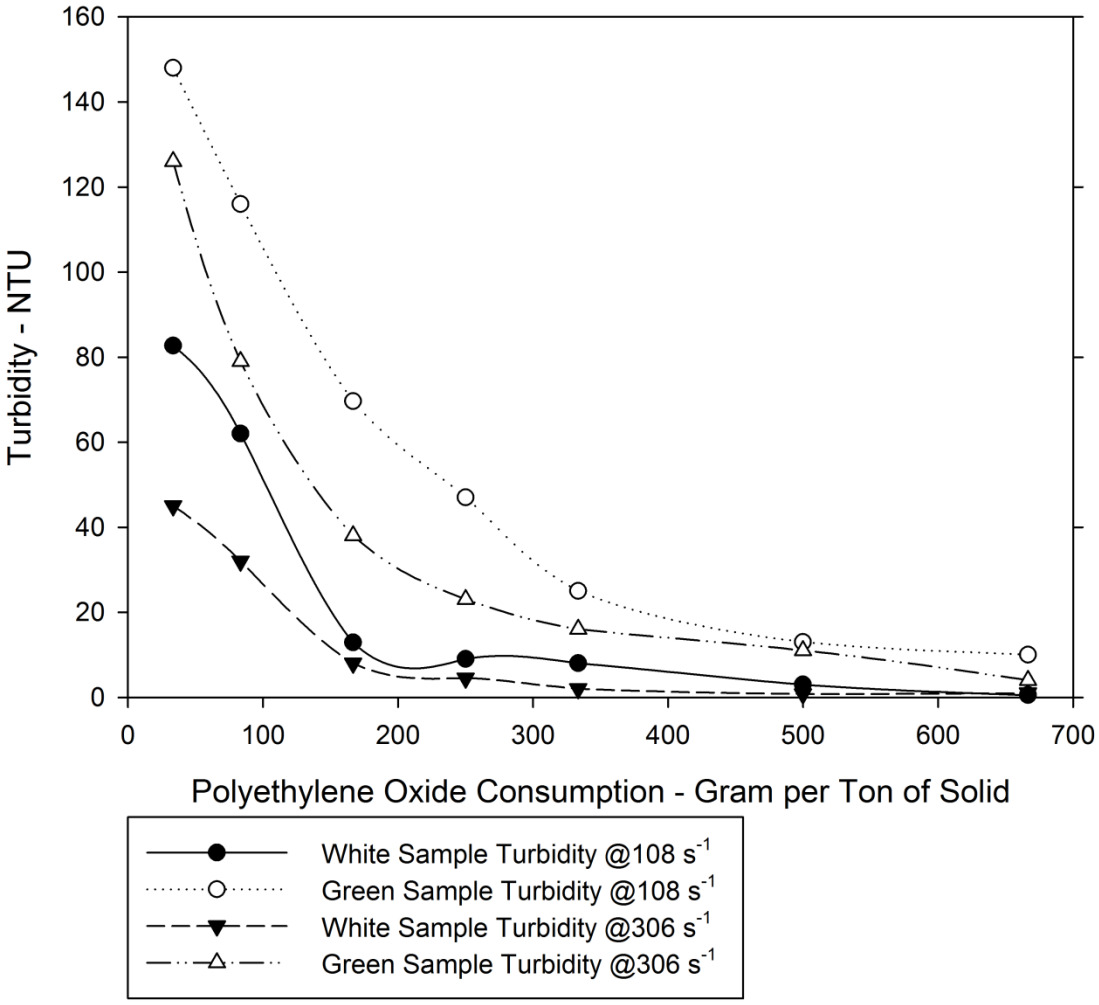

Figure 49. Flocculation results of the suspensions at pH 11.50 (3% solid, 3% borax)

Another favorable result of flocculation at pH 11.50 was observed in the volume of the flocculated sediments. These flocculated sediment volumes (Figure 50) were significantly reduced as compared to the previous results (Figure 40) at pH 9.40. For example, the flocculated sediment of the white sample had a V_f/V_i ratio of 0.14 whereas the flocculated sediment of the green sample had a V_f/V_i ratio of 0.26 when 333 g/t PEO used at a velocity gradient of 108 s^{-1}. As it can be differentiated from these values, the reduction in the sediment volume for the green sample flocs was lesser than the reduction in the sediment volume of the white sample flocs. As it was explained previously, the reason of this was the mineralogical differences between these samples. However, very strong flocs were obtained both for the green and the white sample suspensions at pH 11.50.

In addition to good volume-based reduction ratios, the flocs formed at pH 11.50 had ultra-fast settling rate. The flocs settled within 10 seconds (Figure 50) especially when 333 g/t and higher dosages were implemented. So, the linear lines parallel to x-axis were principally observed instead of the non-linearity in Figure 50 at these dosage values. To make it clear, the colloidal particles in the suspensions were chemically bonded with PEOs and agglomerated into larger globular structures at the initial phase of the mixing. Then, these globular structures attached to each other to cluster into final floc sediment at the final phase of the mixing. As a result, this resultant large single mass sedimented very fast as it was shown in Figure 50.

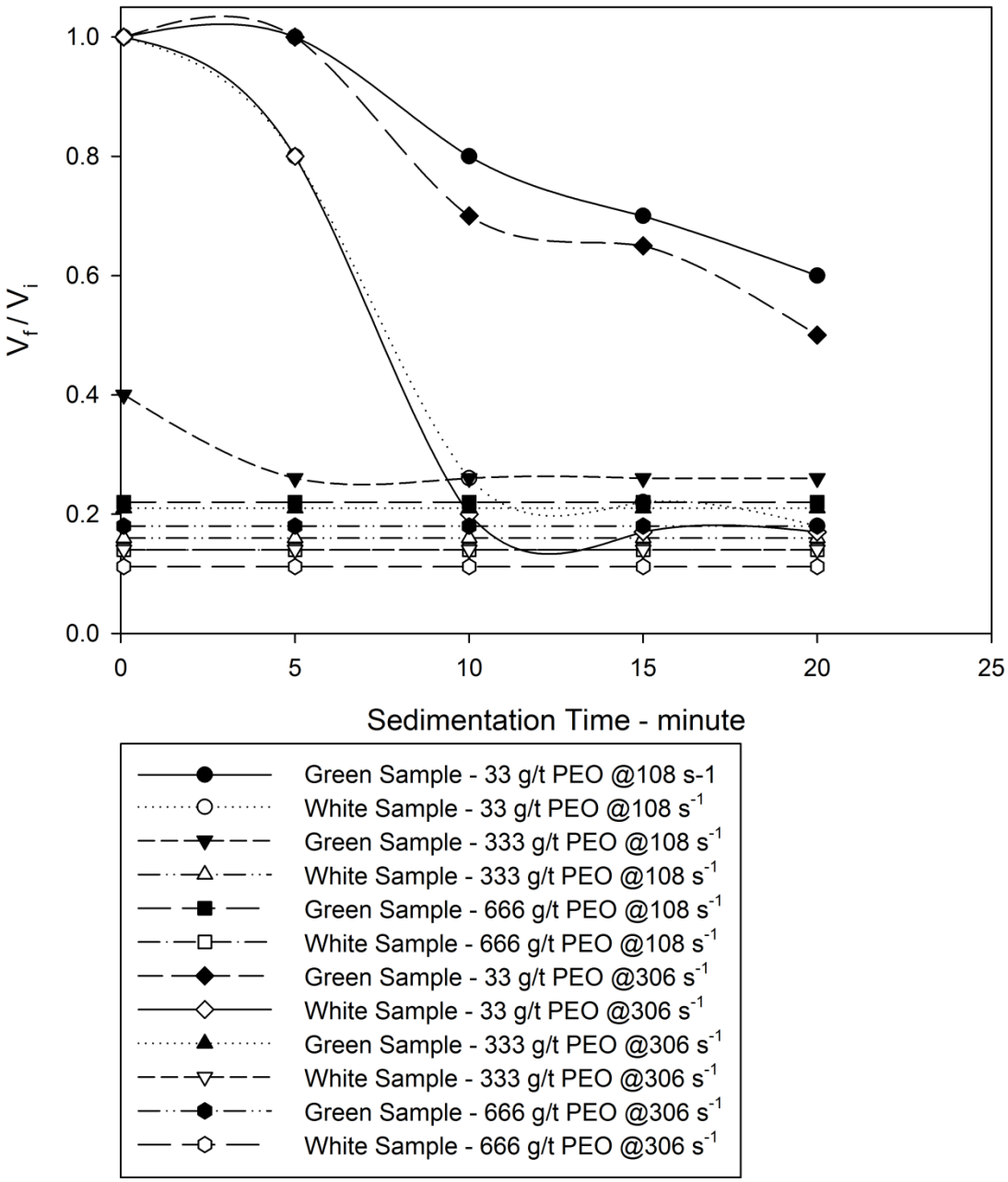

Figure 50. Time-dependent volumetric changes of flocculated sediments pH=11.50 (3% solid, 3%borax).

4.2.3.1. NaOH Consumption vs. pH Adjustment in the Presence and Absence of Borax

pH adjustment of the green and the white sample suspensions was very challenging and it seems to be practically unfeasible. The aim of this part of the study was to prove the difficulty in terms of NaOH consumption during pH adjustment. Firstly, NaOH consumptions were determined to adjust pH for both suspensions in the absence of borax. pH of both the green and the white sample suspensions, which were completely borax free, was easily increased and adjusted to 11.5, because dolomite and silicate minerals inside the solutions did have a low solubility and ignorable buffering capacity as compared to borax. Due to these aqueous chemistry properties, the adjustment of pH was very easy (Figure 51) for the suspensions, which contained only 3% solid. However, pH of the solutions was immediately fixed and buffered at 9.4 when borax was completely dissolved in solid-containing suspensions. Borax has a great buffering capacity due to its solubility of 3-5% by wt in water at 25°C. Owing to this buffering effect, raising the pH to 11.5 required significant consumption of NaOH as shown in Figure 51. 15 – 20 times more NaOH was required to increase pH to 11.5 for the borax-buffered suspensions. The voluminous amounts of base requirements may hinder the practical applications of the pH-dependent flocculation improvement.

Considering the unfavorable effect of borax, the buffering property was tried to be suppressed to make pH adjustment easier. For this purpose, the dissolution reaction of the solid borax mineral (Kistler & Helvaci, 1994) was reversed.

$$2Na^{+}\uparrow + 2H_2O + B(OH)_3 \rightharpoonup H_3O^{+1} + B(OH)_4^{-1} + Na_2B_4O_7.10H_2O\ (Borax)$$

For reversing the reaction, a straightforward chemical manipulation was applied. Sodium ion was introduced into the green and the white sample suspensions in the form of NaCl. NaCl immediately dissolved in water due to its very high solubility. This treatment was applied at a suggested amount by Garrett (1998). Increase in the

concentration of Na-ion made the above chemical reaction to proceed as written and the solubility of borax decreased. When borax became almost insoluble in NaCl dominated solutions, the buffering effect vanished. The resultant pH of the suspensions decreased down to 8.6 (Figure 51) from 9.4 due to the suppression of the borax buffering effect. As a result, pH adjustment became relatively easier due to the NaCl suppression effect. However, it still required a large amount of NaCl and NaOH. The insoluble borax at pH 8.6 in the presence of NaCl started to re-dissolve producing boric acid and tetrahydoxoborate in lesser amounts when pH was changed. Such a presence of these species formed a weaker buffer solution which led lesser NaOH consumption. In conclusion, this procedure to get rid of the boron buffering effect seems to be impractical due to the immense amount of reagent required. There are also other techniques (Xu & Jiang, 2008) to remove boron from the solutions, for instance membrane separation, chemical conversion to less soluble minerals that have non-buffering capacity, adsorption via activated carbon, liquid-liquid extraction, ion-exchange resin, electrodialysis and electrocoagulation etc. However, they similarly require extreme conditions or extreme equipment set-ups which may be considered as non-economic or unimplementable for such a tailing treatment process. These techniques were mostly designed for undersaturated systems (Sharma & Sanghi, 2012) and may not be suitable for efficient boron removal in the case of saturated/oversaturated solutions. The tailing discharged from the borax concentrator contains both dissolved and non-dissolved boron phases and this co-existence indicates saturation/oversaturation (Garrett, 1998). This promotes the complication in the removal procedure because solid borax re-dissolves immediately to reach chemical equilibrium after boron removal technique is applied. The mentioned chemical loop (the removal – re-dissolution cycle) may invalidate the feasibility of the downstream boron removal. However, the upstream boron removal may be considered as more applicable/desirable, relatively. If this can be achieved, the flocculation process would be manageable via pH adjustment and the extracted upstream boron would be turned into an economic value. Unfortunately, none of these techniques can be regarded as viable alternatives for the tailing treatment of the

borax concentrator under the current conditions. Therefore, boron removal test was not studied in depth within the scope of this thesis.

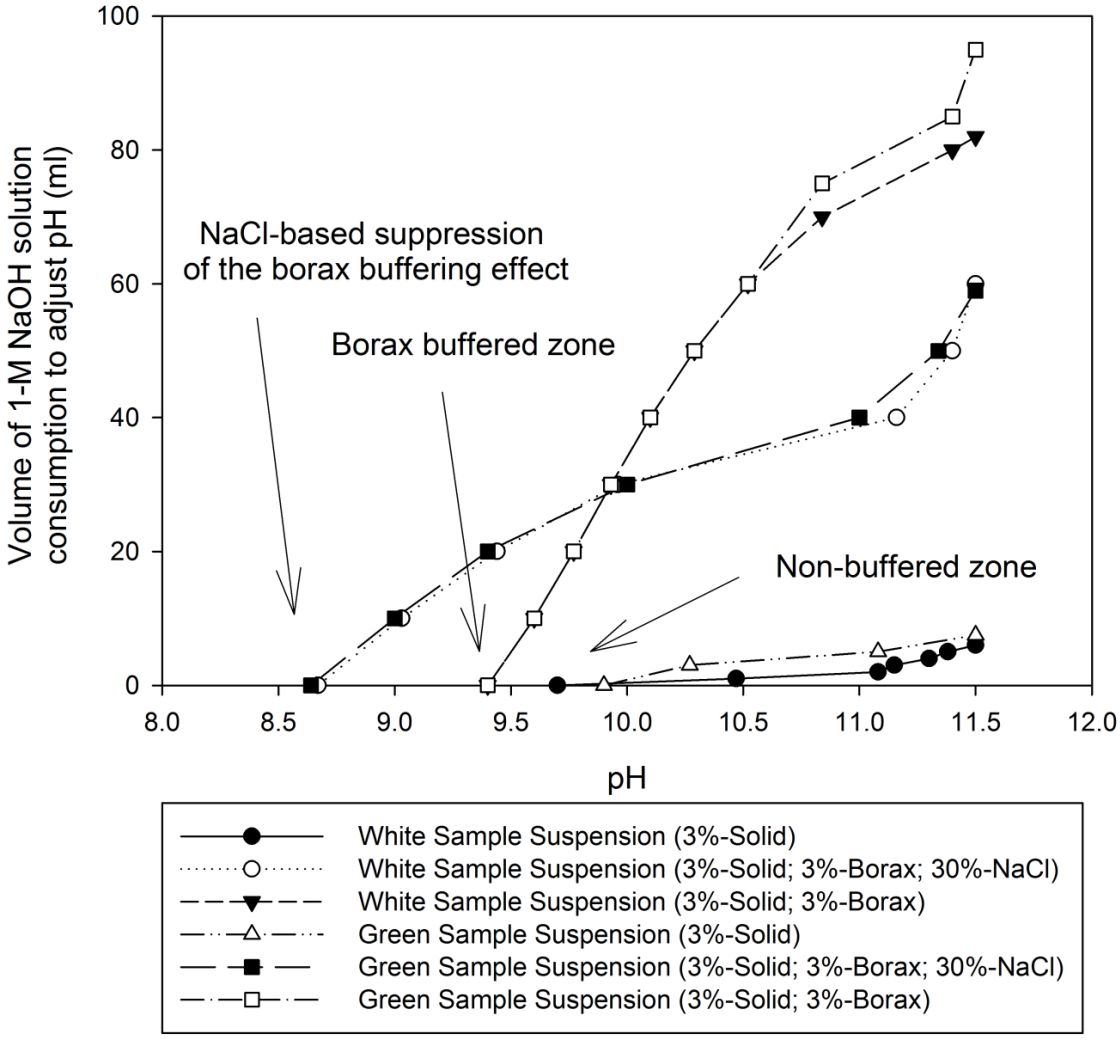

Figure 51. NaOH consumptions to adjust pH for the buffered and non-buffered suspensions

4.2.4. Effect of Temperature on the Flocculation Performance

Effect of temperature was studied as another parameter for the flocculation of the green and the white sample suspensions because some controversial opinions were present in the literature. Although this parameter was slightly out of the main scope, an initial experiment set was carried out to shed light on this subject. Temperatures of the green and the white sample suspensions were increased from 25 °C to 75 °C. The heated suspensions were only treated with a single dosage of 666 g/t PEO at 108 s^{-1} and 306 s^{-1}. In addition to these, the control samples for each of the green and the white suspensions were prepared at 75 °C and these suspensions were not subjected to PEO treatment under hydrodynamic conditioning by simply leaving the heated suspensions to rest for sedimentation. Then, the results of the flocculation experiments were compared to the results of the untreated sedimentation experiments considering the turbidity values of the supernatants. The findings were summarized in Figure 52, indicating that there was a significant difference between the supernatant turbidity values of the green and the white sample suspensions at 75 °C after the flocculation/sedimentation period. The supernatant of the white sample suspension was much more turbid than the supernatant of the green sample suspension. The reason for this can be explained again with the mineralogical difference between the samples. As it was shown in Figure 52, the flocculation/sedimentation of the dolomite-rich white sample was inferior to the flocculation/sedimentation of the silicate/clay rich green sample at 75 °C.

However, an interesting point was observed related to the polymer interaction. The polymer addition for the purpose of flocculation did not produce any further beneficial effect both for the green and the white sample suspensions at 75 °C when it was compared to the sedimentation of these control suspensions at 75 °C without any PEO addition. It can be claimed that the increase in total dissolved solid, activities of dissolved ions, ionic strength etc. due to the elevated temperature made the colloidal particles both in the green and the white sample suspensions destabilized. This destabilization resulted in sedimentation by reducing particle-

particle repulsion especially between the green sample particles. Colloidal particles in the white sample suspension also sedimented without any polymer treatment but they distinctively tended to produce more turbid supernatant. In conclusion, the flocculating efficiency of PEO almost completely lost in the heated suspensions. This can be easily differentiated comparing to the sedimentation of the control suspensions (Figure 52).

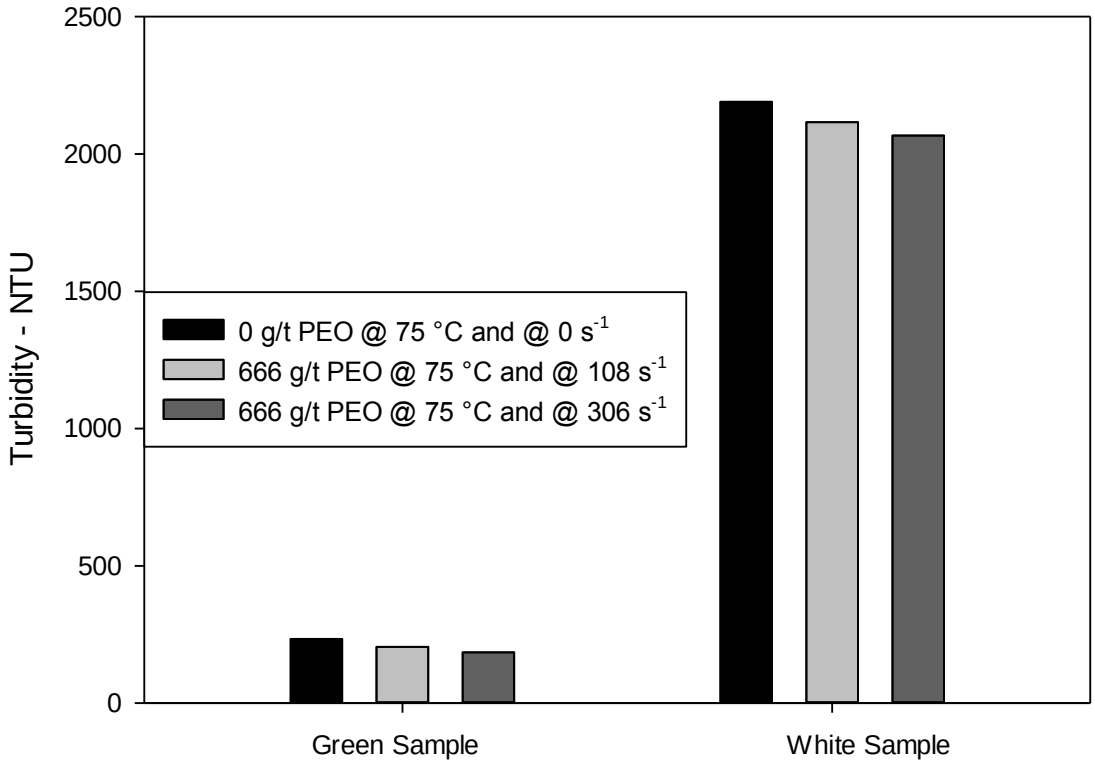

Figure 52. Flocculation/sedimentation results of the suspensions at 75 °C (3% solid, 3% borax, pH=9.40, 108 s^{-1} and 306 s^{-1})

The time-dependent volumetric changes of the sediments at 75°C showed that the reduction of the sediment volumes was much more difficult (Figure 53) for the green sample suspension compared to the white sample suspension. Besides, the polymer addition did not make a difference considering the time-dependent variation in the volume, and the resultant volumes of both for sedimentation and flocculation were almost same (Figure 53). The reason for this can be explained again with the loss of flocculating ability of PEO chains which lead to decrease in polymer-particle interaction. As a matter of fact, no large/firm floc formation was observed during the flocculation/sedimentation experiments carried out at 75 °C. Most probably, this resulted in larger final sediment volumes both for the green and the white sample suspensions because particle-particle repulsion could not be surpassed at the desired level. This polymer-induced problem at the elevated temperature is also encountered in industrial scale. In the boron derivatives plant, the flocculation process of the hot borax solution, including the same colloidal mineral particles as in the green and the white samples used in this study, is crucial for both enrichment and tailing management purposes. However, the borax industry considerably suffers from the inefficiency of the polymer treatment. To overcome this problem, the polymer treatment is separately carried out by using excessive amounts of anionic PAM, nonionic PAM and nonionic PEO in a two-staged thickener system. So, the flocculation of such suspensions including mostly dolomite and clay type silicates was problematic at the elevated temperature and it was thought that the source of the problem was the polymer itself for this temperature-dependent specific case. For this purpose, the problem were tried to be explained with the viscosity measurements of the completely dissolved PEO solution and the result will be presented in Section 4.4.1.

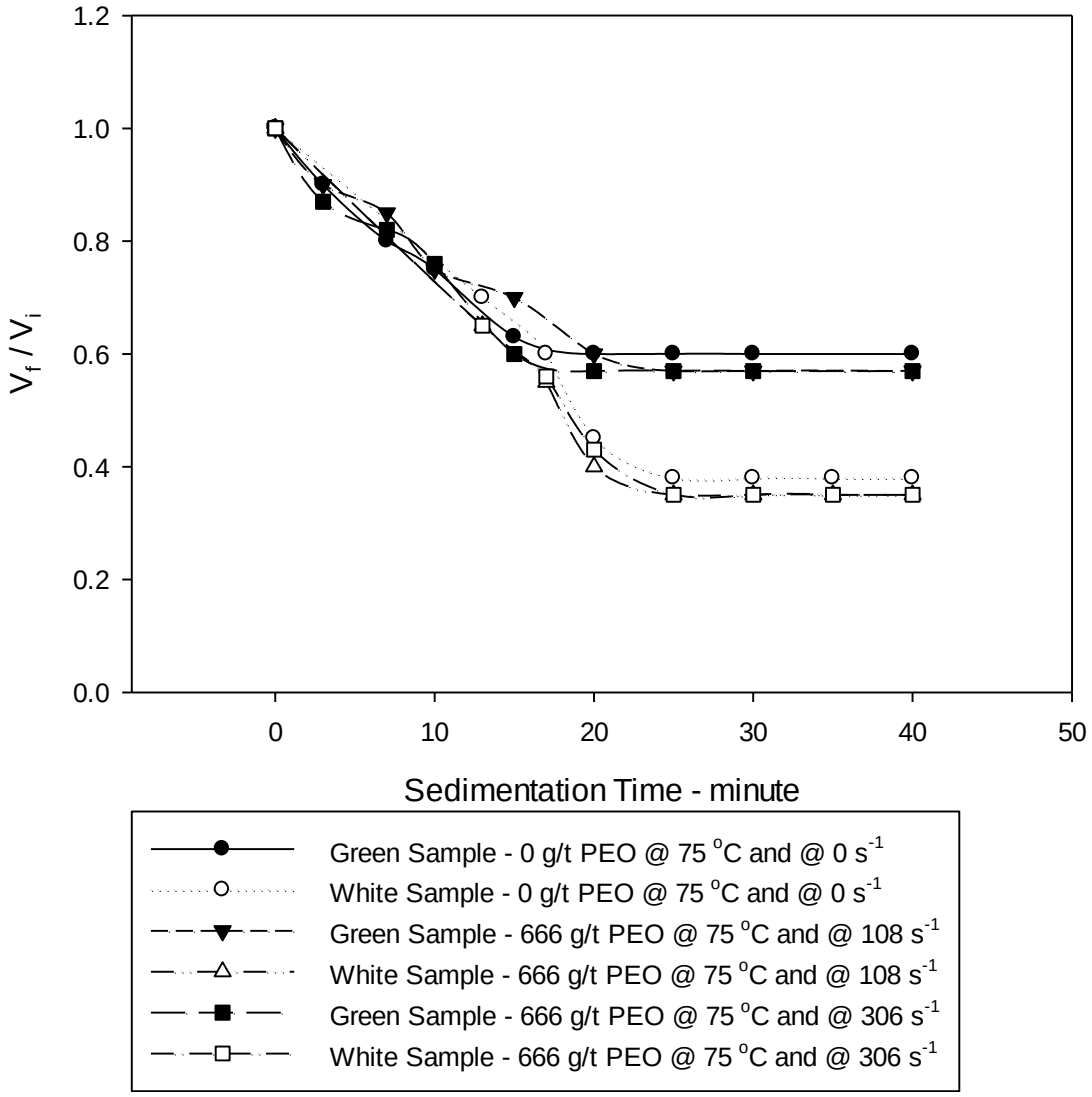

Figure 53. Time-dependent volumetric changes of the sediments at 75 °C (3% solid, 3%borax, pH=9.40, 108 s^{-1} and 306 s^{-1}).

4.2.5. Coagulant Preconditioning Trials for Flocculation Enhancement

The suspensions were preconditioned with Al^{+++}, Cu^{++}, Fe^{+++}, Ca^{++} and Mn^{++} prior to the PEO treatment with the intention of increasing the flocculation performance and the best coagulant were tried to be determined to decrease the supernatant turbidity. However, the expected decrease in the supernatant turbidity could not be observed after the experimentation with Al^{+++}, Cu^{++} and Fe^{+++} preconditioning. Actually, similar trend (Figure 54) in the turbidity lines both for the green and the white sample suspensions were obtained. It seems that the preconditioning with these coagulants does not promote particle-particle and particle-polymer interaction. This was a rather strange finding because especially aluminum and iron coagulants were frequently used in both industrial and experimental studies and considered as efficient reagents for solid/liquid separation.

For instance, Fe^{+++} preconditioning prior to 666 g/t-solid PEO treatment barely decreased the turbidity to 642 NTU for the white sample suspension and 412 NTU for the green sample suspension at velocity gradient of 108 s^{-1}. However, even this small turbidity decrease could not be observed in the case of Al^{+++} and Cu^{++} preconditioning. The reason behind the ineffective turbidity removal of these coagulant trials will be explained with the conceptual aqueous chemistry calculations.

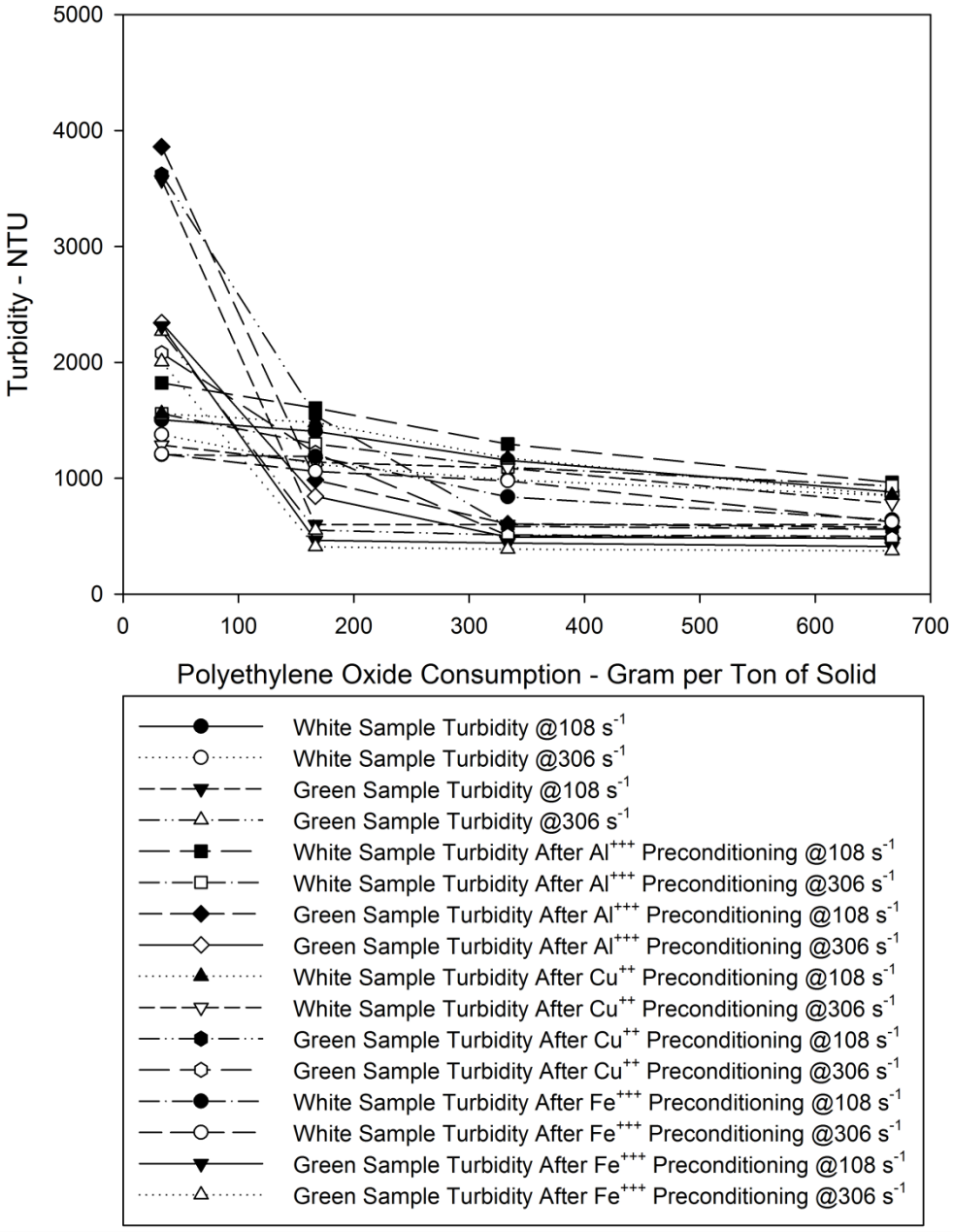

Figure 54. Coagulant preconditioning with Al^{+++}, Cu^{++} and Fe^{+++} (3% solid, 3%borax, pH=9.40 and 500 mg/l coagulant)

On the other hand, Ca^{++} preconditioning prior to the PEO treatment significantly increased the flocculation performance. The turbidity of the green sample supernatant sharply decreased below 200 NTU whereas the turbidity of the white sample supernatant gradually decreased below 200 NTU. In addition to that, such low turbidity values were achieved with relatively lower polymer consumptions. The green sample suspension required around 166 g/t-solid PEO and the white sample suspension required 333 g/t-solid. The remarkable turbidity difference due to Ca^{++} preconditioning can be seen in Figure 55.

In analogy with Ca^{++} coagulant, Mn^{++} coagulant significantly contributed to PEO-induced flocculation performance. With the help of Mn cations, much cleaner supernatant was obtained (Figure 55) and turbidity was easily reduced below 200 NTU with a lesser amount of flocculant consumption compared to the inefficiency of Al, Fe and Cu coagulants (Figure 54). This was a rather interesting result because Mn cations are not commonly known as surface activators or coagulants. Although Mn coagulant has not been used for such purposes in real life cases, the results of Mn-preconditioned flocculation experiments explained the underlying surface activation mechanism in conjunction with the Ca-preconditioned flocculation experiments and this finding shed light on what is needed for the improved flocculation of the green and the white sample suspensions. The related mechanism will be explained under the aqueous chemistry calculation section in detail because the aqueous chemistry governs the whole flocculation process for these challenging suspensions.

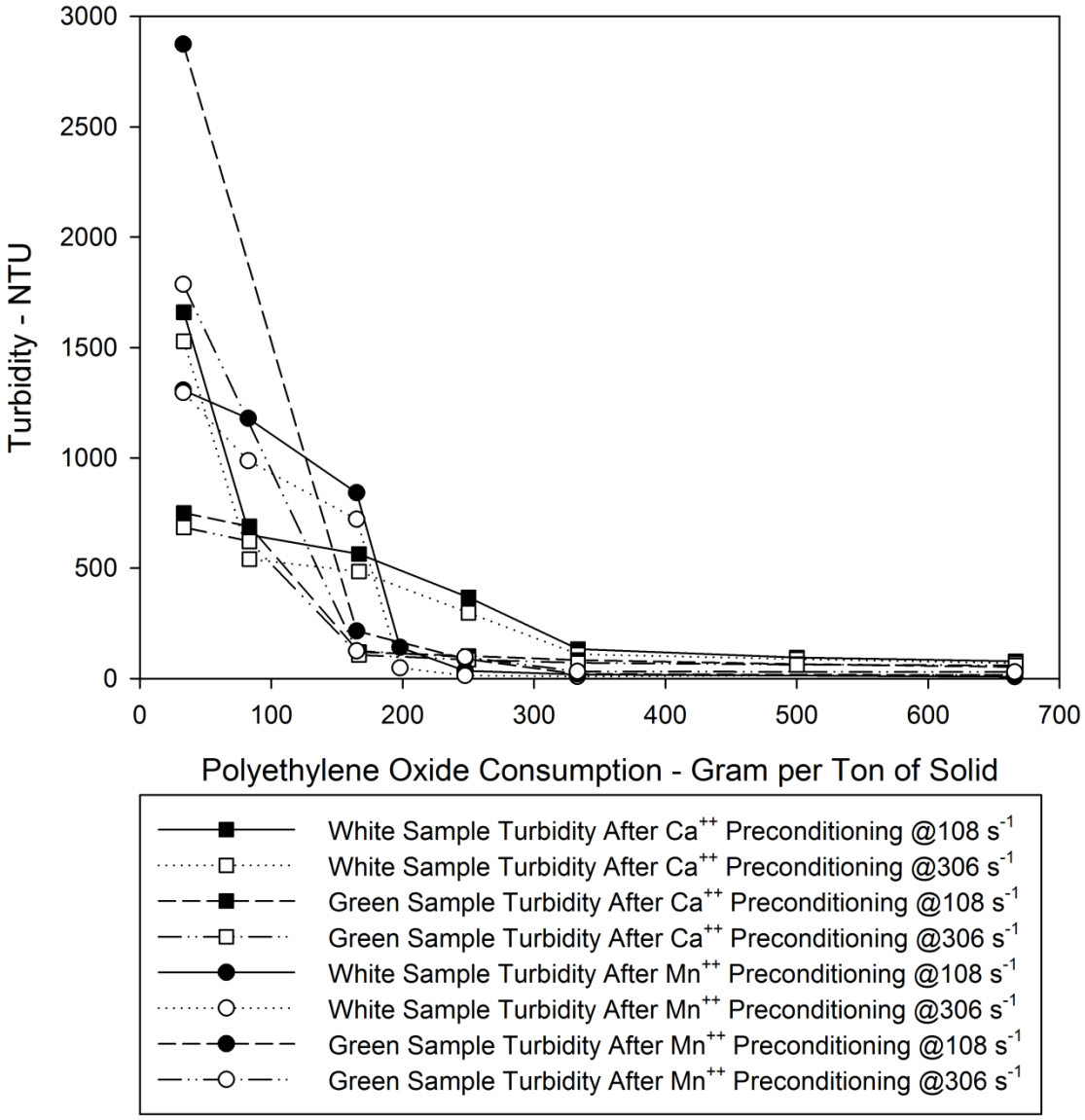

Figure 55. Coagulant preconditioning with Ca^{++} and Mn^{++}
(3% solid, 3%borax, pH=9.40 and 500 mg/l coagulant)

The time-dependent volumetric changes of the green and the white sample sediments with Mn treatment can be seen in Figure 56 and Figure 57. It can be inferred that the green sample particles flocculated much slower than the white sample particles when Ca and Mn preconditioned suspensions were especially treated with small amount (33 g/t-solid) of PEO. The increasing flocculant dosage to 166 g/t-solid relatively enhanced the sedimentation rate and the final sediment volumes for both Ca and Mn preconditioned suspensions. Further increment in the flocculant dosage (333 g/t-solid) resulted in the sudden settlement of the flocs within the first ten seconds of 20 minutes sedimentation time. This sedimentation behavior presented itself as parallel lines to x-axis as shown in Figure 56 and Figure 57. Besides, the final sediment volumes of Mn-preconditioned suspensions were much smaller than the final sediment volumes of Ca-preconditioned suspensions for both the green and the white samples. In conclusion, it seems that Mn coagulant produced more compact sediment volumes and slightly lesser supernatant turbidity in comparison to Ca coagulant. However, both of these Mn and Ca coagulants can be considered as efficient boosters for the PEO-induced flocculation of these colloidal suspensions at pH 9.40 in contrast to Cu, Al and Fe coagulants.

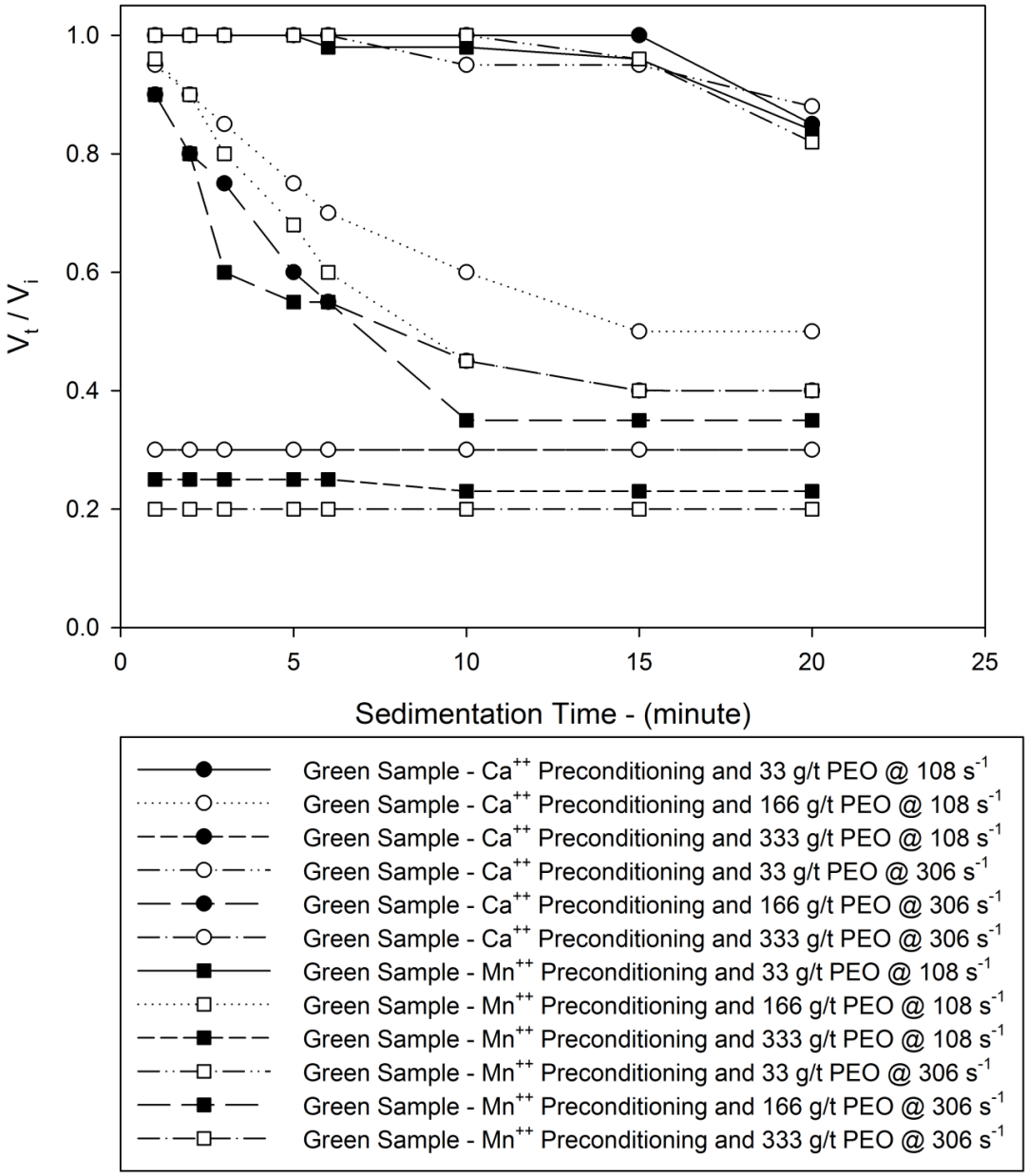

Figure 56. Time-dependent volumetric changes of the green sample sediments (3% solid, 3%borax, pH=9.40 and 500 mg/l Ca^{++} and Mn^{++} coagulant)

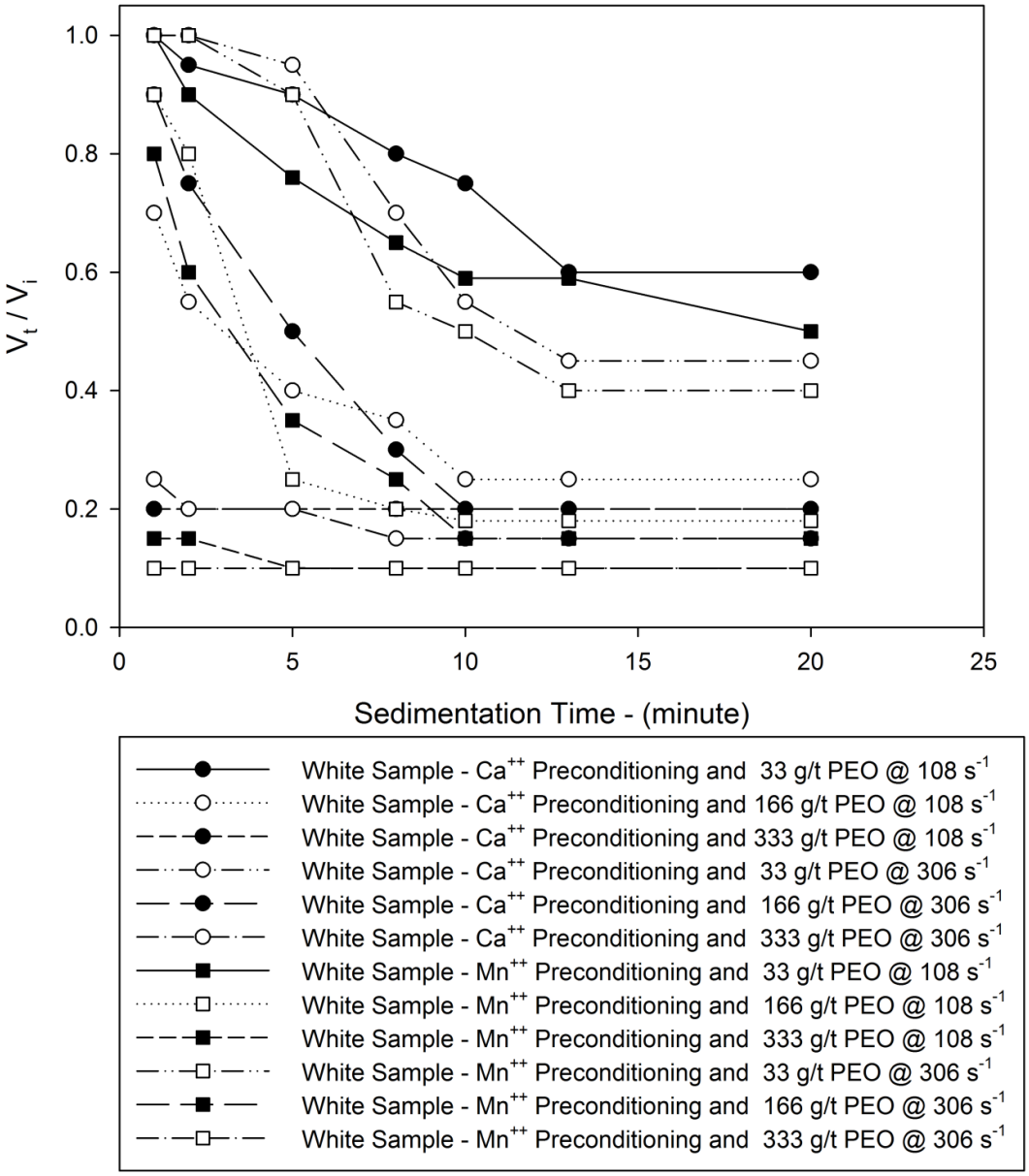

Figure 57. Time-dependent volumetric changes of the white sample sediments (3% solid, 3%borax, pH=9.40 and 500 mg/l Ca^{++} and Mn^{++} coagulant)

4.2.6. Cationic Polyacrylamide Preconditioning Trial for Flocculation Enhancement

The green and the white sample suspensions were preconditioned with cationic polyacrylamide (PAM) prior to PEO treatment. The initial aim for this PAM conditioning was to neutralize the negatively charged particle surfaces with this cationic polymer and prepare the surface for fundamental PEO adsorption. However, the results of the flocculation tests revealed that 2-staged polymer treatment complicated the system and flocculation performance could not be improved as aimed (Figure 58). Most probably, such a treatment leads to a non-homogeneous polymer distribution by preventing efficient particle – polymer interaction. This phenomenon made the floc sediments more viscous but colloidal particles that were still present in the supernatant could not be destabilized successfully. Turbidity removal performance deteriorated and very high turbidity results were obtained. Increasing the velocity gradient slightly improved the turbidity results, however, no sharp decrease in the turbidity trends was observed. This means that the tests including PAM preconditioning increased the total amount of polymer requirement for the destabilization. For instance, when 166 g/ton-solid PAM and 666 g/t-solid PEO injected into the suspensions, the turbidity barely decreased around 100 NTU both for the green and the white sample suspensions in spite of such a high amount of polymer. In conclusion, the cationic polymer preconditioning did not improve the flocculation performance due to polymer-polymer interaction domination over polymer-particle interaction.

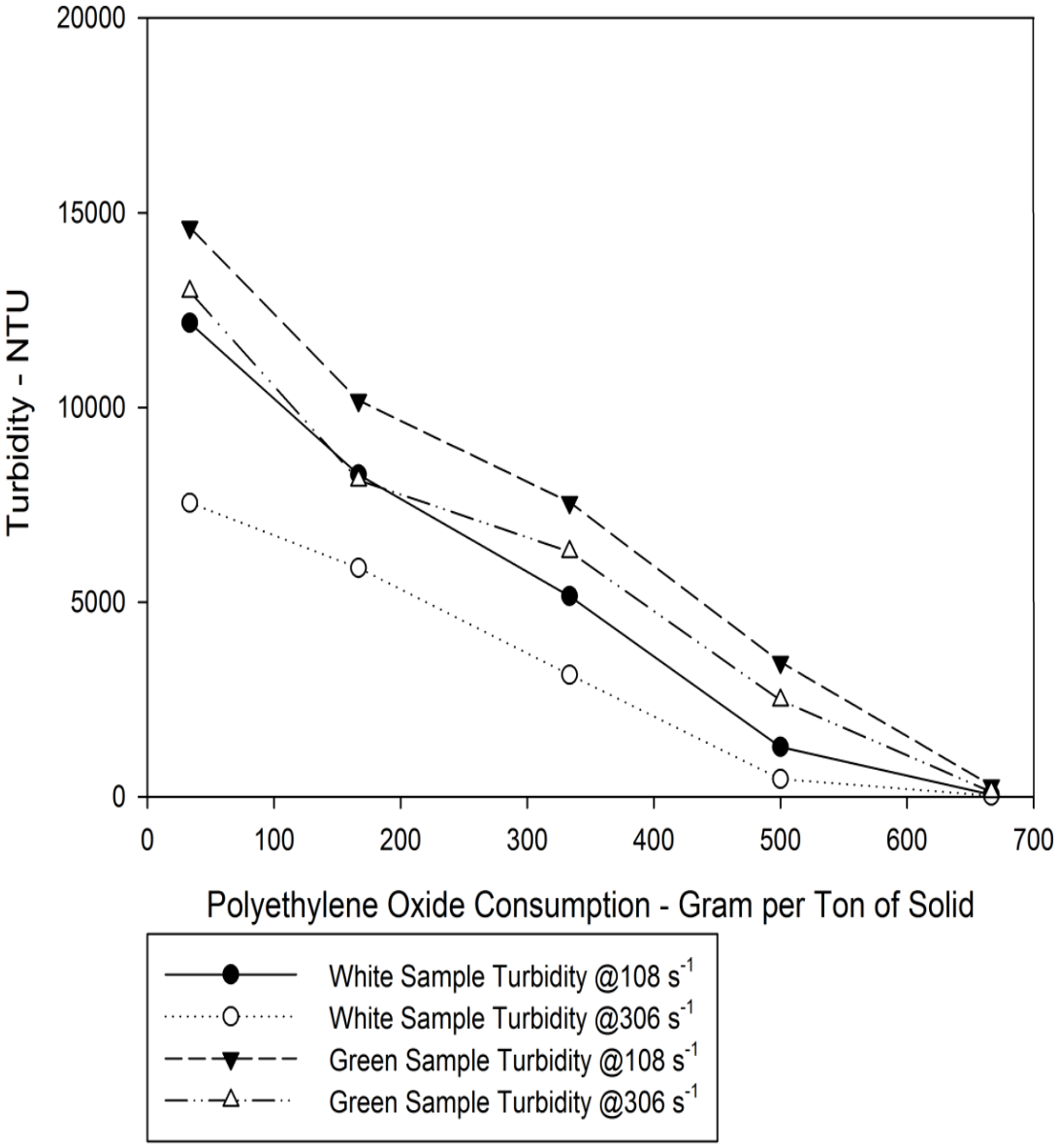

Figure 58. Cationic PAM preconditioning (166 g/t-solid) prior to PEO treatment

4.2.7. Clinker Ballasting Trial for Flocculation Enhancement

The suspensions of the green and the white samples proved as very stable and the colloidal character of the particles showed significant resistance to polymer-induced destabilization. Therefore, readily flocculatable clinker in powder form was introduced into the non-flocculatable colloidal suspensions of the green and the white sample. The aim of this procedure was to destabilize colloidal particles together with this ballast material via hetero-flocculation mechanism. After these ballasted systems were completely mixed, the flocculation performance of PEO was tested and the results were presented in Figure 59. Although a very low amount of PEO (33 g/t-solid) was added into the suspensions, the turbidity values significantly decreased below 250 NTU for both the green and the white sample suspensions. Turbidity generating particles were most probably physically and/or chemically entrapped into the reticular structure of PEO – clinker flocs and as a result turbidity removal performances significantly improved. Furthermore, increasing the velocity gradient contributed to enhancement of the particle agglomeration into floc structure producing less turbid supernatant. So, the ballasting method should be considered as an alternative treatment method for the coagulant preconditioning and pH adjustment prior to the flocculation because it decreased the polymer consumptions as well as the supernatant turbidity values.

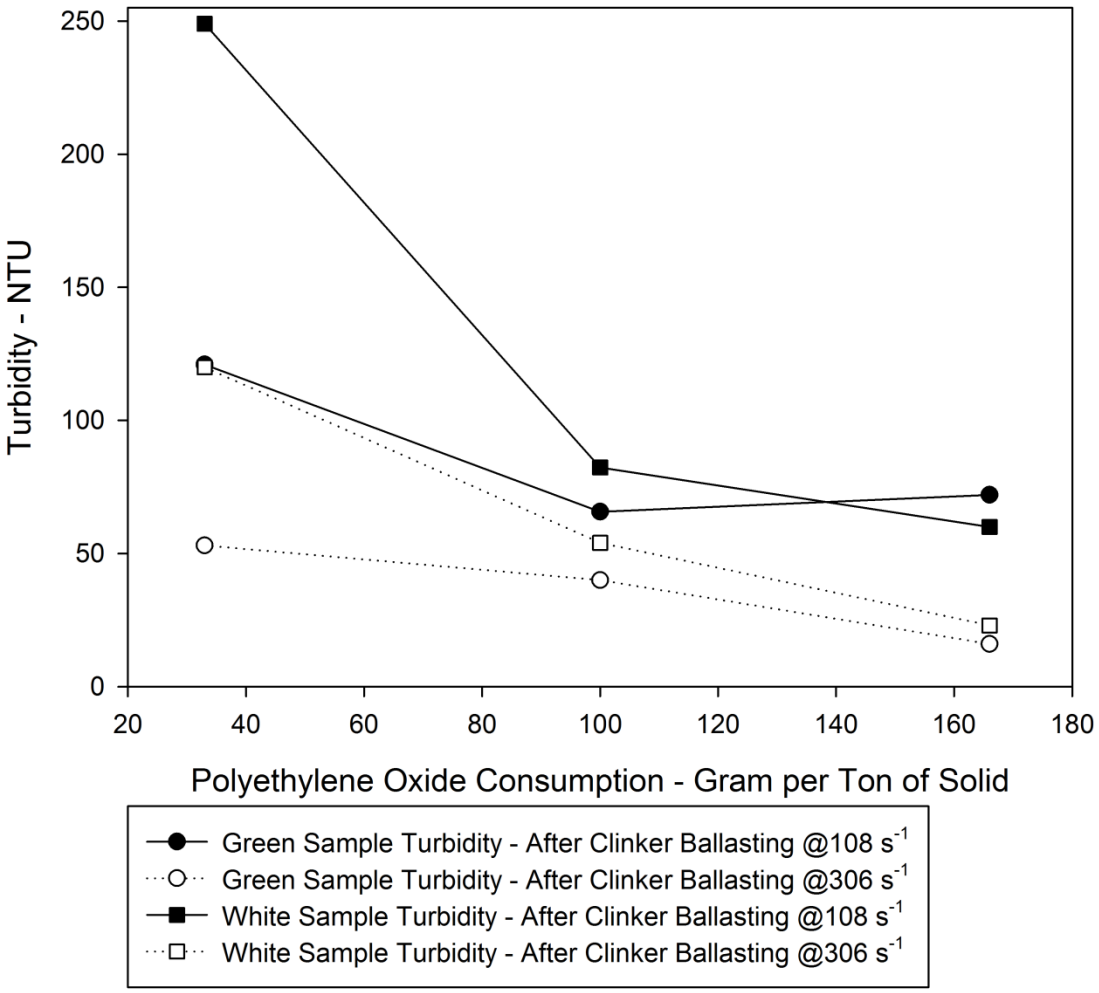

Figure 59. Clinker ballasting (10 g/l) prior to the PEO treatment
(3% solid, 3%borax, pH=9.40)

Furthermore, clinker ballasting procedure prior to the PEO-induced flocculation significantly reduced the volume of the flocculated sediments (Figure 60-a; Figure 60-b). And, the ballasted flocs were sedimented very rapidly (Figure 60-b) when 166 g/t PEO added into the suspensions. This rapid settlement stemmed from the dense, firm flocs formation due the polymer bridging property and high specific gravity of

artificial clinker minerals (Ohama et al., 1997) entrapped into the floc structure like tri-calcium silicate (S.G. 3.13), bi-calcium silicate (S.G. 3.28), tetra-calcium aluminoferrite (S.G. 3.77). In addition to that, calcium component of those clinker minerals seems to establish strong bonds with ether oxygen of PEO leading to complex web-like structure. Owing to these properties, the particles in the green and the white sample suspensions were efficiently caught into the ballasted floc structure. High-intensity mixing also contributed to the process improvement by enhancing the entrapment probability of the colloidal particles into the ballasted floc structure. In conclusion, hetero-flocculation can be an esteemed alternative to coagulant pretreatment in the case of PEO-induced flocculation of the green and the white sample suspensions.

a-)

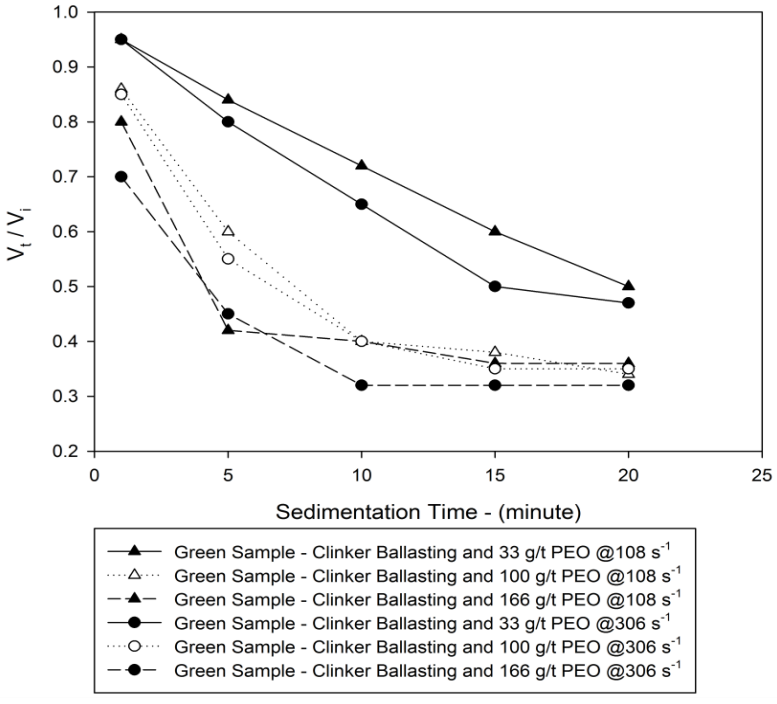

Figure 60. Time-dependent volumetric changes of clinker ballasted (10 g/l) flocculated sediments

((a) the green sample (b) the white sample, 3% solid, 3%borax, pH 9.40).

b-)

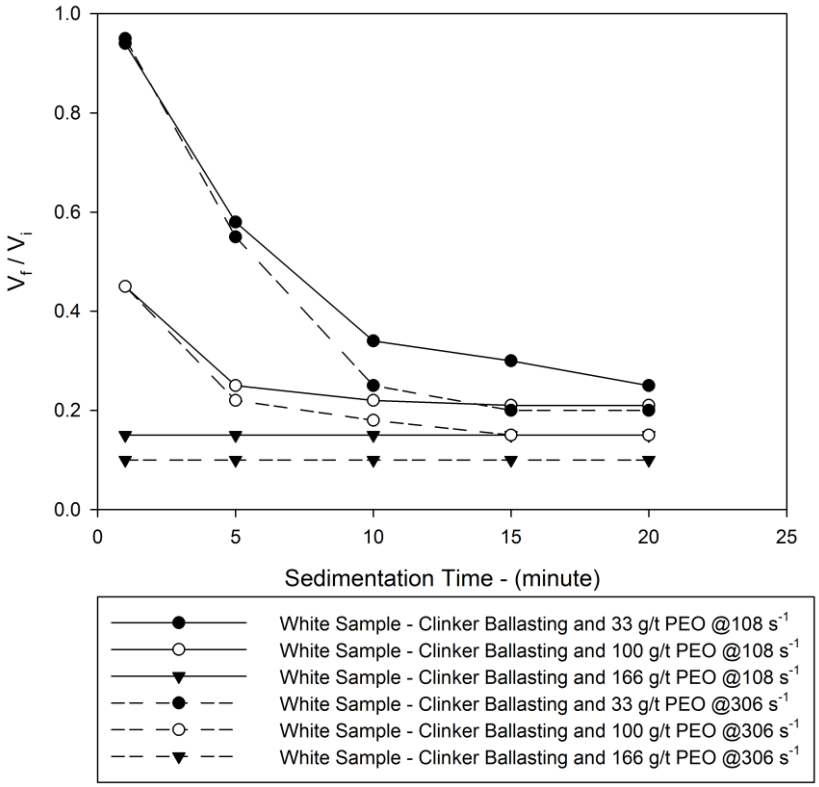

Figure 60. (continued)

In conclusion, clinker seems to be a good ballast material for the PEO-induced flocculation of these colloidal samples. The reason behind this fact can be explained with the following:

1-) Clinker was not adversely affected from intense mixing conditions due to the strong and abrasive nature and did not produce extra turbidity when it was used as ballast material for the flocculation procedure.

2-) Although clinker can be considered as an unconventional ballast material, it had some superiority over conventional ballast material such as micro-sand. In the case of the conventional micro-sand ballast treatment, (1) coagulant preconditioning – (2)

micro-sand conditioning – (3) polymer conditioning stages were applied to the suspensions respectively and the flocculation procedure becomes more complex, challenging and costly. However, the clinker ballasting instead of micro-sand eliminated the coagulant preconditioning requirement by successfully decreasing turbidity and polymer consumption at borax buffered pH in this study.

3-) Furthermore, clinker particles seem to readily form strong chemical bonds with PEO leading to strong reticular floc structures, and the colloidal particles were entrapped into these primary flocs. The resultant strong and large floc structures did not disintegrate owing to the influential interaction between clinker and PEO when the suspensions were subjected to intense mixing.

4-) The clinker particles had a great tendency to settle down by itself. Based on this property of clinker, the resultant ballasted floc structures rapidly sedimented. So, the sedimentation rate was also improved with this ballasting technique in addition to turbidity removal performance.

Currently, there is no practical use of clinker in the tailing treatment but it is used for the purpose of agglomeration in mineral processing, specifically in heap leach operations (Mular et al., 2002; Marsden & House, 2006). However, clinker may be utilized as flocculant aid in the flocculation procedures considering the above benefits.

4.3. Aqueous Chemistry Calculations

4.3.1 pH-Dependent Aqueous Chemistry Calculations of Dolomite/Clay/Borax-Containing Systems

The aqueous chemistry calculations were carried out to explain generalized pH-dependent behavior of the dilute solutions at equilibrium with the green and the white samples in borax presence. So, the diluted concentrations were preferred for

ease of calculations and reliable, interpretable results instead of the actual concentrations used in the flocculation experiments. The PHREEQC findings obtained here supported the flocculation studies with significant information.

First of all, the ionic strength values at original pH values of 9.40 were found as 6.30E-03 for the diluted green sample solution (Figure 61) and 6.28E-03 for the diluted white sample solution (Figure 62). These ionic strength values were rather high due to the dissolved borax. In spite of these high ionic strength values of the solutions, the destabilization of the green and the white sample suspensions were very challenging even if polymeric flocculants were used as mentioned previously. However, it can be claimed that the green and the white sample solutions were dominated by dissolved borax at original pH 9.40 so their aqueous chemistry resembled each other as well as the resultant figures. Then, NaOH was used to increase solution pH as in the case of previous flocculation study carried out at pH 11.50. Both of two solutions required significant amount of NaOH to adjust pH. The reason for this was the buffering effect of the dissolved borax around pH 9.40. Based on the calculation results, a perfect parallelism between NaOH consumption and ionic strength values were ascertained and this parallel behavior depending on pH between 9.40 and 12.00 were presented in Figure 61 and Figure 62. When pH was adjusted to alkaline values, ionic strength of the solutions (which was very important for the flocculation studies) was directly governed by huge amount of strong base. In conclusion, the most abundant cation in the solutions was defined as Na which came from dissolved borax and added NaOH and this predominance became stronger with increasing pH.

It was believed that increase of the ionic strength and the high amount of dissolved sodium owing to pH adjustment from 9.40 to 11.50 improved the flocculation performance (Figure 49), because increased ionic strength of the solutions made the thickness of the electrical double layers around the particles compressed. Such compression may lead to destabilization of colloidal particles by decreasing particle-particle repulsion and facilitating effective polymer adsorption on particle surfaces.

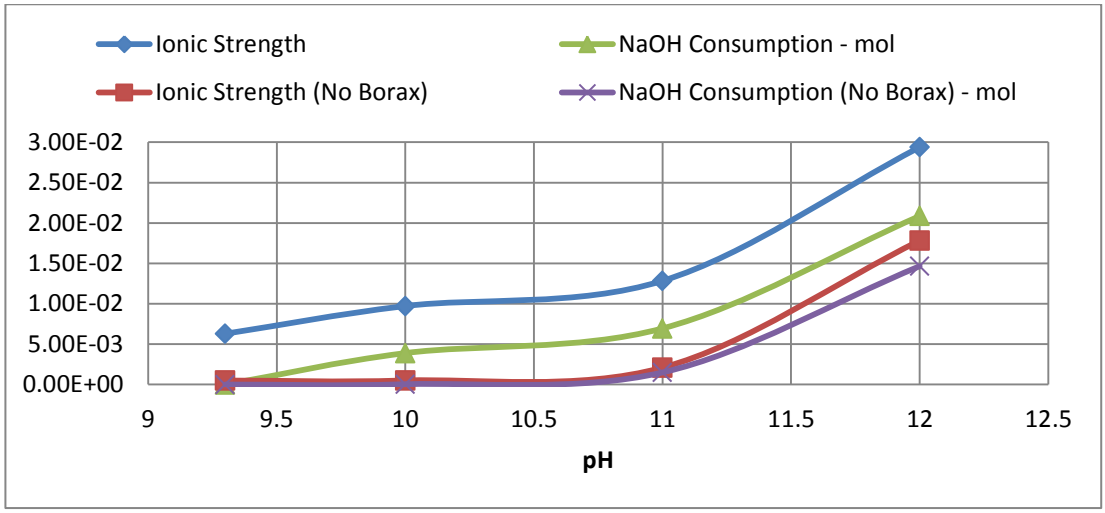

Figure 61. Ionic strength and NaOH consumption of the diluted green sample solution as a function of pH (1g solid, 1g dissolved borax in 1L pure water)

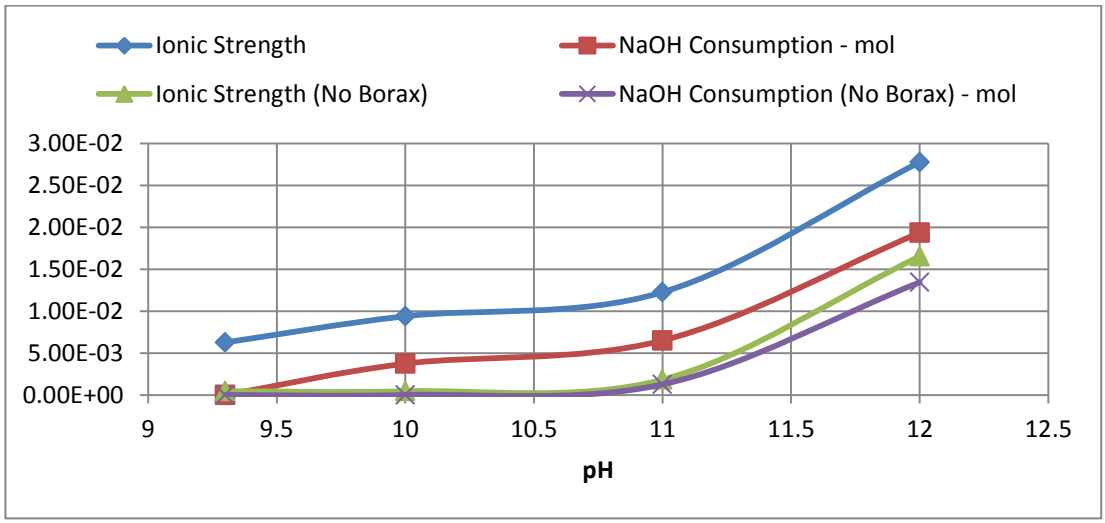

Figure 62. Ionic strength and NaOH consumption of the diluted white sample solution as a function of pH (1g solid, 1g dissolved borax in 1L pure water)

Furthermore, the cations and their aqueous species were very important in terms of the coagulation and flocculation studies (Duan & Gregory, 2003). Especially, it was proved (Bratby, 2006) that hydrolyzed species of cations had a pronounced tendency for adsorption on mineral surfaces and this tendency significantly dependent on pH of solutions. Considering these, the significant aqueous species of calcium and magnesium in terms of the flocculation were calculated with PHREEQC (llnl.dat - database) considering the reactions in Table 10.

Table 10. Important aqueous Ca and Mg species in terms of flocculation

$1.00\ H_2O + 1.00\ Ca^{++} \rightleftharpoons CaOH^{+} + 1.00\ H^{+}$
$4.00\ Mg^{++} + 4.00\ H_2O \rightleftharpoons Mg_4(OH)_4^{++++} + 4.00\ H^{+}$
$1.00\ H_2O + 1.00\ Ca^{++} + 1.00\ B(OH)_3 \rightleftharpoons CaB(OH)_4^{+} + 1.00\ H^{+}$
$1.00\ Mg^{++} + 1.00\ H_2O + 1.00\ B(OH)_3 \rightleftharpoons MgB(OH)_4^{+} + 1.00\ H^{+}$

The results in Figure 63 and Figure 64 showed that $CaOH^{+}$ increased approximately 350-fold from pH 9.40 to 11.50 both for the green and the white samples' diluted solutions. This positively charged hydrolyzed calcium species was thought as the main reason of the previous flocculation performance improvement at pH 11.50, because this calcium species strongly adsorbed on mineral surfaces and activated the surface for effective polymer adsorption. In flotation studies, pH of the solutions was also adjusted to pH 11.50 to activate quartz surface with calcium (Fuerstenau & Elgillani, 1966). Similar to the quartz flotation, it was believed that particle surfaces were activated by this hydrolyzed calcium species at this alkaline pH and ether oxygen of PEO chains established strong hydrogen bond with particles via adsorbed $CaOH^{+}$. In conclusion, $CaOH^{+}$ served as cation bridge between polymer chains and particles and improved the turbidity removal percentages, which was presented previously in Figure 49, significantly producing robust floc structures.

Another calcium species which increased with increasing pH was found out as $CaB(OH)_4^+$ and presented for both the green and white samples solutions in Figure 63 and Figure 64. These figures showed that $CaB(OH)_4^+$ species dominate $CaOH^+$ species at all pH values. Such domination of $CaB(OH)_4^+$ species is also consistent with the previous studies related to this subject and confirmed by the researchers (Mattigod et al., 1985). Increasing amunth of $CaB(OH)_4^+$ species from pH 9.40 to 11.50 is very important because this species strongly adsorb on mineral surfaces (Chaudhary et al., 2005). Mattigod, Frampton, & Lim (1985)'s study also agreed with this and they claimed further that $CaB(OH)_4^+$ species effectively competed with other species like Ca^{+2}, Mg^{+2} etc. for the available sites on mineral surfaces. In conclusion, this species had much higher affinity for the negatively charged mineral surfaces under alkaline conditions than others (Swaine & Goodarzi, 1995) and it was anticipated that $CaB(OH)_4^+$ species in pH 11.50 contributed to the flocculation performance and served as cation bridge like $CaOH^+$. Unfortunately, very limited information is present on this subject especially linking $CaB(OH)_4^+$ species to flocculation mechanism.

Contrary to hydrolyzed calcium species, the amount of $MgB(OH)_4^+$ and $Mg_4(OH)_4^{+4}$ decreased (Figure 63 and Figure 64) from pH 9.40 to 11.50 both for the diluted solutions of the green and the white samples. Although hydrolyzed cationic species were beneficial for coagulation and flocculation, it was not the case for magnesium. Many different and independent studies (Abrol et al., 1988; Agassi, 1996; Dontsova & Norton, 1999; Goyal et al., 2003; Donstova et al., 2004; Singh, 2005; Çırak, 2010) agreed with this unfavorable effect of the magnesium. It was believed that magnesium consolidated the dispersion of negatively charged particles despite the expectation for destabilization. So, magnesium species lost its significance for the benefit of coagulation and flocculation processes. The undesirable dispersion effect of small magnesium cation was explained with its very high hydration energy. When the high hydration energy combined with this compactness in size, water molecules took place firmly around magnesium. So, six water molecules were in direct contact with the central magnesium ion forming the primary hydration shell in a very tight

structure. For this reason, adsorbed magnesium on particle surfaces may decrease particle-particle and particle-polymer interaction by blocking the aggregation process.

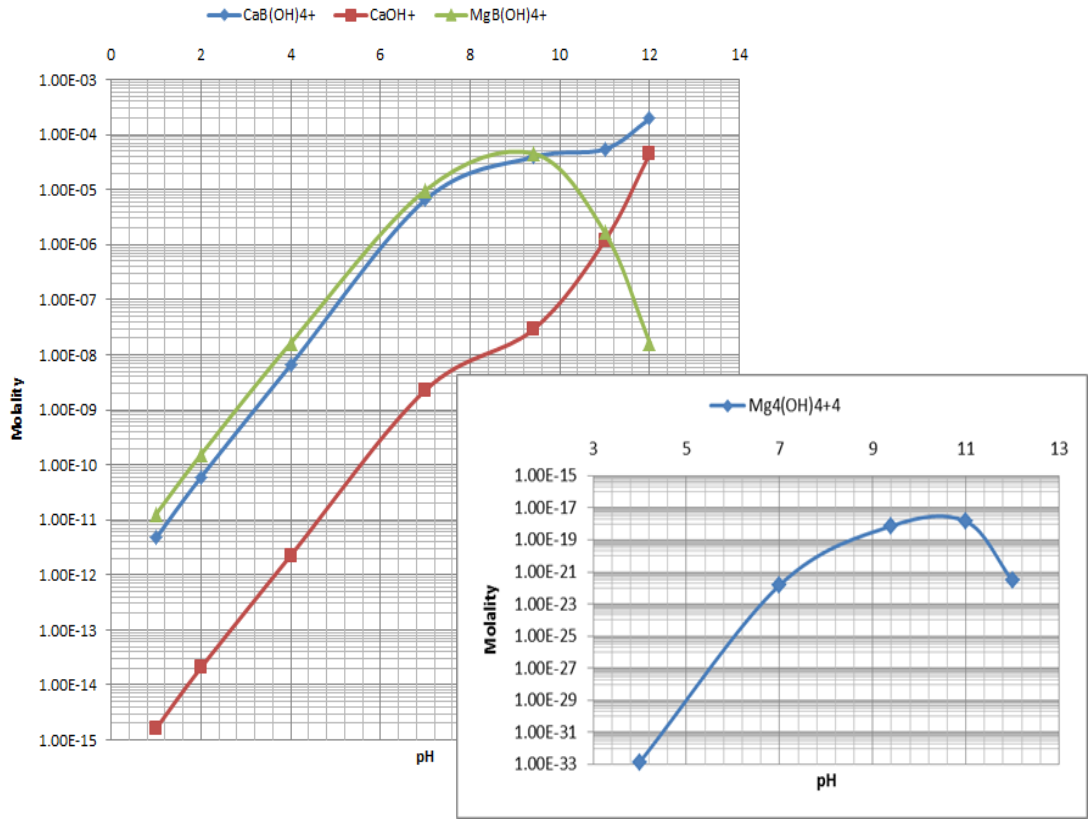

Figure 63. $CaB(OH)_4^+$, $CaOH^+$, $MgB(OH)_4^+$ and $Mg_4(OH)_4^{+4}$ species variation in the diluted green sample solution as a function of pH (1g solid, 1g dissolved borax in 1L pure water)

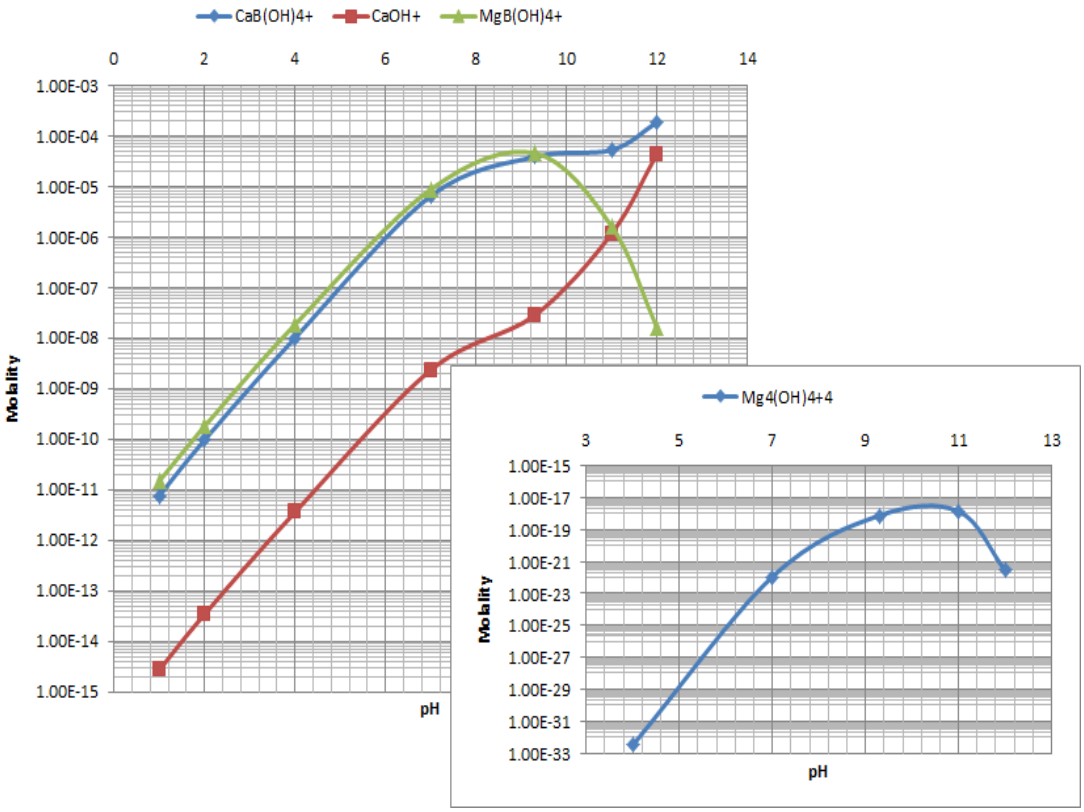

Figure 64. $CaB(OH)_4^+$, $CaOH^+$, $MgB(OH)_4^+$ and $Mg_4(OH)_4^{+4}$ species variation in the diluted white sample solution as a function of pH (1g solid, 1g dissolved borax in 1L pure water)

Considering the unfavorable effect of magnesium, increasing pH from 9.40 to 11.50 might also contribute to flocculation performance improvement. Because, when original pH of the green and the white sample solutions increased to 11.50, the total amount of dissolved magnesium in both solutions decreased and calcium domination over magnesium was observed. The ratios of Ca_{Total}/Mg_{Total} were given in Figure 65 and Figure 66 and these figures also explained the decrease in $MgB(OH)_4^+$ and $Mg_4(OH)_4^{+4}$ species in Figure 63 and Figure 64. Furthermore, a very similar result related to Ca_{Total}/Mg_{Total} ratio as a function of pH was reported in a recent flotation study by Laskowski & Castro (2012). The reason of decrement of magnesium in both solutions was disclosed with the transition to a solid phase. Saturation indexes of

several possible solid phases were calculated in this study and it was found that only $Mg(OH)_2$ had a saturation index exceeding zero. The increase in the saturation indexes of $Mg(OH)_2$ phases was presented in Figure 65 and Figure 66. This means that magnesium in the solutions precipitated as $Mg(OH)_2$ at high pH values according to Table 11.

Table 11. $Mg(OH)_2$ precipitation according to the related coding line in PHREEQC-llnl.dat

$1.00\ Mg^{++} + 2.00\ H_2O \Rightarrow Mg(OH)_{2(Solid)} + 2.00\ H^{+}$

If magnesium caused a dispersion of the green and the white sample particles, the removal of the dissolved magnesium in the form of a solid precipitate at pH 11.50 may also help the flocculation of the green and the white sample suspensions in previous study (Figure 49). This property of magnesium was recently revealed in mineral processing studies, especially, the dispersion/depression effect of magnesium in industrial and batch lab size flotation studies was clearly shown by the researchers (Cheng et al., 2010; Haselhuhn et al., 2012).

In addition to the calcium and magnesium species, boron species of the green and the white sample containing solutions were also analyzed and presented in Figure 67 and Figure 68. The results showed that the amounts of total dissolved boron were fixed at all pH values so B_{Total} trend lines in Figure 67 and Figure 68 were horizontal to x – axis. This means that no boron phases precipitated as a function of pH at room temperatures differing from metal cations like aluminum, iron etc. For this aqueous chemistry behavior of boron, the removal of the element from the solutions becomes very costly, troublous and laborious (Cornwell et al., 2006; Rahman, 2009; Acton, 2012; Yilmaz et al., 2012). As well as the removal procedure, the stable boron

presence throughout pH ranges 2-12 makes the management of the buffered solution more difficult as in this study.

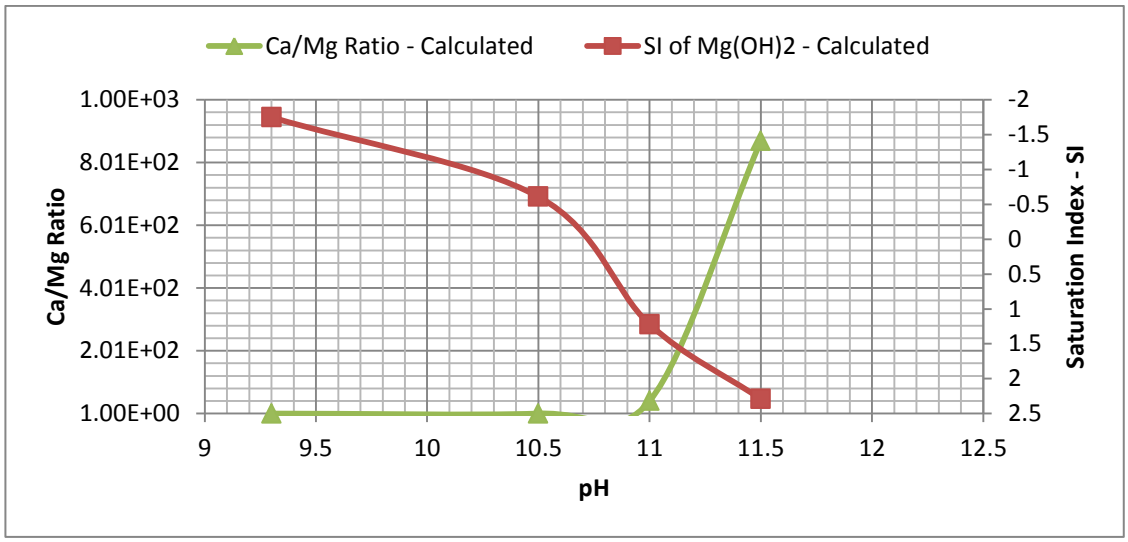

Figure 65. Ca_{Total}/Mg_{Total} variation in the diluted green sample solution as a function of pH (1g solid, 1g dissolved borax in 1L pure water)

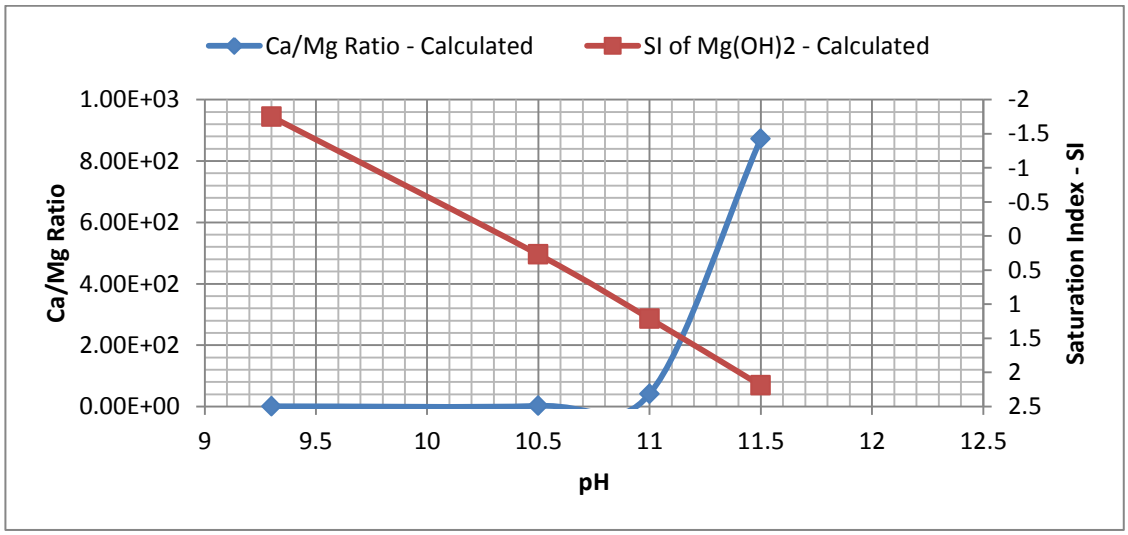

Figure 66. Ca_{Total}/Mg_{Total} variation in the diluted white sample solution as a function of pH (1g solid, 1g dissolved borax in 1L pure water)

Furthermore, the amount of calcium-boron, $CaB(OH)_4^+$ and sodium-boron, $NaB(OH)_4$ species increased with increasing pH, but not the magnesium-boron, $MgB(OH)_4^+$ species due to the previously mentioned chemical balance. The role of these species on the flocculation mechanism has not been studied in the literature; however, calcium-boron and magnesium-boron species may lead to coagulation of negatively charged colloids via charged neutralization. Based on this inference, sodium-boron species can be considered as useless due to zero electro-valency. When Figure 67 and Figure 68 were analyzed according to the domination of species, it can be roughly divided into two major regions. First region was dominated by boric acid species at pH values smaller than 9-10 and second region was dominated by tetrahydroxoborate species at pH range greater than 9-10 (Schweitzer & Pesterfield, 2009). As a matter of fact, the pH value between 9 and 10 in Figure 67 and Figure 68 refers to the chemical equilibrium point of the introduced mineral phases of the green and the white samples in the presence of borax. The pH measurement of the actual prepared suspensions confirmed these calculated equilibrium points revealing a buffering zone exactly at pH 9.4. Unlike boric acid and tetrahydroxoborate species domination of the solutions, a very weak boron species presence was observed. This anionic species (Yamahira et al., 2007) was in the form of $B_2O(OH)_5^-$. Nevertheless, its importance in terms of the solution chemistry and the destabilization may be ignored due to the small amount throughout the pH values.

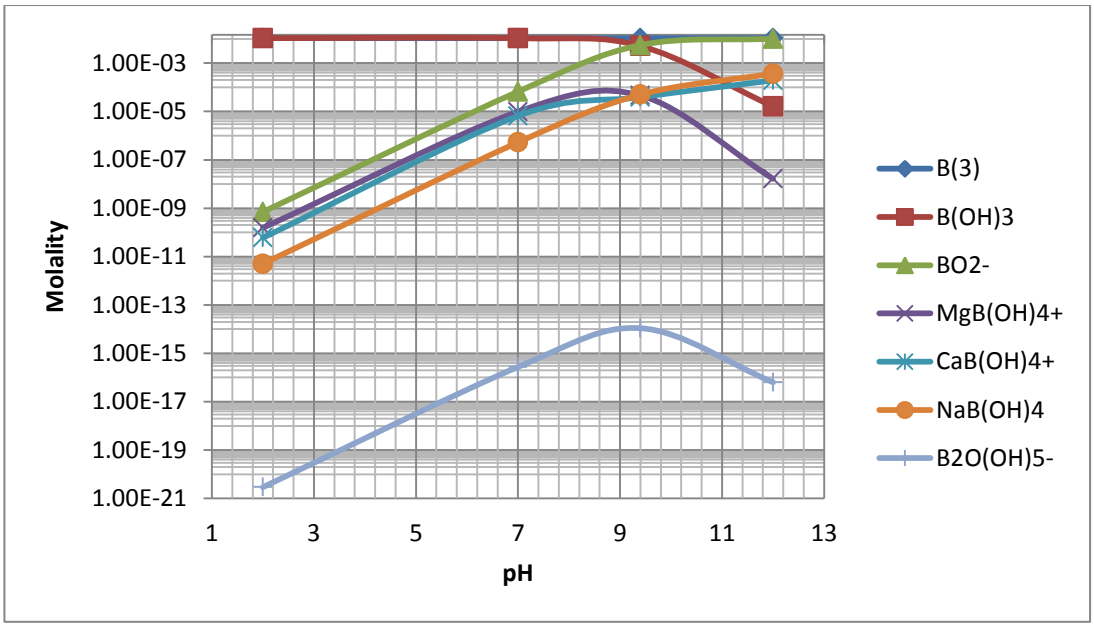

Figure 67. Boron species variation in the diluted green sample suspension as a function of pH (1g solid, 1g dissolved borax in 1L pure water)

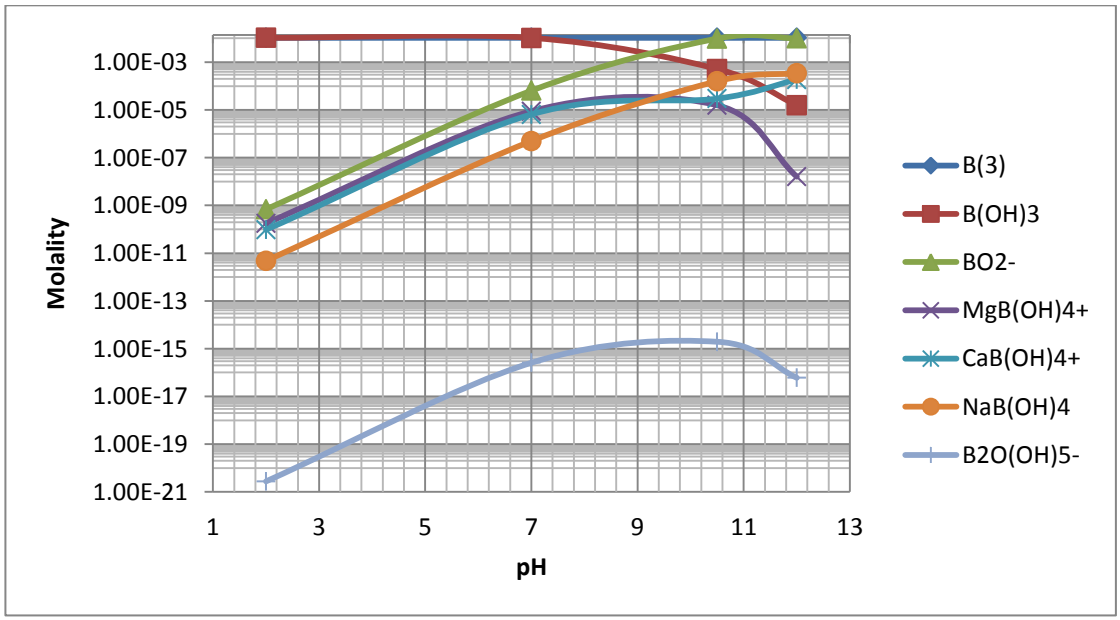

Figure 68. Boron species variation in the diluted white sample suspension as a function of pH (1g solid, 1g dissolved borax in 1L pure water)

Note: B(3), B(OH)3, MgB(OH)4+, CaB(OH)4+, NaB(OH)4, B2O(OH)5- and BO2- in coding refers to B_{Total}, $B(OH)_3$, $MgB(OH)_4^+$, $CaB(OH)_4^+$, $NaB(OH)_4$, $B_2O(OH)_5^-$ and BO_2^- ,respectively.

As a summary, increasing pH from original 9.40 to 11.50 improved flocculation performance due to these three main reasons:

1- The amounts of $CaOH^+$ and $CaB(OH)_4^+$ species increase with increasing pH. Most probably, particle-polymer interaction was enhanced due to these species which serves as efficient cation bridge between them.
2- Ionic strength increase with increasing pH that may lead to compression of the electrical double layer around particle due to significant amount of NaOH addition into the borax-buffered solutions.
3- Mg_{Total}, $MgB(OH)_4^+$ and $Mg_4(OH)_4^{+4}$ species decrease in the solution due to pH increase because Mg may cause dispersion due to its high hydration energy.

In conclusion, these findings may explain the mechanism and the requirement for the efficient flocculation process of the green and the white sample suspensions. As it was previously presented, adjusting pH to 11.50 significantly removed turbidity and very clean supernatant was obtained with a well-compacted sediment volume after the flocculation via PEO.

4.3.2. Durability of Individual Globular Pellet Floc Formed at pH 11.50 and Aqueous Chemistry Calculation inside the Polymeric Barrier

As mentioned previously, PEO addition to the green and the white sample suspensions at pH 11.50 produced firm globular flocs. These globular structures looked like pellets and so they generally called as pellet flocs. These pellet flocs were very intriguing due to their durability. To individually analyze the robustness of this type of globular floc structure, two dispersions were prepared including 1 g solid sample and 1 g dissolved borax in 0.5 kg distilled water. Then, all dispersed colloidal particles were agglomerated into a single globular pellet floc with each of each green and white sample using 666 g/t PEO at 108 s^{-1} and pH 11.50. As a result of this

procedure, a single globular pellet floc was obtained in clean water which had turbidity values of almost zero for both the green and the white sample.

Later on, these green and white globular pellet flocs were subjected to severe mixing conditions at 563 s^{-1} for 40 minutes (Figure 69). The aim of this was to observe any breakage of the green and white globular pellet flocs as a function of turbidity at very high velocity gradient value. However, expected turbidity change due to the intense mixing could not be validated even at the end of the long mixing period. No turbidity change proved that these green and white globular pellet flocs were very firm as a single mass and these polymer-induced structures were very durable against severe mixing.

Then, highly acidic condition at pH 2.00 associated with severe hydrodynamic disturbance at 563 s^{-1} to test the breakage of the green and the white globular pellet flocs (formed at pH 11.50) as a function of turbidity for 40 minutes. At this time, the pellet flocs were tried to be destroyed both physically and chemically however single globular mass was conserved for each case even under acidic conditions and no significant turbidity change was observed (Figure 69). This was a rather strange case because polymer chains and also flocs were known to be fragile / sensitive to mixing especially under acidic conditions (Bratby, 2006). However, this was not the case for the globular pellet flocs formed at pH 11.50.

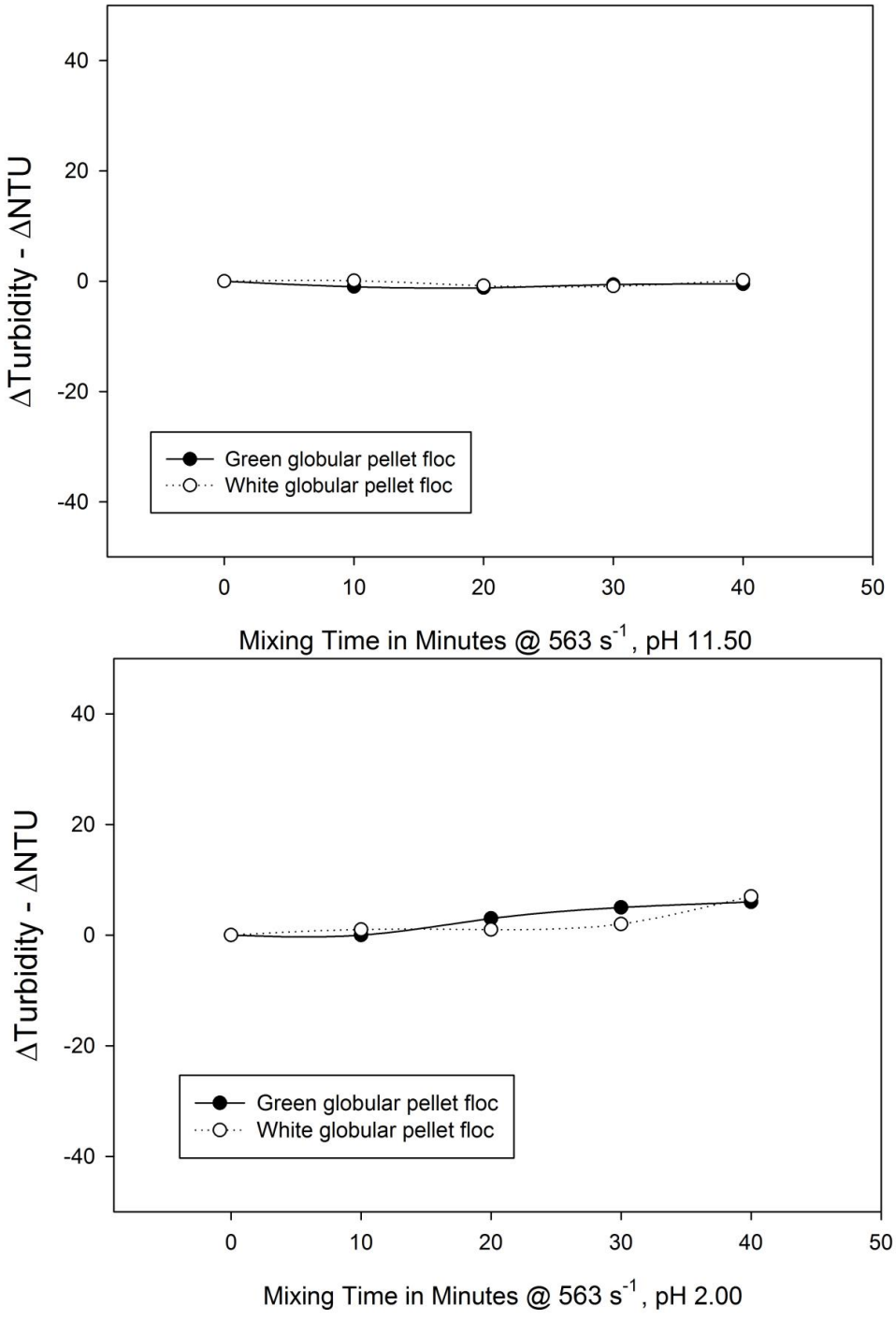

Figure 69. Turbidity change against intensive mixing condition during 40 minutes period right after the globular pellet flocs formed.

In addition to remarkable robustness of these globular pellet flocs presented above, a peculiar behavior was observed for those which were subjected to acidic conditions together with severe mechanical mixing. The fine particles that agglomerated into the globular pellet flocs did not decompose and disperse into the suspension and, they preserved their pellet like forms. Nonetheless, the globular pellet flocs started to rise and float inside the beaker when pH was decreased from pH 11.50 down to around 5.50 for both the green and the white samples. Furthermore, the globular pellet flocs completely floated at pH 2.00. Although the hydrophobicity initially came into mind, PHREEQC calculations, which were carried out to identify the variation in the composition of the aqueous chemistry inside these pellet flocs, revealed the actual mechanism lied behind this behavior. According to the results, dolomite minerals captured in the globular pellet floc structure started to dissolve with decreasing pH as follows (Marini, 2007):

$$Ord - dolomite + 2H^{+} = Ca^{+2} + Mg^{+2} + 2HCO_3^{-}$$

As expected, dolomite released Ca, Mg and HCO_3^-. However, it was intriguing that PEO around the globular pellet floc behaved like a polymer barrier. This barrier had semi-permeable character. Small hydrogen ions managed to diffuse through this semi-permeable polymeric barrier and the hydrogen concentration inside the pellet floc increased leading to decrease in the internal pH. This increase in the concentration of H^+ and HCO_3^- promoted the following reaction and as a result liquid water and $CO_{2(g)}$ were formed (Marini, 2007):

$$HCO_3^{-} + H^{+} = H_2O + CO_{2(g)}$$

The saturation index of $CO_{2(g)}$ inside the pellet structure was calculated as a function of pH and presented in Figure 70. The saturation index of $CO_{2(g)}$ always had a negative value between pH 11.50 and 5.5. However, when pH decreased further to acidic levels ≤ 5.5, the saturation index of $CO_{2(g)}$ became equal and greater than zero. This referred that $CO_{2(g)}$ started to form at pH 5.5 and below inside the floc structure. Although, small hydrogen ions diffused through the semi-permeable PEO barrier, large $CO_{2(g)}$ could not pass through this barrier. As a result, $CO_{2(g)}$ – bubble was

entrapped (Figure 71) inside the pellet floc due to potently adsorbed PEO barrier around the globular pellet floc. In conclusion, the formation of $CO_{2(g)}$ - bubble made the density of the pellet floc smaller by increasing its volume and promoted the peculiar flotation behavior.

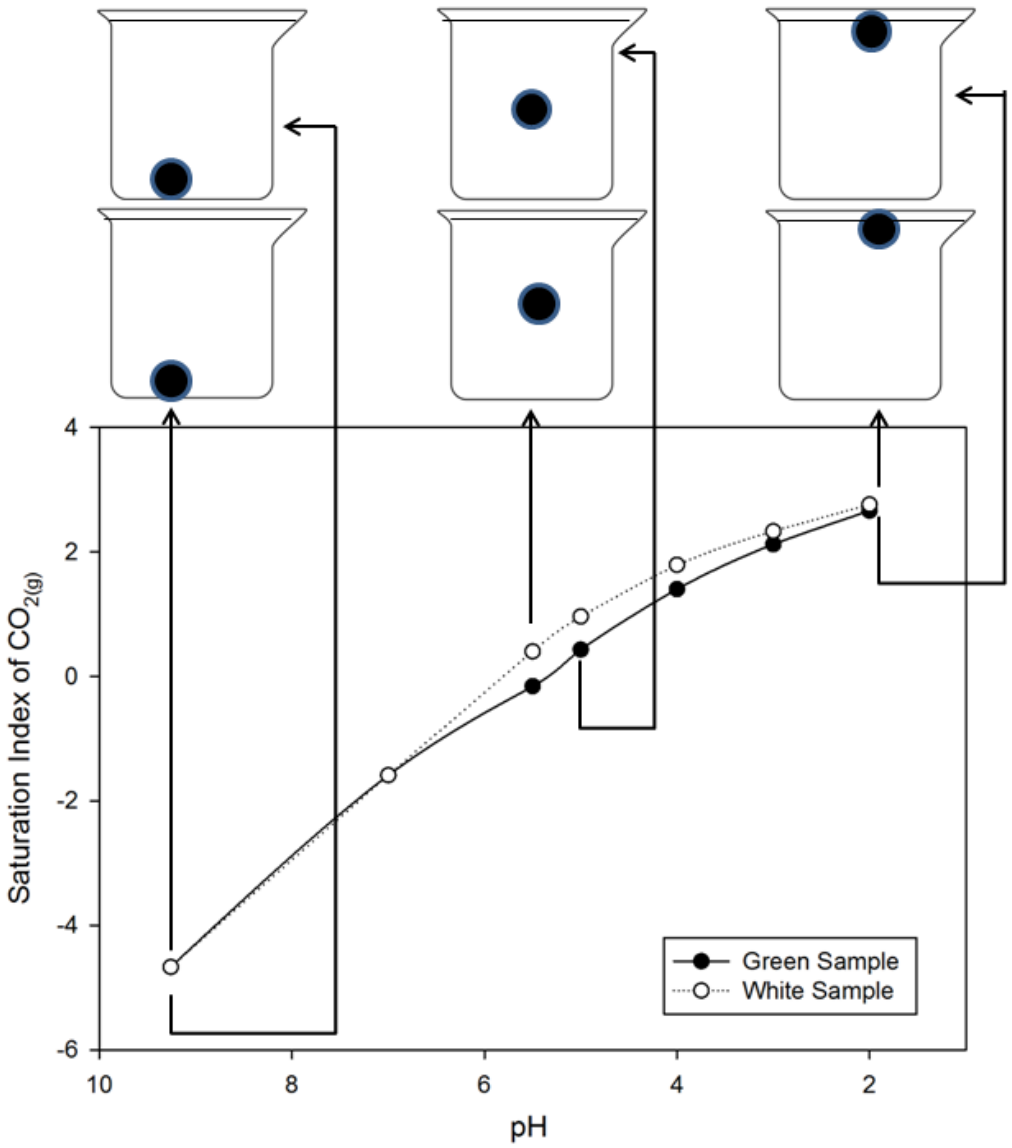

Figure 70. Saturation Index of $CO_{2(g)}$ inside the pellet floc
(via Pitzer.dat database)

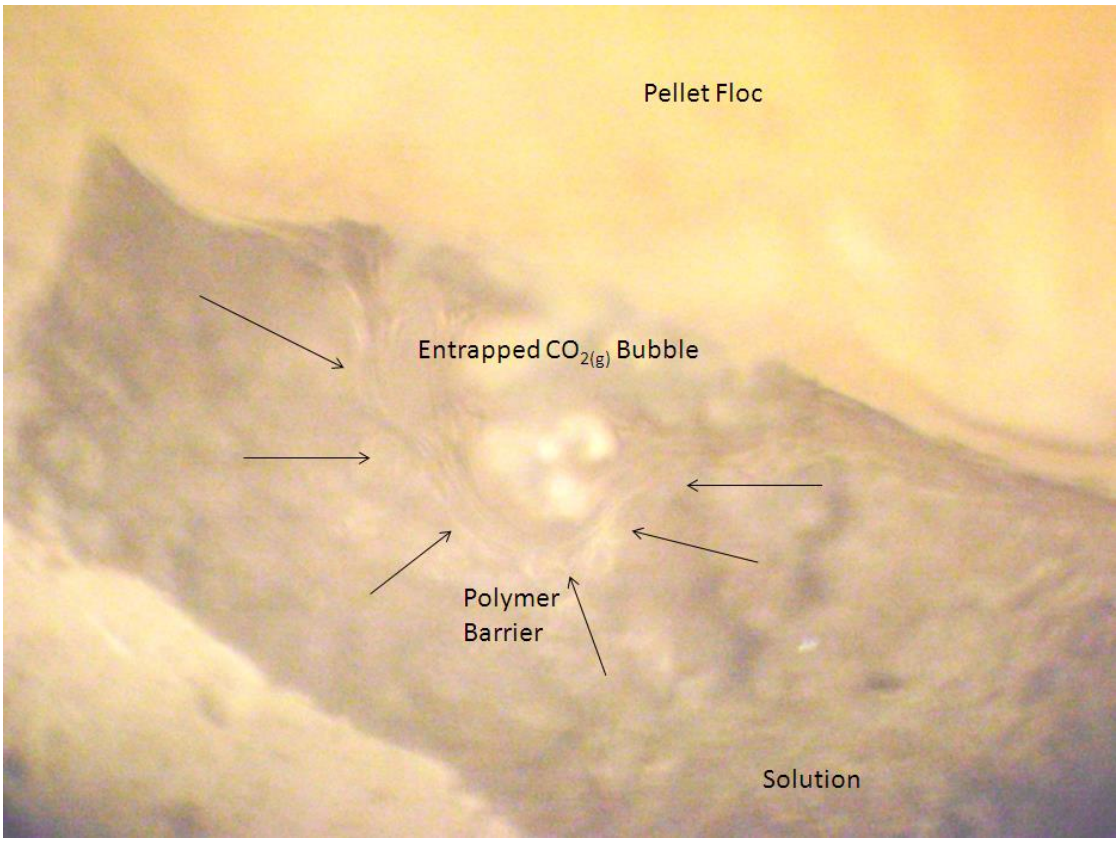

Figure 71. An example of $CO_{2(g)}$ bubble exposed to surface of the pellet floc.

4.3.3. pH-Dependent Aqueous Chemistry Calculations of Coagulant Solutions

Firstly, Cu^{++} coagulant was tested to improve flocculation performance of the green and the white sample suspensions. However, the result of the flocculation tests proved previously that Cu^{++} coagulants were inefficient. This inefficiency was related to the aqueous chemistry of the suspensions and explained with the PHREEQC calculations. The original pH of the copper solution was highly acidic at 4.0 and copper completely dissolved at this pH. But, the borax presence increased pH of the solution and made all dissolved copper in the solution precipitated. PHREEQC results (Table 12) indicated an obvious solid phase presence with a saturation index of zero at pH 9.4. This solid phase was found as light blue crystals (Figure 72) in the

form of $Cu(OH)_2$. The related literature information was also agreed with this finding (Young & Thomas , 1999). So, there was no copper cation in the solution to adsorb on the negatively charged particle surfaces and this shortcoming that stemmed from the aqueous chemistry resulted in the insufficient destabilization of colloidal particles although the suspensions were preconditioned with a very high amount of copper coagulants.

Secondly, Al^{+++} coagulant was used for the purpose of preconditioning. As mentioned before, it did not affect the stability of the system as expected. The reason behind this fact was tried to be explained with the help of aqueous chemistry calculations. When aluminum sulphate was dissolved in distilled water, pH decreased down to 3.3 (Table 13). It means that aluminum sulphate solution had an acidic character. It was seen at this pH that aluminum sulphate was completely dissolved by producing clear solution. However, Al^{+++} cations started to precipitate immediately when the solution was equilibrated with borax because borax presence increased the solution pH up to 9.4. At this high pH value, aluminum sulphate was completely dissociated and precipitated as a different solid phase (also confirmed by (Eble & Mersmann, 1999)). PHREEQC calculations showed that only phase reached to the saturation index of zero (Table 13) at pH 9.4 was AlO(OH). This means that the aluminum cations precipitated as white crystal (Figure 72) in the form of AlO(OH). In conclusion, no dissolved aluminum became present in this alkaline solution. Based on this fact, aluminum aquacomplex and their hydrolysis products did not formed in the solution and due to the lack of these dissolved aluminum ions in the system they could not promote the flocculation of the colloidal particles in the suspensions.

Thirdly, another widely used coagulant, ferric sulphate was tested for the purpose of flocculation performance improvement. Similar to copper sulphate and aluminum sulphate coagulants, ferrous sulphate preconditioning did not produce expected turbidity removal of the green and the white sample suspensions. When the ferric sulphate solution, which was originally acidic in nature, was analyzed with

PHREEQC considering the buffered pH by dissolved borax, it was found that iron cations precipitated (Table 14) as red-brown crystals (Figure 72) in the form of FeO(OH) (confirmed by Hill & Holman, (2000)). Since no dissolved iron species was present in the solutions, the expected iron adsorption on the particle surface did not actualize. In conclusion, the high amount of the ferric sulphate coagulant dosing did not affect the flocculation procedure at desired level due to the precipitation at high pH.

Table 12. Copper Sulphate Solutions at the original and the buffered pH

Copper Sulphate Solution – 1 (in distilled water; no borax)	Copper Sulphate Solution – 2 (in distilled water; 3% borax)
pH = 4.0 (Original pH)	pH = 9.4 (Increased from original pH)
Initial Copper Sulphate Phase = $10x10^{-2}$ in moles	Initial Copper Sulphate Phase = $10x10^{-2}$ in moles
Final Copper Sulphate Phase = 0.00 in moles	Final Copper Sulphate Phase = 0.00 in moles
Saturation Index of $Cu(OH)_2$ = -1.45	Saturation Index of $Cu(OH)_2$ = 0.00
Amount of $Cu(OH)_2$ Phase = 0.00 in moles	Amount of $Cu(OH)_2$ Phase ~$10x10^{-2}$ in moles

Table 13. Aluminum Sulphate Solutions at the original and the buffered pH

Aluminum Sulphate Solution – 1 (in distilled water; no borax)	Aluminum Sulphate Solution – 2 (in distilled water; 3% borax)
pH = 3.3 (Original pH)	pH = 9.4 (Increased from original pH)
Initial Aluminum Sulphate Phase = $10x10^{-2}$ in moles	Initial Aluminum Sulphate Phase = $10x10^{-2}$ in moles
Final Aluminum Sulphate Phase = 0.00 in moles	Final Aluminum Sulphate Phase = 0.00 in moles
Saturation Index of AlO(OH) = -0.20	Saturation Index of AlO(OH) = 0.00
Initial AlO(OH) Phase = 0.00 in moles	Final AlO(OH) Phase ~$20x10^{-2}$ in moles

Table 14. Ferric Sulphate Solutions at the original and the buffered pH

Ferric Sulphate Solution – 1 (in distilled water; no borax)	Ferric Sulphate Solution – 2 (in distilled water; 3% borax)
pH = 2.0 (Original pH)	pH = 9.4 (Increased from original pH)
Initial Ferric Sulphate Phase = $10x10^{-2}$ in moles	Initial Ferric Sulphate Phase = $10x10^{-2}$ in moles
Final Ferric Sulphate Phase = 0.00 in moles	Final Ferric Sulphate Phase = 0.00 in moles
Saturation Index of FeO(OH) = -0.49	Saturation Index of FeO(OH) = 0.00
FeO(OH) Phase = 0.00 in moles	FeO(OH) Phase ~$20x10^{-2}$ in moles

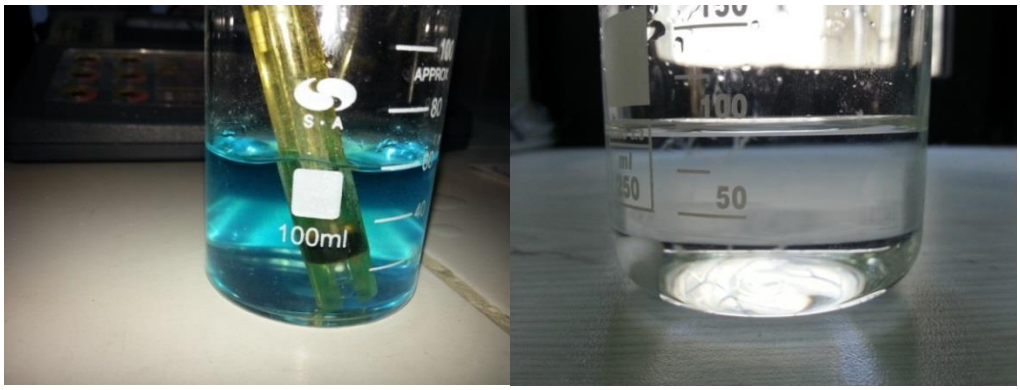

a-) Copper Sulphate Solution b-) Aluminum Sulphate Solution

c-) Ferric Sulphate Solution

Figure 72. Coagulant solutions and their precipitates at pH 9.4

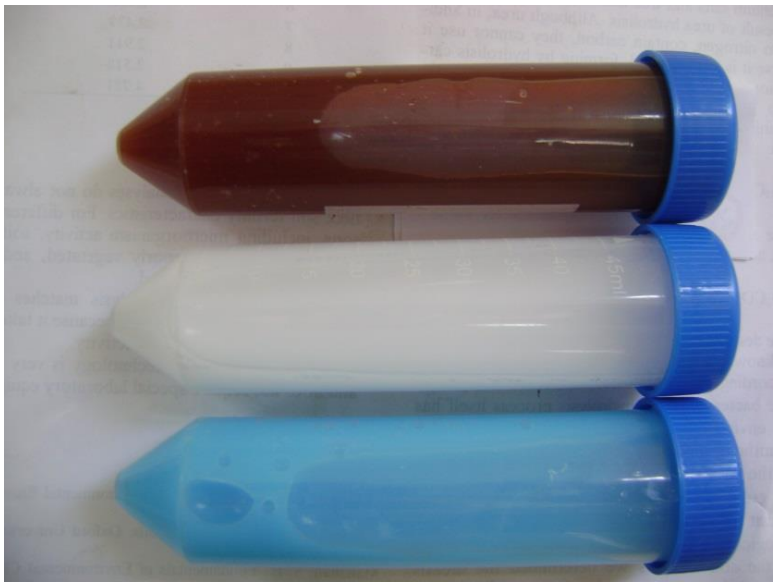

d-) Precipitation of metal coagulants at pH 9.4 (precipitated copper at the bottom; precipitated aluminum at the middle; precipitated iron at the top)

Figure 72. (continued)

Contrary to aluminum, copper and iron coagulants, calcium chloride preconditioning significantly contributed to the turbidity removal procedure of the green and the white sample suspensions. When calcium chloride solution was analyzed via PHREEQC, it was seen that calcium was completely dissolved in distilled water. Furthermore, it was also in a completely dissolved state at pH 9.4 unlike previous coagulants. According to aqueous chemistry calculations, $Ca(OH)_2$ was the closest phase to precipitate at high pH. However, the saturation index of $Ca(OH)_2$ was found as -10.08 in its original pH and -5.28 in buffered pH (Table 15). These values had a negative sign and referred to no precipitation of $Ca(OH)_2$. For this reason, calcium chloride produced very clear solutions without color generating solid phase at these pH values. Moreover, the beneficial calcium species amount increased with increasing pH like $CaOH^+$ as proven previously. At the borax-buffered pH, this species was present but not maximized. So, it should be remembered that the calcium

preconditioning improve the flocculation but it could not take full advantage of $CaOH^+$ at pH 9.4. To make the most of hydrolyzed calcium species, pH of the solutions should be increased to 11.5 as mentioned previously.

Table 15. Calcium Chloride Solutions at original and buffered pH

Calcium Chloride Solution – 1	Calcium Chloride Solution – 2
pH = 7.0 (Original pH)	pH = 9.4 (Increased from original pH)
Initial Calcium Chloride Phase = $10x10^{-2}$ in moles	Initial Calcium Chloride Phase = $10x10^{-2}$ in moles
Final Calcium Chloride Phase = 0.00 in moles	Final Calcium Chloride Phase = 0.00 in moles
Saturation Index of $Ca(OH)_2$ = -10.08	Saturation Index of $Ca(OH)_2$ = -5.28
$Ca(OH)_2$ Phase = 0.00 in moles	$Ca(OH)_2$ Phase = 0.0 in moles

Similar to the calcium preconditioning, manganese preconditioning prior to the PEO treatment substantially improved the flocculation performance both for the green and the white sample suspensions. To understand manganese effect as coagulant, its solution was analyzed with PHREEQC in the absence and presence of borax. The results were shown in Table 16. The saturation indexes of all solid Mn-phases were smaller than zero at the original pH. These results indicated that manganese sulphate completely dissolved in distilled water. Contrary to the previous calcium case presented in Table 15, manganese sulphate solution produced solid precipitates at borax-buffered pH 9.40. The saturation index of $Mn(OH)_2$ phase reached to zero at this high pH and %90 of the added Mn-cations chemically transformed into this light pink solid phase (Figure 73-b). Although most of the manganese precipitated at pH 9.40, the remaining Mn-cations significantly improved the flocculation of the colloidal suspensions. The reason behind this fact tried to be explained with the speciation calculations. The findings (Figure 74) showed that the hydrolyzed species $Mn_2(OH)_3^+$ became maximized exactly at pH 9.40 in spite of the previously

mentioned $Mn(OH)_2$ precipitation. $Mn_2(OH)_3^+$ species adsorbed strongly on the colloid surfaces like $CaOH^+$ and it served as an activator between the particles and the flocculant in the presence of borax. Very similar activating property of manganese was observed in the previous quartz flotation study (Fuerstenau et al., 1985) carried out at pH 9.40. It can be concluded that manganese cations can successfully activate the surfaces of the colloidal particles in both the green and the white sample at pH 9.40 for improved PEO adsorption.

Table 16. Manganese Sulphate Solutions at original and buffered pH

Manganese Sulphate Solution – 1	Manganese Sulphate Solution – 1
pH = 4.5 (Original pH)	pH = 9.4 (Increased from original pH)
Initial Manganese Sulphate Phase = $10x10^{-2}$ in moles	Initial Manganese Sulphate Phase = $10x10^{-2}$ in moles
Final Manganese Sulphate Phase = 0.00 in moles	Final Manganese Sulphate Phase = 0.00 in moles
Saturation Index of $Mn(OH)_2$ = -13.63	Saturation Index of $Mn(OH)_2$ = 0.00
$Mn(OH)_2$ Phase = 0.00 in moles	$Mn(OH)_2$ Phase = $9.16x10^{-2}$ in moles

a-) 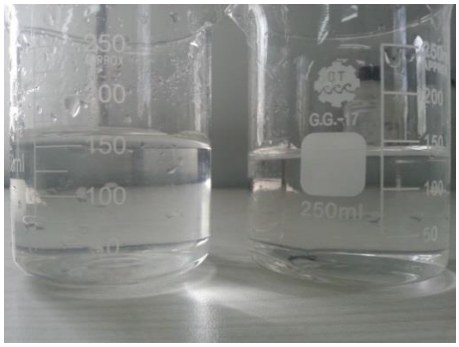

b-) 

Figure 73. Calcium (-a-) and Manganese (-b-) solutions at original (beakers at the left) pH and at buffered pH (beakers at the right).

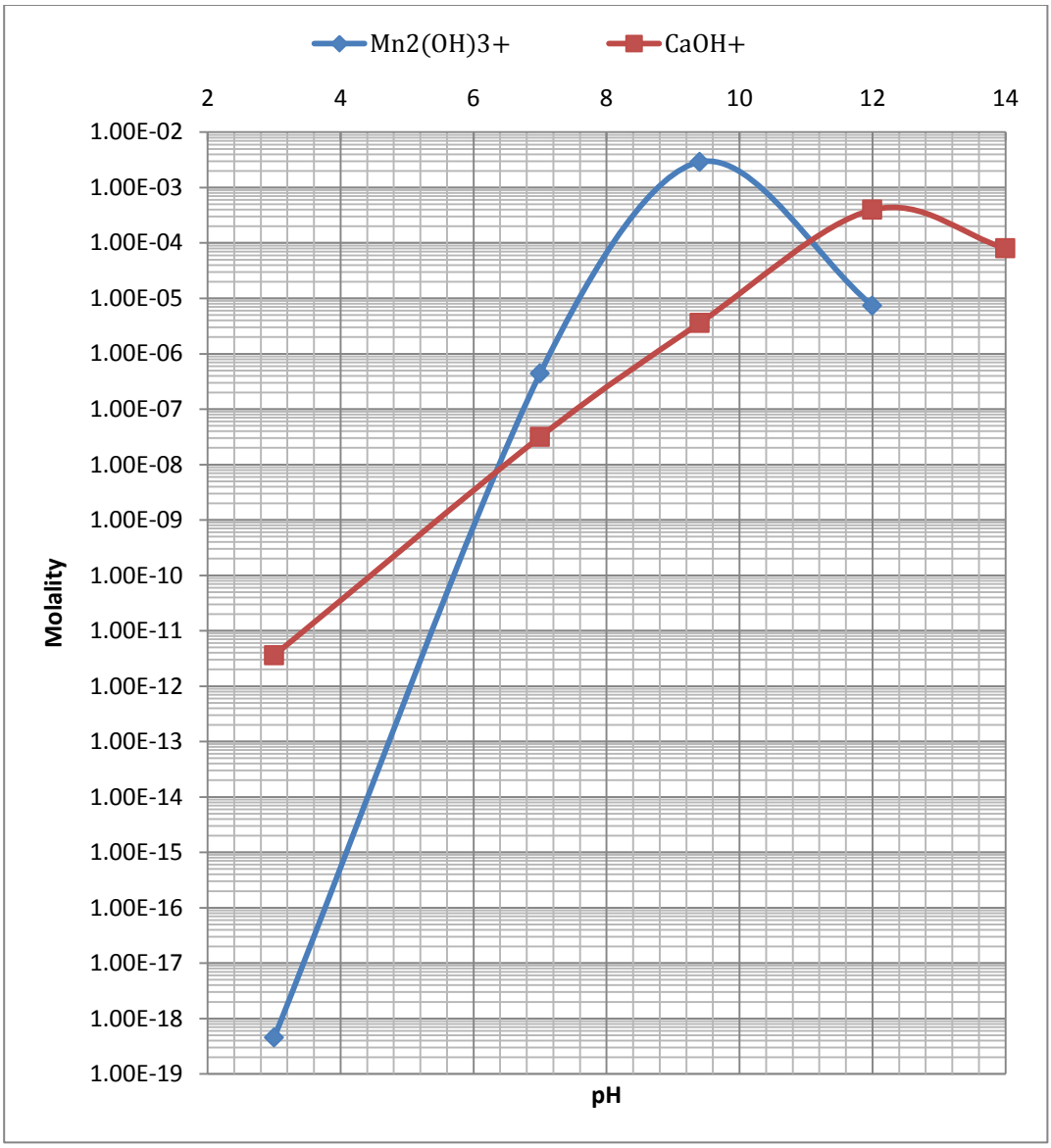

Figure 74. Comparison of $Mn_2(OH)_3^+$ and $CaOH^+$ species depending on pH in 0.1 M calcium coagulant solution and 0.1 M manganese coagulant solution

4.4. Viscosity Measurements

4.4.1. Viscosity Measurement of the Polymer Solution

Viscosity measurements produced an impressive amount of information about the PEO behavior in 0.05% aqueous solution. The findings illuminated especially the flocculation studies related to mixing intensity and high temperature effect. The standard Brookfield disk spindle was used for the viscosity measurement of the PEO solution. With the help of this attachment, percent torque and rpm values were measured and plotted in log-log form in Figure 75 (at 25 °C) and Figure 76 (at 75 °C). A linear line with increasing tendency was observed for each of these graphs. Linear regression was applied to the collected data to mathematically express these lines. The aim of this was to find the flow behavior index for the polymers as suggested by (Steffe & Daubert, 2006). The flow behavior index actually is represented by the coefficient of x in the form of a linear regression formula (y=ax+b). The summary of the regression statistic based on the collected data was demonstrated in Table 17. According to the regression results, the constant of x was found as 1.5441 for the line in Figure 75 and 1.9789 for the line on Figure 76. The reference value for the flow behavior index is 1. If it was equal to 1, it would be a Newtonian fluid. Water can be given as a most specific example and its viscosity was always constant independent to applied shear rate. If it was less than 1, it would be a pseudoplastic a specific case of non-Newtonian fluid. These type non-Newtonian fluids were very common and most of the polymeric flocculants (Williams, 1992; Fourie, 2006; Rashidi, 2010) can be given as example. Especially, high molecular mass non-ionic water soluble polymers (Burggraaf & Cot, 1996) including PEO solutions (Tripathy & De, 2006) were mostly known with their strong pseudoplasticity. However, the flow behavior indexes of the polymer solutions in this study were found greater than 1. These values were less common and rarely encountered in general rather than the other cases. The large flow behavior indexes referred to another specific case of non-Newtonian fluid which called as dilatant.

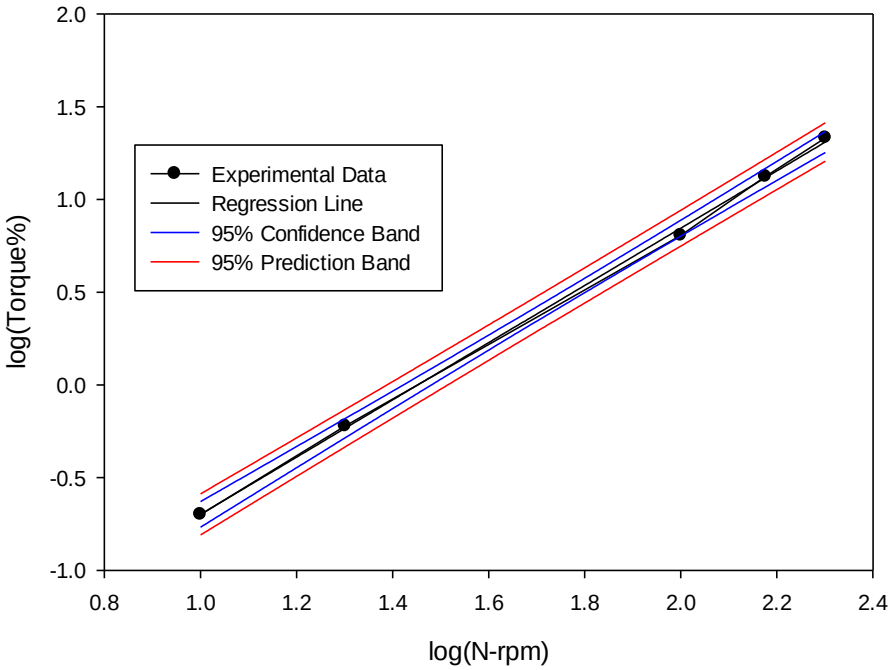

Figure 75. Regression for the measured data at 25 °C

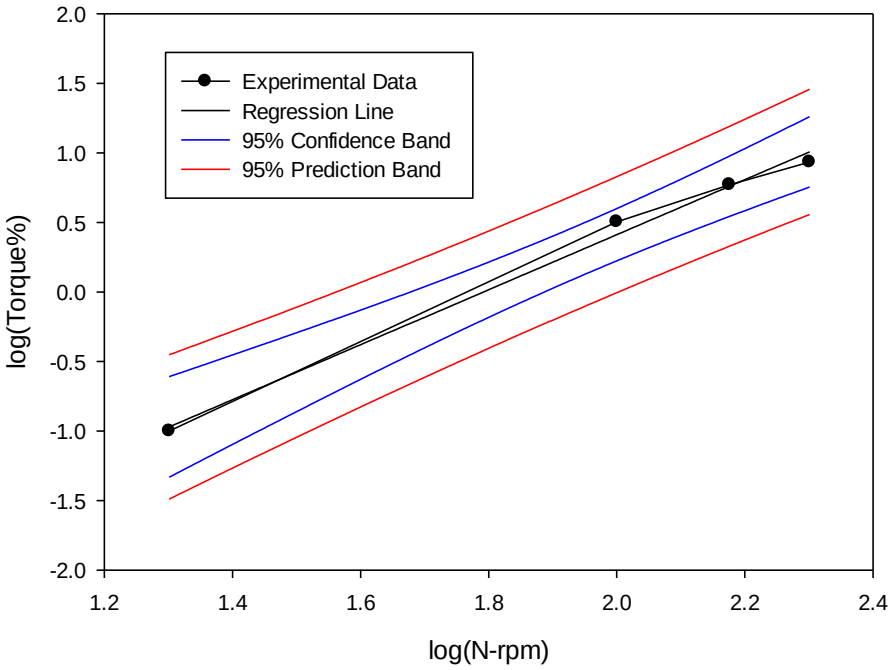

Figure 76. Regression line for the measured data at 75 °C

Table 17. Statistics of regression procedure

Prepared polymer solution at 25 °C Equation: Linear in the form of (y = b + a*x)				
R	**Rsqr**	**Adj. Rsqr**	**Standard Error of Estimate**	
0.9996	0.9993	0.9991	0.0272	
	Coefficient	**Std. Error**	**t**	**P**
b	-2.2426	0.0434	-51.6343	<0.0001
a	***1.5441***	0.0237	65.0193	<0.0001
Prepared polymer solution at 75 °C Equation: Linear in the form of (y = b + a*x)				
R	**Rsqr**	**Adj. Rsqr**	**Standard Error of Estimate**	
0.9968	0.9936	0.9905	0.0865	
	Coefficient	**Std. Error**	**t**	**P**
b	-3.5455	0.2219	-15.9806	0.0039
a	***1.9789***	0.1119	17.6842	0.0032

After defining the flow behavior index for PEO solution, the measured viscosity values were shown as a function of temperature. As it can be seen in Figure 77, the viscosity of the PEO solution increased with increasing the rate of spindle rotation at 25°C. When the spindle speed was set to 200 rpm, the viscosity of the polymer solution reached slightly above 40 centipoise at 25°C (almost 4 times greater than the initial viscosity at 10 rpm). However, this substantial increase observed at 25°C was deteriorated when the temperature increased to 75°C. When the spindle speed was set to 200 rpm at 75°C, the viscosity value barely reached 13 centipoise. Nevertheless, a very weak increase in the viscosity values was still observed at 75°C. Such increases

in viscosity, both at 25°C and 75°C, indicated non-Newtonian character and also it was proved that the polymer chain behaved differently in the solution in contrast to the expectations of pseudoplasticity/shear-thinning. Actually, this uncommon case was called as shear-thickening because the polymer solution increased in viscosity at higher rpm values. This means that the polymer chains concentrated more at the center of the vessel under agitated conditions rather than the perimeter. At the same time, water molecules were squeezed out from between the PEO macromolecules. As a result, PEO chains interacted with each other more strongly and a resultant web-like polymeric structure formed. Such a strong concentrated polymeric structure may also physically entrap the colloidal particles into flocs. Most probably, the reason of the flocculation performance improvement under highly agitated condition was this unique shear-thickening property of the PEO solution.

The flocculation performance deteriorated at the elevated temperature as shown previously (Figure 52 and Figure 53). The adverse effect of the high temperature on flocculation was also explained with the viscometry and related the problem to the polymer itself. Although a similar weak shear-thickening behavior was observed at 75 °C, the viscosity significantly decreased compared to the viscosity values obtained at 25 °C. This means that the quality of the polymer was adversely affected from high temperature by causing deterioration of the flocculation performance (Mpofu et al., 2004).

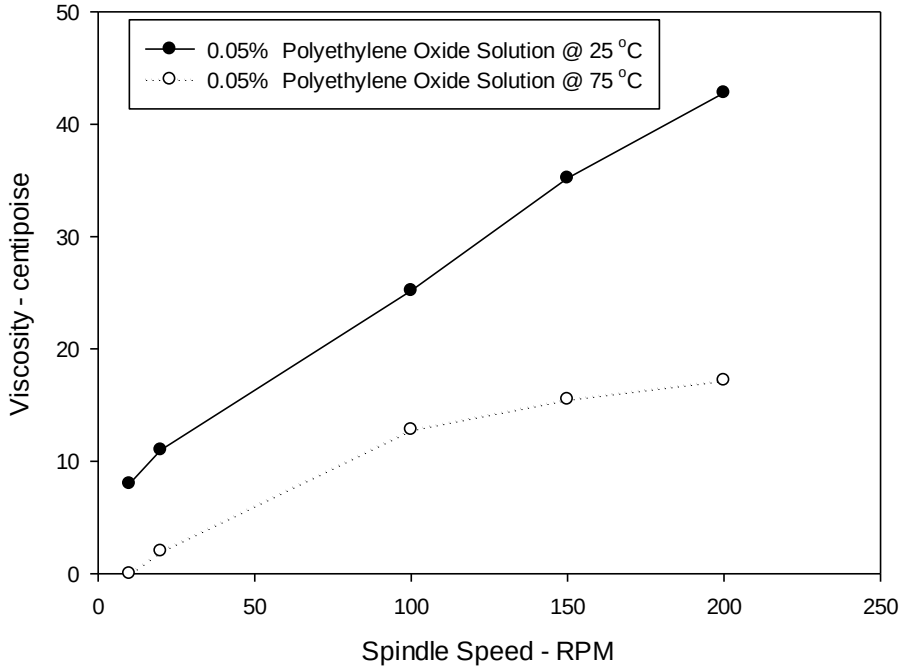

Figure 77. The viscosity measurement of the PEO solution at 25°C and 75°C

As it can be seen in previous flocculation studies, intense mixing improved flocculation performance to some extent. Firstly, PEO macromolecules were very enduring and the polymer chains were not broken or deteriorated under highly agitated conditions and even the coiled-up states of the polymers turned into elongated states that contributed to catching up more colloidal particles into floc structure. Secondly, proved shear-thickening character of PEO solution revealed the behavior of macromolecules inside the hydrodynamic environment. As a result, these two properties were considered as main improving factors for flocculation performance and these improvements were practically observed. However, it should be noted that the green and the white sample suspensions were treated with PEO in a delicately controlled manner to take advantage of these properties of PEO. This was very substantial for the destabilization of the colloidal particles. If the polymer treatment procedure was uncontrolled (for instance, swift injection of highly

concentrated PEO solution directly into the center of the beaker), the flocculation would be deteriorated because advantage of non-Newtonian character of PEO would be converted into disadvantage. This adverse effect had been actually observed by the naked eye during preliminary flocculation tests (which were not presented in this study) and the viscosity findings in this part of the thesis directly pointed out the problem. The uncontrolled injection of the polymer resulted in a non-homogenous distribution of the polymer chains in the particle crowded system and polymer-polymer interaction dominated particle-polymer interaction. Due to the non-Newtonian shear-thickening behavior, elongated polymer chains were tended to concentrate at the center of the vortex in mixing zone. The interaction between polymer chains was also maximized at this central zone. The interacted polymer chains together with some entrapped colloidal particles formed a gel like structure (Figure 78). This gel-like structure showed visco-elastic property of non-Newtonian fluid. While non-visco-elastic fluids are thrown outwards and upwards against the wall of the beaker as a result of centrifugal forces during mixing, visco-elastic fluids are drawn up by the rotor shaft against the force of gravity and such phenomenon is known as the Weissenberg effect (Schramm, 1998). Similarly, in this study, the gel-like structure was drawn to the center of mixing zone and furthermore started to climb up the rotor shaft (Figure 78). The fiber like structure of the polymer also contributed to this undesirable and irreversible accumulation around the shaft in a similar vein to rope enwinding. Once a small gel-like structure formed as in Figure 78, it immediately jeopardized the flocculation procedure. Further addition of the polymer did not remove turbidity after this but enlarged and strengthened the gel-like structure in an evolving state because additional polymer molecules tended to interact with this gel-like structure under highly agitated conditions instead of the suspended solid particles. As a result of uncontrolled PEO treatment, flocculation performance significantly deteriorated due to the non-homogenous polymer distribution and weak particle-polymer interaction. To prevent this, particle surfaces should be activated for enhanced particle-polymer interaction and the suspensions should be treated with the polymer in a delicately controlled manner to take advantage of viscometric properties of PEO.

a-)

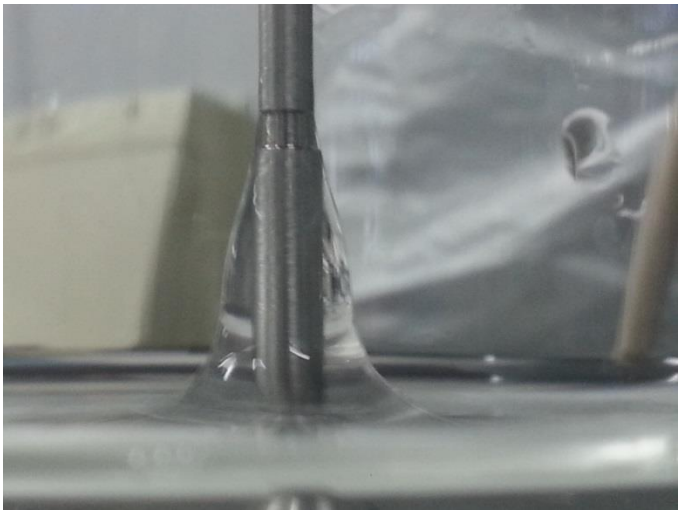

b-)

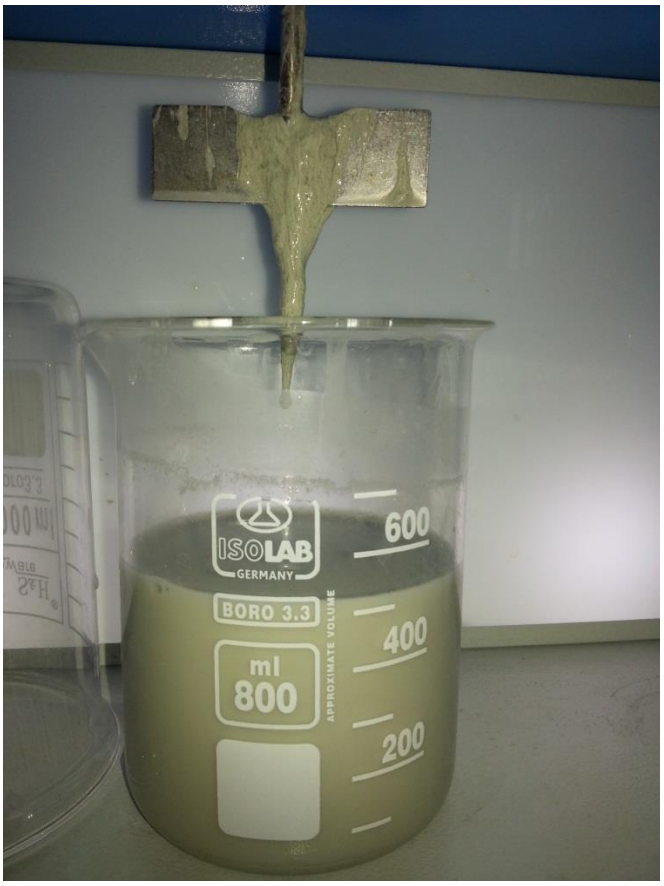

Figure 78. The Weissenberg phenomenon on PEO solution (-a-) and adverse effect of the Weissenberg phenomenon on the flocculation (-b-), an example for unwanted floc formation.

4.4.2. Viscosity Comparison of the Floc Sediments

In addition to previous supernatant turbidity results, the flocculated sediments of different experiment sets were analyzed with the help of viscosity measurement. The aim of the viscosity measurements was to compare the parameters effect (Table 6) on the resultant flocs under controlled condition. So, time and rpm-dependent behavior of different flocs were defined via up-down rate ramp method and the findings were presented in Figure 79 and Figure 80.

All viscosity measurements of the studied flocs showed non-Newtonian property, as expected. The viscosity values decreased for every measurement set when rpm of the spindle increased. Such a decreasing viscosity tendency against increasing rpm referred to pseudoplasticity which is also named as shear-thinning. This proved that PEO – particle flocs formations actually behaved differently (shear-thinning) than the PEO solution itself (shear-thickening).

In this part of the study, polymer dosage was fixed to 666 g/t to collect reliable and interpretable data within the measurement range of the equipment setup. Although 666 g/t PEO was added into the green and the white sample suspensions in the presence of borax at a velocity gradient of 3 s^{-1}, the lowest viscosity values were obtained for Floc-1 & Floc-7 among the other measurements. These viscosities showed that the formed flocs were very weak due to the low-intensity mixing and inefficient particle-polymer interaction. Moreover, the declining and rising part of the viscosity curves (Floc-1 & Floc-7) were not congruent. There was an area between these two parts. This area was known as hysteresis area and it defined the extent of the time-dependent behavior. It means that the flocs were affected from agitation due to its weakly bonded/bridged structure. Most probably, this decrease in the viscosity of the flocs may refer to the floc disintegration. As a result, the flocculation tests with high amount of PEOs consumption did not produced strong/dense flocs and poor turbidity removal at a velocity gradient of 3 s^{-1}. Such fragile floc formations only observed for flocculation experiments at velocity

gradient of 3 s^{-1} (Floc-1 & Floc-7) but not at velocity gradients of 306 s^{-1}. So, for further evaluation of the viscosity highest velocity gradient was preferred.

Floc-2 and Floc-8 showed improved viscosity properties as compared to Floc-1 and Floc-7. The only reason for this was the calcium conditioning at higher velocity gradient of 306 s^{-1}. The declining and rising part of the viscosity curves were congruent and the viscosity values reached their original value at the end of the up-down rate ramp period. This means that these floc structures (Floc-2 and Floc-8) were not fragile and did not disintegrate as a function of time. It was obvious that PEO dosaging of suspensions at higher velocity gradient (306 s^{-1}) in the presence of calcium significantly improved flocculation in terms of both viscosity of sedimented flocs and turbidity removal of supernatant. The severe mixing and calcium conditioning seems to physically and chemically force the stable colloidal particles into agglomeration. Furthermore, probability of particle-polymer collision increased due to calcium activation of particle surfaces under severe agitation leading to enhanced densification and consolidation of this agglomeration process. In conclusion, very viscous/firm floc sediments (Floc-2 and Floc-8) were obtained with the intense agitation, the calcium activation and the PEO-induced flocculation.

Manganese preconditioning of the suspensions also produced very firm structures both for the green and the white sample flocs. The viscosity values (Floc-3 & Floc-9) were very high. The initial and final viscosities did not diverge from each other indicating undisturbed floc sediments. When these viscosities (Floc-3 & Floc-9) are compared to previous ones (Floc-2 & Floc-8), it can be claimed that the manganese-preconditioned flocculation experiments gave slightly more viscous flocs than calcium-preconditioned flocculation experiments. The reason for that can be explained with the maximized hydrolyzed species of manganese cations at pH 9.40. On the other hand, the hydrolyzed species of calcium reached its maximum amount at pH 11.50 but not at pH 9.40. For this reason, there was a slight viscosity difference between calcium and manganese preconditioned flocculation tests.

At the next step, the effect of pH adjustment to 11.5 on the flocs viscosity was evaluated. The resultant flocs (Floc-4 and Floc-10) revealed that viscosity of the flocs improved more than the previous ones (Floc-1, Floc-2, Floc-3; Floc-7, Floc-8, Floc-9). As it was known from previous explanation related to conceptual water chemistry calculations, the amount of $CaOH^+$ and $CaB(OH)_4^+$ species were maximized at pH 11.5. These species had high affinity for the particle and they strongly adsorbed rendering the surfaces with the active anchorage sites for PEO. In conclusion, the surfaces of the colloidal particles were activated for enhanced particle – polymer interaction and the activation with pH adjustment significantly increased both viscosity of sedimented floc structures and turbidity removal performances. However, it should be noted again that although the pH adjustment of the suspensions for flocculation lead to very successful outcomes, it may be very challenging on an industrial scale due to the buffering capacity of borax.

As previously stated, the flocculation performance can also be improved without the activation of the colloid surfaces. The hetero-flocculation via clinker ballasting was an outstanding example for this case. This unconventional ballasting procedure successfully contributed to the viscosity of the sedimented floc structures as well as the turbidity removal. The resultant flocs' viscosity values were presented in Figure 79 - Figure 80 and clinker particles provided a strong bridging leading to properly agglomerated and compacted sediments. Furthermore, these clinker ballasted Floc-5 & Floc-11 (constituted of the colloidal particles – clinker – PEO) gave higher viscosity readings than the previous measurements of Floc-1, Floc-2, Floc-3, Floc-4; Floc-7, Floc-8, Floc-9, Floc-10. Hetero-flocculation via clinker ballasting can be considered as an influential viscosity enhancer and it can be implemented as an alternative to commonly used coagulants and silicate ballasts for this purpose.

At the final step, the suspensions that were preconditioned with cationic PAM were subjected to flocculation with the main flocculant, PEO. The resultant flocs were analyzed with Brookfield Viscometer. The obtained viscosity values were impressive among the other test results. For instance, the viscosity of Floc-6 reached around

5000 mPa.s for the green sample flocs and the viscosity of Floc-12 reached around 10000 mPa.s for the white sample flocs after two consecutive polymer treatments. In conclusion, most viscous flocs were obtained for these Floc-6 and Floc-12. So, it seems to be helpful method in terms of flocs firmness (Bulutçu et al., 1986); however, it should be remembered that the turbidity removal became difficult in the case of two different flocculant additions into the suspensions. To decrease the turbidity, the greater amount of polymer was required. The reason behind this fact was explained that the interaction between PAM and PEO molecules became dominant in the system. The improved polymer-polymer interaction deteriorated the flocculation performance due to the decrease in particle-polymer interaction. As a result, multi-flocculant treatments of the suspensions should be carried out delicately because it may enhance the structure of sedimented flocs whereas it may impair the turbidity removal.

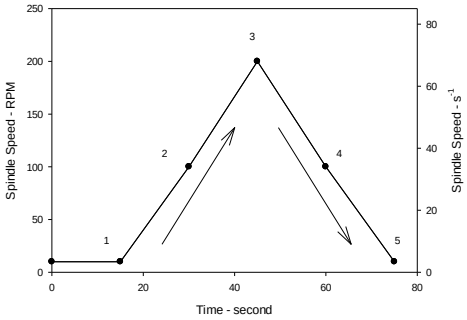

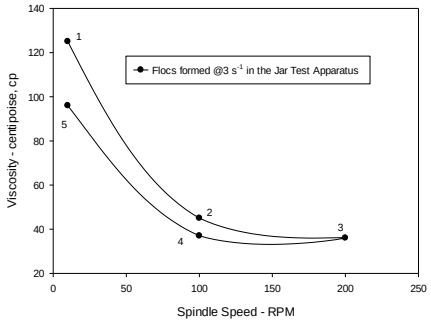

Floc-1: 666 g/t PEO

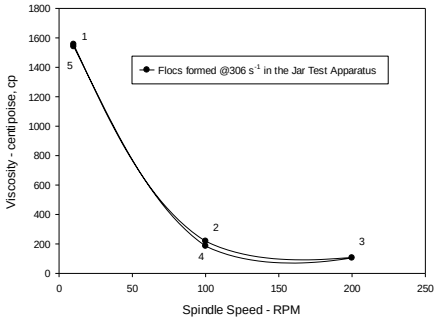

Floc-2: 500mg/l $CaCl_2$ & 666 g/t PEO

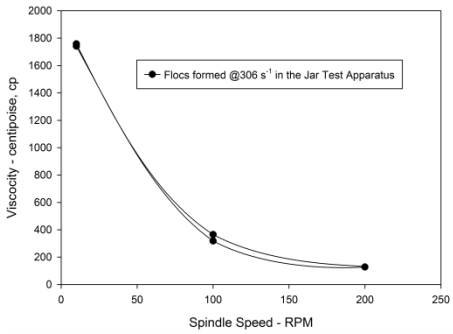

Floc-3: 500mg/l $MnSO_4$ & 666 g/t PEO

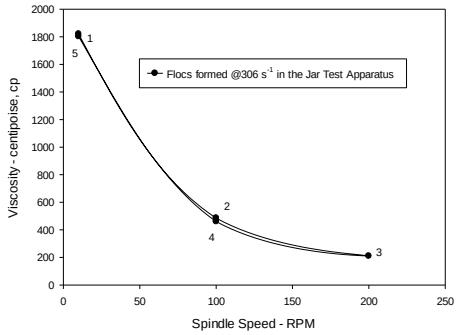

Floc-4: pH 11.50 & 666 g/t PEO

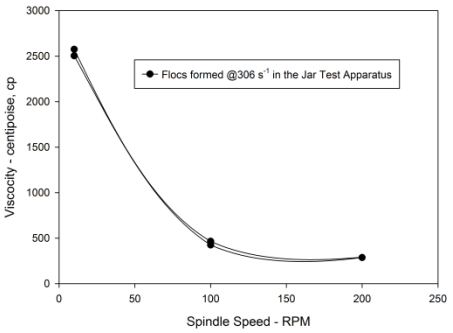

Floc-5: 10 g/l clinker & 666 g/t PEO

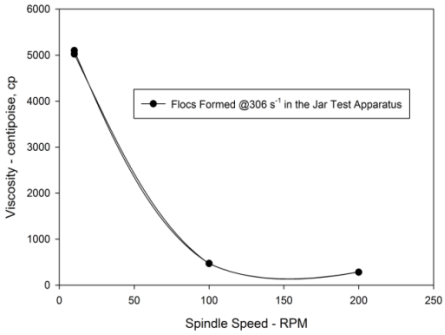

Floc-6: 166 g/t C-PAM & 666 g/t PEO

Figure 79. Viscosity measurements of the green sample flocs

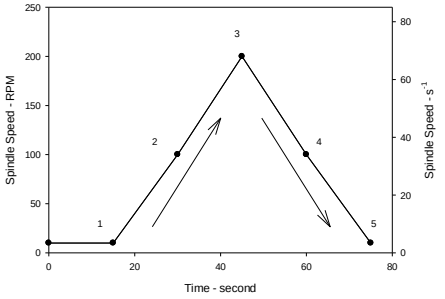

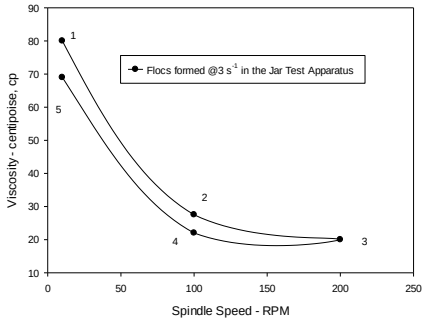

Floc-7: 666 g/t PEO

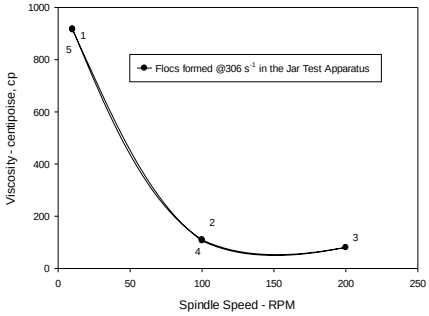

Floc-8: 500mg/l $CaCl_2$ & 666 g/t PEO

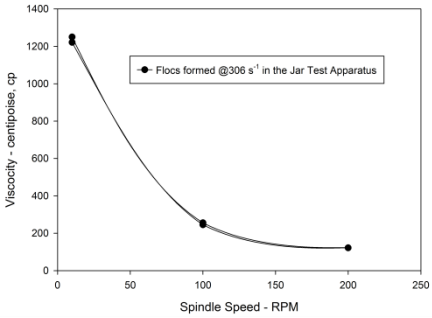

Floc-9: 500mg/l $MnSO_4$ & 666 g/t PEO

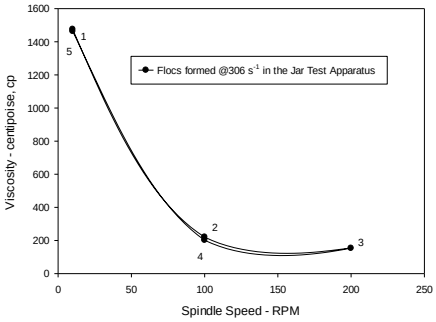

Floc-10: pH 11.50 & 666 g/t PEO

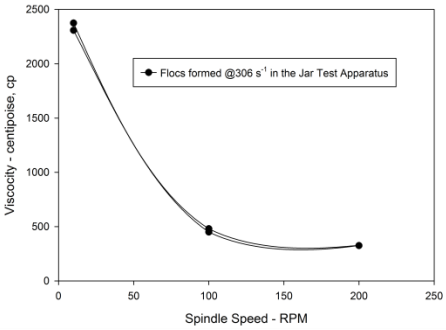

Floc-11: 10 g/l clinker & 666 g/t PEO

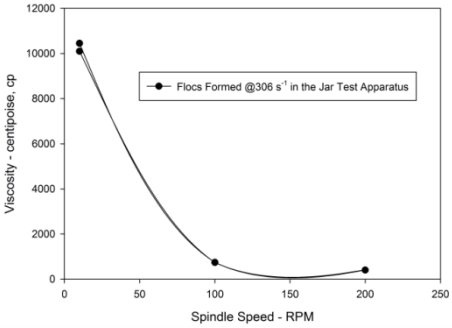

Floc-12: 166 g/t C-PAM & 666 g/t PEO

Figure 80. Viscosity measurements of the white sample flocs

4.5. Optimization of the Flocculation Process Using RSM

The response and the variables utilized in the experimental design and optimization procedure was given in Table 18. Y_1 and Y_2 were represent the variable the turbidity whereas X_1 X_4 ; X_2 X_5; X_3 X_6 represented the variables PEO, calcium chloride and velocity gradient respectively (Table 18).

Table 18. The responses and the variables used in the experimental design

Parameters of the Green Sample Flocculation	Parameter of the White Sample Flocculation	
X_1 - Variable	X_4 - Variable	Polyethylene Oxide Dosage – g/t
X_2 - Variable	X_5 - Variable	Calcium Chloride Dosage – mg/l
X_3 - Variable	X_6 - Variable	Velocity Gradient – G, s^{-1}
Y_1 - Response	Y_2 - Response	Turbidity of the Supernatant - NTU

Response surfaces were generated with the experimental data input and the related mathematical relationships between the responses and the variables expressed for the flocculation of the green and the white sample suspensions in the presence of borax as follows

$$Y_{Green} = 6595.05 - 10.0237*X_1 - 15.2008*X_2 - 30.0214*X_3 + 0.00540304*X_1^2 + 0.007376*X_1*X_2 + 0.0129951*X_1*X_3 + 0.0142309*X_2^2 + 0.0180896*X_2*X_3 + 0.0481025*X_3^2$$

$$Y_{White} = 7056.22 - 11.4153*X_4 - 22.9377*X_5 - 15.1163*X_6 + 0.0112821*X_4^2 + 0.00262082*X_4*X_5 + 0.00657145*X_4*X_5 + 0.0252322*X_5^2 + 0.0256496*X_5*X_6 + 0.00541698*X_6^2$$

R-squared value for the model Y_{Green} was quite high that the given model successfully explained 97.7085% of the variability in turbidity (NTU). The adjusted R-squared value of the model Y_{Green} was 93.5839% and this value was also satisfyingly high. On the other hand, the adjusted R-squared value of the model Y_{White} was 85.5827%. Although this value was a little smaller, it was sufficiently high for the response surface methodology. Considering R-squared value of this model, it explained 94.8509% of the variability in the response. Therefore, the response surface models for each study accomplishedly reflected the essence of the turbidity removal behavior. The mean absolute error was found as 154.15 for the green sample design and 295.73 for the white sample design. These values represented the average values of the residuals for each design and they confirmed the success of the statistical procedure. The Durbin-Watson statistic tested these design to determine if there were any significant correlations based on the order in the collected data set. Since the P-values of the Durbin-Watson (0.85 for the green sample design and 0.64 for the white sample design) were greater than 0.05, there was no indication of serial autocorrelation in the residuals at 5.0% significance level.

The second-order functions statistical summaries (ANOVA) were given in Table 19. According to this table, all introduced variables for the flocculation of the green sample suspensions were found as statistically significant due to their P-values which were smaller than 0.05. However, P-values of only X_1; X_2; $X_1.X_2$; $X_1.X_3$; $X_2.X_2$ were found smaller than 0.05 in the case of the white sample. This means that only these parameters were actually statistically significant not the ones greater than 0.05 like X_3; $X_1.X_2$; $X_2.X_3$; $X_3.X_3$.

Table 19. ANOVA tables of the statistical procedures

Analysis of Variance Table for Flocculation of the Green Sample Suspension						*Analysis of Variance Table for Flocculation of the White Sample Suspension*					
Source	Sum of Squares	Df	Mean Square	F-Ratio	P-Value	Source	Sum of Squares	Df	Mean Square	F-Ratio	P-Value
X_1:PEO	3.62449E6	1	3.62449E6	31.15	0.0025	X_1:PEO	4.70077E6	1	4.70077E6	10.45	0.0231
X_2:Ca	8.17945E6	1	8.17945E6	70.29	0.0004	X_2:Ca	1.86248E7	1	1.86248E7	41.42	0.0013
X_3:G	4.62152E6	1	4.62152E6	39.72	0.0015	X_3:G	1.17169E6	1	1.17169E6	2.61	0.1674
X_1 X_1	821837.	1	821837.	7.06	0.0450	X_1 X_1	3.58335E6	1	3.58335E6	7.97	0.0370
X_1 X_2	1.40132E6	1	1.40132E6	12.04	0.0178	X_1 X_2	176917.	1	176917.	0.39	0.5580
X_1 X_3	1.23285E6	1	1.23285E6	10.60	0.0226	X_1 X_3	315265.	1	315265.	0.70	0.4406
X_2 X_2	2.89365E6	1	2.89365E6	24.87	0.0042	X_2 X_2	9.09684E6	1	9.09684E6	20.23	0.0064
X_2 X_3	1.27164E6	1	1.27164E6	10.93	0.0213	X_2 X_3	2.55662E6	1	2.55662E6	5.69	0.0628
X_3 X_3	1.8271E6	1	1.8271E6	15.70	0.0107	X_3 X_3	23170.8	1	23170.8	0.05	0.8294

The Pareto charts of each design were visually showed the statistical significances (Figure 81 and Figure 82) of X_i - values for the models. These values were consistent with the previous P-values and their effect on the model can be differentiated easily according to the statistical emphasis on the response. Based on these figures, the most important parameter on the flocculation performance can be named as coagulant (calcium chloride) addition for both the green and the white sample suspensions. Dissolved calcium presumably adsorbed by the particle surfaces in the suspensions and promoted the surface activation. For this motive, the coagulant preconditioning had very substantial effect on the destabilization of the colloidal particles. Once the surfaces were activated via calcium, intense mixing and PEO treatment contributed to the flocculation to a greater extent. As a summary, the Pareto charts clearly proved the variables effect and the significance on the response.

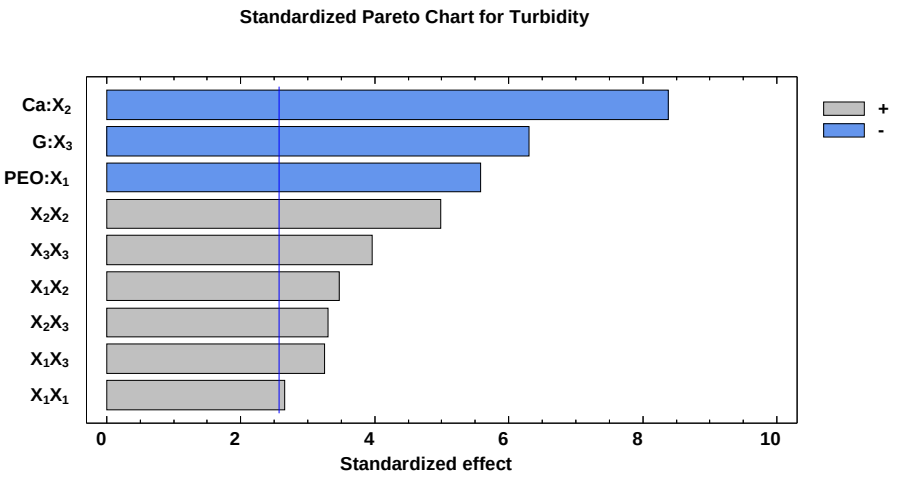

Figure 81. Pareto chart for the parameters of the green sample suspension flocculation design

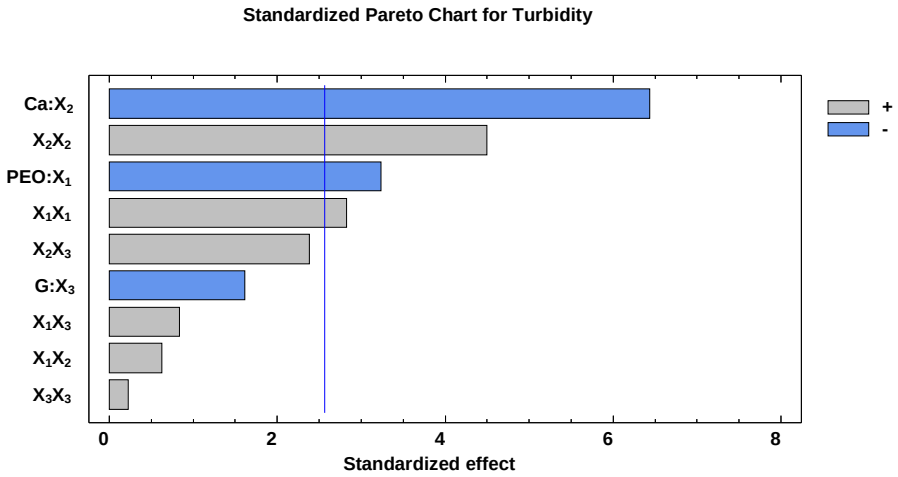

Figure 82. Pareto chart for the parameters of the white sample suspension flocculation design

Based on the second-order previous equations, the response surfaces were drawn in three dimensional graphs for the green and the white sample design. Figure 83 and Figure 84 clearly summarized the relation between three parameters and the response. These parameters were calcium preconditioning, mixing intensity and PEO treatment and all of these parameters proved to be useful to decrease turbidity of the stable the green and the white sample suspensions. The standardized effects (Figure 81 and Figure 82) of these factors in the Pareto charts were manifested their effects on the turbidity in a more interactive and easily interpretable way in Figure 83 and Figure 84. According to these figures (Figure 83 and Figure 84), it can be concluded that PEO's flocculation efficiency on the green and the white sample suspensions can be improved significantly in combination with calcium preconditioning and high-intensity mixing. These estimated response surfaces were analyzed to determine optimum conditions for the successful flocculation performance. For the green sample flocculation design, PEO consumption decreased and optimized to 241.197 g/t-solid with the help of 266.407 mg/L calcium chloride and velocity gradient at 108.327 s^{-1}. On the other hand, PEO consumption optimized to 238.087 g/t-solid with the help of 497.280 mg/L calcium chloride and velocity gradient at 111.856 s^{-1}. In the previous literature information related to the flocculation of Kırka's silicate-carbonate gangue containing suspensions (Gür et al., 1994; Garrett, 1998; Sabah & Yeşilkaya, 2000; Çırak, 2010), the optimum polymer dosages had been very high (1000-2000 g/t-solid) comparing to these findings presented in Table 20. It can be concluded considering the results of these previous studies that the flocculation performance can be improved by implementing three parameters altogether and the costly polymer consumption can be decreased significantly. The flocculation studies on this subject mostly focused on only polymer type and dosage. However, this study showed that polymer treatment should be supported with coagulant pretreatment and high-intensity mixing for better flocculation performance because increasing only polymer dosage did not remove the supernatant turbidity values as intended. For this reason, the optimization study of the white sample design suggested increasing coagulant dosage instead of increasing polymer dosage to decrease supernatant turbidity. As shown in Table 20, the optimum flocculant dosage of two samples were

very close to each other 241.197 g/t-solid for the green sample and 238.087 g/t-solid for the white sample but the optimum coagulant dosage of the white sample, 497.280 mg/L was almost twice as much as the green sample, 266.407 mg/L.

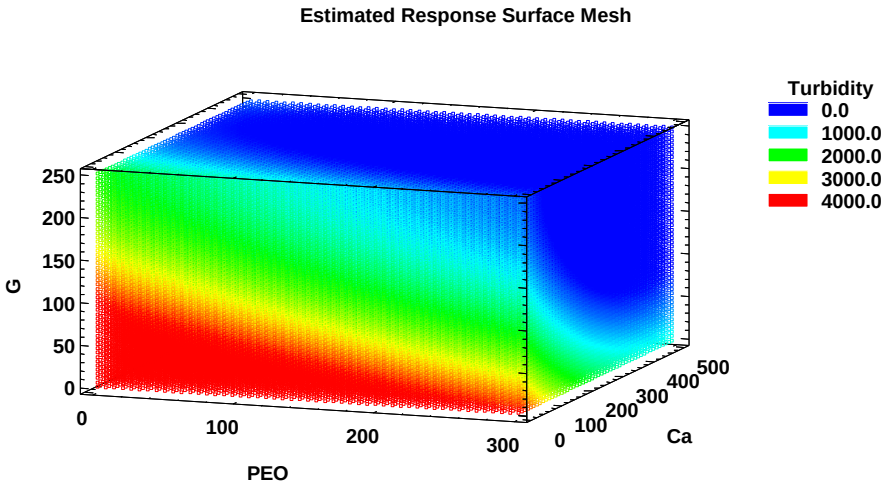

Figure 83. Response surface meshes of the green sample design in 3-D

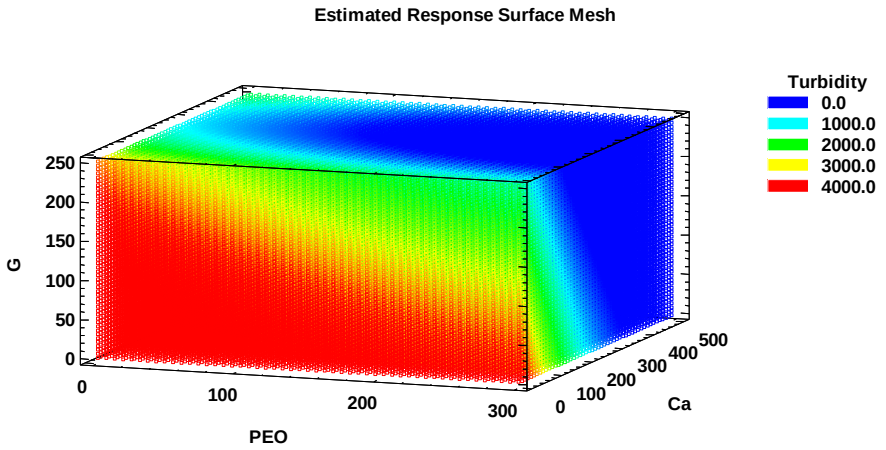

Figure 84. Response surface meshes of the white sample design in 3-D

Table 20. Optimization of the flocculation parameters for each design.

Optimization for the green sample design	***Factor***	***Low***	***High***	***Optimum***
	PEO (g/t)	33.0	666.0	241.197
	Ca (mg/L)	0.0	500.0	266.407
	G (s^{-1})	3.0	306.0	108.327

Optimization for the white sample design	***Factor***	***Low***	***High***	***Optimum***
	PEO (g/t)	*33.0*	*666.0*	*238.087*
	Ca (mg/L)	*0.0*	*500.0*	*497.28*
	G (s^{-1})	*3.0*	*306.0*	*111.856*

CHAPTER 5

CONCLUSIONS AND RECOMMENDATIONS

Based on the data and discussions presented in this study, the following conclusions were derived:

1-) The characterization studies provided significant explanatory information about the dolomite/clay-containing samples collected from Kırka. XRF and XRD analyses revealed the chemical and mineralogical differences between the samples. Clay mineral based technical complications in the quantitative phase analysis had been overcome with Rietveld refinement technique and this method proved as a reliable/applicable technique for the clayey samples. As a result, most abundant phases were identified as Mg-rich trioctahedral smectite and ideal/ordered dolomite. Furthermore, the particle size and zeta potential studies explained the reason of the high degree of stability of the colloidal suspensions. In addition to that, infrared studies identified the interfacial problem in the flocculation process with the lack of active (isolated – OH) groups on particle surfaces.

2-) Dolomite/clay/borax-containing systems formed very stable suspensions which caused difficulties in solid/liquid separation. PEO-induced flocculation could not efficiently destabilize and remove the turbidity due to the insufficient particle-polymer interaction at borax-buffered pH 9.40. For this reason, additional supplementary parameters may be required to assist flocculation procedure of such colloids.

3-) Unique difficulties in the PEO-induced flocculation were observed for dolomite/clay/borax-containing suspensions and these were associated with the

mineralogical constituents. The flocculation of the silicate-rich green sample particles produced greater floc sediment volumes whereas the flocculation of the dolomite-rich white sample particles produced greater supernatant turbidity values.

4-) High-intensity mixing during the PEO conditioning was found beneficial to improve flocculation performance at high velocity gradient values of 108 s^{-1} and 306 s^{-1}. With the help of the highly agitated conditioning, the probability of particle-polymer collision was enhanced and turbidity removal was improved because more colloidal particles were entrapped into the floc structure. In addition to this, the volume of the flocculated sediment was reduced due to the denser floc formation during mixing. However, the further enhancement was still required in addition to this physical flocculation parameter to obtain more compact floc structure and much cleaner supernatant.

5-) For the purpose of further improvement in the flocculation performance, various coagulants were added into the suspensions to activate particle surfaces prior to PEO treatment at high velocity gradient values. Nevertheless, none of the widely used coagulants including iron and aluminum actually worked for destabilization of these colloidal suspensions. Inefficiency of these well-known coagulants was explained with the direct precipitation of iron and aluminum metals at pH 9.40, because they completely transformed into non-adsorbable / neutral charged solid phases and they lost their destabilizing ability. On the other hand, calcium and manganese coagulants produced promising results for the effective removal of the turbidity values. Their effectiveness was elucidated with the presence of hydrolyzed species of calcium and manganese at pH 9.40 and these species were identified as $CaOH^{+}$ and $Mn_2(OH)_3^{+}$. They were strongly adsorbed by the particle surfaces and served as a bridging agent between particle and PEO leading to outstanding flocculation performances.

6-) Temperature adversely affected the flocculation of the dolomite/clay/borax-containing suspensions. When the suspension temperature was increased to 75°C, the PEO flocculation capability was almost completely lost and no visible floc formation

was observed. The viscosity measurements also confirmed that the quality of PEO significantly deteriorated at high temperatures. The mentioned temperature sensitivity of the polymer was not fully comprehended in the practical applications. Due to this obscurity, extortionate amount of three different flocculants is currently applied to hot solutions of dolomite/clay/borax-containing suspension in an actual plant operation to overcome this unnoticed problem. Consequently, this temperature related finding should be taken into consideration in such applications of PEO to improve performances of both enrichment and solid/liquid separation processes.

7-) When pH of the suspension was increased up to 11.50, the amount of $CaB(OH)_4^+$ and $CaOH^+$ was maximized in the suspensions and the significant flocculation improvements were observed for the dolomite/clay/borax-containing suspensions. Based on this fact, it can be concluded that the cations are needed to be hydrolyzed to form charged hydroxo-complexes for the purpose of efficient flocculation inasmuch as these hydroxo-complexes are strongly adsorbed by the particles and lead to the activation of the surfaces.

8-) Unconventional clinker ballasted flocculation was also tested to enhance the solid/liquid separation process of the dolomite/clay/borax-containing suspensions. When the results of these experiments were analyzed, it was ascertained that the flocculation performance of the suspensions significantly improved owing to the hetero-flocculation mechanism triggered by clinker particles. Considering this favorable effect of clinker on the flocculation, it might be suggested that clinker ballasting can be used as an esteemed alternative to the other common pretreatment methods, such as coagulant pretreatment and pH adjustment.

9-) The viscosity measurements proved that PEO chains were durable against the high velocity gradient values. Furthermore, the PEO solutions showed shear-thickening property instead of the expectations of shear thinning. This unique property of the PEO solutions might contribute to the flocculation of the colloidal suspensions under intense mixing conditions. On the other hand, another viscometric

phenomenon called Weissenberg effect was observed during the test. This uncommon behavior of PEO might result in inhomogeneous polymer distribution inside the suspensions causing insufficient probability of particle-polymer collision/interaction. So, these advantageous and disadvantageous viscosity properties of PEO should be evaluated properly for high velocity gradient-induced flocculation processes.

10-) Response surface methodology (RSM) was used to determine optimum flocculation conditions both for the green and the white sample suspensions in the presence of borax. This statistical procedure principally utilized three beneficial flocculation parameters, namely the mixing intensity, the amount of the calcium coagulant and the dosage of PEO, in order to obtain the best possible supernatant turbidity. According to the results of the optimization, increasing PEO dosage was not suggested above around 240 g/t-solid. Instead of that, the amount of calcium coagulant should be increased to improve the flocculation performance, for instance 497 mg/L for the white sample suspensions. The underlying reason behind this statistical decision was to primarily enable surface activation and to increase the amount of the anchor sites on the particle surfaces with calcium hydroxo-complexes for more effective PEO adsorption. Comparing to the previous flocculant dosages (1000 – 2000 g/t-solid) proposed by different researchers, it can be claimed in this study that the polymer consumptions decreased to more reasonable values with the help of the physical and chemical flocculation parameters.

After the completion of this dissertation, some further studies can be proposed as below:

1-) Solid/liquid separation process of these dolomite/clay/borax-containing suspensions should be tested inside an ultra-flocculator at velocity gradient between 1000 and 10 000 s^{-1} for further enhancement of collision probability between particles and polymeric macromolecules.

2-) In addition to the PEO-induced flocculation improved with coagulant pretreatment and high-intensity mixing in this study, various filtering techniques should be applied to this challenging suspension to decrease its solid/liquid ratio.

3-) Alternative flocculants should be tested for the industrial treatment of hot borax solutions. If these alternative flocculants fail completely at high temperatures due to the deterioration of polymeric chains, the suggested coagulants of calcium and manganese in the scope of this thesis should be used as a primary chemical in exchange for polymers.

4-) Electro-coagulation / electro-flocculation should be tested for the purpose of solid/liquid separation.

5-) Proposed physical and chemical flocculation parameters should be experimented on a pilot plant operation to observe any possible real-life challenges for further scale-up works.

REFERENCES

Abrol, I. P., Yadav, J. S., & Massoud, F. I. (1988). *Salt effected soil and their management.* Rome: FAO SOILS BULLETIN 39.

Acton, A. Q. (2012). *Polyethylene Glycols—Advances in Research and Application: 2012.* Atlanta: Scholarly Editions.

Agassi, M. (1996). *Soil Erosion, Conservation and Rehabilitation.* New York: Marcell Dekker.

Akdeniz, Y., Özmıhçı, F., Duvarcı, Ç. Ö., Balköse, D., & Ülkü, S. (2003). Characterization of colloidal phase in hot aqueous solutions of Kırka tincalconite mineral. *XI. National Clay Symposium* (pp. 603-613). İzmir: Turkish National Committee of Clay Science.

Aygun, A., & Yilmaz , T. (2010). Improvement of coagulation-flocculation process for treatment of detergent wastewaters using coagulant aids. *International Journal of Chemical and Environmental Engineering, 1*(2), 97-101.

Behl, S., & Moudgil, B. M. (1993). Mechanisms of polyethylene oxide interactions with dolomite and apatite. *Journal of Colloid and Interface Science, 161*(2), 443-449.

Besra, L., Sengupta, D. K., Roy, S. K., & Ay, P. (2004, July). Influence of polymer adsorption and conformation on flocculation and dewatering of kaolin suspension. *Separation and Purification Technology, 37*(3), 231-246.

Bish, D. L., & Post, J. E. (1993). Quantitative mineralogical analysis using the Rietveld full-pattern fitting method. *American Mineralogist, Vol. 78*, 932-940.

Bratby, J. (2006). *Coagulation and Flocculation in Water and Wastewater Treatment.* London: IWA.

Bulutçu, A. N., Türkay, S., & Tolun, R. (1986). Pellet flocculation of tincal slimes in double flocculant system. *I. International Mineral Processing Symposium.* İzmir, Turkey.

Burggraaf, A. J., & Cot, L. (1996). *Fundamentals of Inorganic Membrane Science and Technology*. Amsterdam: Elsevier.

Camp, T. R. (1946). Sedimentation and the design of settling tanks . *ASCE*, 909.

Camp, T. R. (1955). Flocculation and flocculation basins. *ASCE*, 1-16.

Camp, T. R. (1969). Discussion to agglomerate size changes in coagulation. *ASCE*, 1210-1214.

Çebi, H., Yersel, E., Poslu, K., Behar, A., Nesner, R., & Langenbrick, H. (1994). Solid-liquid separation of Etibank Kırka borax plant effluents by centrifugal decanter. *Progress in Mineral Processing Technology*, (s. 513-516).

Chaudhary, D. R., Shukla, L. M., & Gupta, A. (2005). Boron equilibria in soil - a review. *Agric. Rev*, *26*(4), 288-294.

Cheng, F., Zhang, H., Jiao, Y., & Zhu, C. (2010). Effects of hydrated Mg on KCL flotation. *XXV International Mineral Processing Congress Proceedings* (pp. 1783-1791). Brisbane: Curran Associates, Inc.

Cheng, Y. C. (1985). *The Effect of Surface Hydration on the Adsorption and Flocculation of a Model Silica Suspension Using Polyethylene Oxide.* Gainesville: University of Florida.

Çırak, M. (2010). *Flocculation Behavior of Two Different Clay Samples From Kırka Tincal Deposit.* Ankara: METU - MSc. Thesis.

Çolak, M. (1995). *The Emet and Kirka Borate Mines (Turkey) 1: Mineralogy and chemistry of the clays, 2: Ceramic applications of their tailing products.* Fribourg: University of Fribourg-Switzerland.

Cornwell, D., Gouellec, Y. L., & Cheng, R. C. (2006). *A Novel Approach to Seawater Desalination Using Dual-Staged Nanofiltration.* Denver: American Water Works Association.

Counties, L., & Counties , T. (1965). Dolomite soft sediment from Pluvial Lake Mound. *Abstracts for 1965: Abstracts of papers submitted for six meetings with which the Society was associated* (s. 123). New York: Geological Society of Ametica.

Donstova, K. M., Norton, D., Jonston, C., & Bigham, J. (2004). Influence of exchangeable cations on water adsorption by soil clays. *Soil Science Society of American Jornal*, 1218-1227.

Dontsova, K., & Norton, L. D. (1999). Effects of exchangeable Ca:Mg ratio on soil clay flocculation, infiltration and erosion. *Sustaining the Global Farm: 10th International Soil Conservation Organization Meeting* (pp. 580-585). Lafayette: International Soil Conservation Organization.

Duan , J., & Gregory, J. (2003). Coagulation by hydrolysing metal salts. *Advances in Colloidal and Interface Science, 100-102*, 475-502.

Eble, A., & Mersmann, A. (1999). Interaction of kinetics governing the precipitation of nanoparticles. *14th International Symposium on Industrial Crystallization* (s. 1-12). Warwickshire: Institution of Chemical Engineers, UK.

Everett , D. H. (1988). *Basic Principles of Colloid Science.* London: Royal Society of Chemistry .

Fourie, A. B. (2006). *Paste and Thickened Tailings: A Guide.* Australian Centre for Geomechanics.

Fuerstenau, M. C., & Elgillani, D. A. (1966). Minerals beneficiation - calcium activation in sulfonate and oleate flotation of quartz. *AIME Transactions, 235*, 405.

Fuerstenau, M. C., Miller, J. D., & Kuhn, M. C. (1985). *Chemistry of Flotation.* New York: Society of Mining Engineers.

Garrett, D. E. (1998). *Borates: Handbook of Deposits, Processing, Properties and Use.* California: Academic Press.

Gaucher, E. C., Blanc, P., Matray, J. M., & Michau, N. (2004). Modeling diffusion of an alkaline plume in a clay barrier. *Applied Geochemistry*, *19*(10), 1505-1515.

Ghafari, S., Aziz, H. A., Isa, M. H., & Zinatizadeh, A. A. (2009). Application of response surface methodology (RSM) to optimize coagulation-flocculation treatment of leachate using poly-aluminum chloride (PAC) and alum. *Journal of Hazardous Materials, 163*(2-3), 650-656.

Ghosh, P. (2009). *Colloid and Interface Science.* Sonepat: PHI Learning Private Limited.

Goyal, S. S., Sharma, S. K., & Rains, D. W. (2003). *Crop Production in Saline Environments.* New York: The Haworth Press.

Gunasekaran, S., & Anbalagan, G. (2007). Spectroscopic study of phase transitions in dolomite mineral. *Journal of Raman Spectroscopy, Vol. 38*, 846-852.

Gür, G., Türkay, S., & Bulutçu, A. N. (1994). The effects of the process conditions on the flocculation of tincal slimes. *Progress in Mineral Processing Technology* (pp. 501-503). Ankara : Taylor & Francis.

Gür, G., Türkay, S., & Bulutçu, A. N. (1996). Comparison of polyethylene oxide and polyacrylamides as flocculatiion agent for the flocculation of tincal slimes. *Changing Scopes in Mineral Processing*, (pp. 649-653). Kuşadası.

Haselhuhn, H. J., Carlson, J. J., & Kawatra, S. K. (2012). Water chemistry analysis of an industrial selective flocculation dispersion hematite ore concentrator plant. *International jornal of Mineral Processing, 102-103*, 99-106.

Helvaci, C., Mordogan, H., Çolak , M., & Gundogan , İ. (2003). Presence and distribution of lithium in borate deposits and some recent lake waters of west-central Turkey. *International Geology Review, 45*, 177-190.

Hill, G., & Holman, J. (2000). *Chemistry in Context.* London: Nelson Thornes Ltd. .

Howe, K. J., Hand, D. W., Crittenden, J. C., Trussell, R. R., & Tchobanoglous, G. (2012). *Principles of Water Treatment.* Wiley.

Kanungo, S. B. (2005, September). Effect of some commercial flocculating agents on settling and filtration rates of low grade, fragile manganese ores of Andhra Pradesh. *Indian Journal of Chemical Technology, 12*, 550-558.

Karaömerlioğlu, B. (2011). *Research on Boron Removal from Soil Using Medicago Sativa L. and Vicia Sativa L. Plants.* Adana : Çukurova Üniversitesi.

Kistler , R. B., & Helvaci, C. (1994). Boron and borates. In D. D. Carr, *Industrial Minerals and Rocks* (6th ed., pp. 171-178). Littleton: Society of Mining, Metallurgy and Exploration.

Kistler, R. B., & Helvaci, C. (1994). Boron and borates. D. D. Caff içinde, *Industrial Minerals and Rocks* (s. 171-186). Society of Mining, Metallurgy and Exploration.

Kökkılıç, O., Sirkeci, A. A., & Acarkan, N. (2005). Removal of boron from the effluents of Kırka borax tailing ponds. In R. Venugopal, T. Sharma, V. K. Saxena, & N. R. Mandre (Ed.), *International Seminar on Mineral Processing Technology* (pp. 400-406). Dhanbad: The McGraw-Hill Companies.

Langmuir, D. (1997). *Aqueous Environmental Geochemistry.* Livingstone: Prentice Hall.

Laskowski, J. S., & Castro, S. (2012). Hydrolyzing ions in flotation circuits: seawater flotation. *13th International Mineral Processing Symposyum*, 219-228.

Laskowski, J. S., & Ralston, J. (1992). *Colloidal Chemistry in Mineral Processing* (Cilt Developments in Mineral Processing,12). Amsterdam: Elsevier.

Lawson, J. (2010). *Design and Analysis of Experiments with SAS.* Boca Raton: CRC Press.

Leentvaar, J., & Ywema, T. S. (1980). Some dimensionless parameters of impeller power in coagulation-flocculation process. *Water Res., 40*, 135-140.

Lemons, K. W., & McAtee, J. L. (1983). The parameters of induced thermoluminescence of some selected phyllosilicates: a crystal defect structure study. *American Mineralogist, 68*, 915-923.

Lu, S., Pugh, R., & Frossberg, E. (2005). *Interfacial Separation of Particles.* Amsterdam: Elsevier.

Lucia, M. D., Bauer, S., Beyer, C., Kühn, M., Nowak, T., Pudlo, D., et al. (2012). Modelling CO2-induced fluid-rock interactions in the Altensalzwedel gas reservoir. *Environ Earth Sci, 67*, 563-572.

Lutterotti, L., Matthies, S., & Wenk, H. R. (1999). MAUD (Material Analysis Using Diffraction): a user friendly Java program for Rietveld Texture Analysis and more. *Proceeding of the Twelfth International Conference on Textures of Materials (ICOTOM-12), 1*, s. 1599.

Madejova, J. (2003). FTIR techniques in clay mineral studies. *Vibrational Spectroscopy, Vol.31*, 1-10.

Marini, L. (2007). *Geological Sequestration of Carbon Dioxide Thermodynamics, Kinetics, and Reaction Path Modeling* (Cilt Developments in Geochemistry-11). Oxfird: Elsevier.

Marsden, J. O., & House, C. I. (2006). *The Chemistry of Gold Extraction.* Littleton, Colorado: Society for Mining, Metallurgy, and Exploration, Inc. (SME).

Mathur, S., & Moudgil, B. M. (1997). Adsorption mechanism(s) of polyethylene oxide on oxide surfaces. *Journal of Colloid and Interface Science, 196*, 92-98.

Mattigod, S. V., Frampton, J. A., & Lim, C. H. (1985). effect of ion-pair formation on boron adsorption by kaolinite. *Clays and Clay Minerals, 33*(5), 433-437.

Merkel, B. J., & Planer-Friedrich, B. (2005). *Groundwater Geochemistry: A Practical Guide to Modeling of Natural and Contaminated Aquatic Systems.* Berlin: Springer.

Mitschka , P. (1982). Simple conversion of Brookfield R.V.T readings into viscosity functions. *Rheologica Acta, 21*, 207-209.

Mittal, K. L., & Shah, D. O. (2002). *Adsorption and Aggregation of Surfactants in Solution.* New York: Taylor and Francis.

Moore, D. M., & Reynolds, R. C. (1997). *X-Ray Diffraction and the Identification and Analysis of Clay Minerals* (Second Edition b.). Oxford: Oxford University Press.

Moudgil, B. M., & Behl, S. (1993). Flocculation behaviour of dolomite. *XVIII International Mineral Processing Congress*, (pp. 1309-1314). Sydney.

Moudgil, B. M., Mathur, S., & Behl, S. (1997, February 14-17). Flocculation behavior of dolomite with poly(ethylene-oxide). *SME Annual Meeting*, 1-14.

Moudgil, B. M., Matur, S., & Behl, S. (1995). Flocculation behavior of dolomite with polyethylene oxide. *Minerals and Metallurgical Processing, 12*(4), 219-224.

Mpofu, P., Addai-Mensah, J., & Ralston, J. (2003). Investigation of polymer structure type on flocculation, rheology and dewatering behaviour of kaolinite dispersion. *International Journal of Mineral Processing, 71*, 267-268.

Mpofu, P., Addai-Mensah, J., & Ralston, J. (2004, March). Flocculation and dewatering behaviour of smectite dispersions: effect of polymer structure type. *Minerals Engineering, 17*(3), 411-423.

Mpofu, P., Addai-Mensah, J., & Ralston, J. (2004). Temperature influence of nonionic polyethylene oxide and anionic polyacrylamide on flocculation and dewatering behavior of kaolinite dispersion. *Journal of Colloid Interface Science, 271*(1), 145-156.

Mular , A. L., Halbe, D. N., & Barratt, D. J. (2002). *Mineral Processing Plant Design, Practice and Control.* Littleton, Colarado: Society for Mining, Metallurgy, and Exploration, Inc. (SME).

Ohama, Y., Kawakami, M., & Fukuzawa, K. (1997). *Polymers in Concrete.* London: Chapman & Hall.

Ostrom, M. E. (1961). Separation of clay minerals from carbonate rocks by using acid. *Journal of Sedimentary Petrology*, 123-129.

Pashley, R. M. (1982). Hydration forces between mica surfaces in elecytrolyte solutions. *Advances in Colloid and Interface Science, 16*(1), 57-62.

Pokrovsky, O. S., Mielczarski, J. A., Barres, O., & Schott, J. (2000). Surface Speciation models of calcite and dolomite / aqueous solution interfaces and their spectroscopic evaluation. *Langmuir, Vol. 16*(No. 6), 2677-2688.

Rahman, I. (2009). *Removal of Boron from Produced Water by Co-Precipitation / Adsorption for Reverse Osmosis Concentrate.* California: California Polytechnic State University (MSc. Thesis).

Rashidi, M. (2010). *Physico-Chemistry Characterization of Sulfonated Polyacrylamide Polymers for Use in Polymer Flooding.* Bergen: University of Bergen (PhD. Thesis).

Ravina, L., & Moramarco, N. (1993). *Everything You Want yo Know About Coagulation & Flocculation.* Virginia: Zeta-Meter Inc.

Records, A., & Sutherland, K. (2001). *Decanter Centrifuge Handbook.* Oxford: Elsevier.

Rubio, J., & Kitchener, J. A. (1976). The mechanism of adsorption of polyethylene oxide flocculant on silica . *Journal of Colloid and Interface Science, 57*(1), 132-141.

Sabah, E., & Yeşilkaya, L. (2000). Evaluation of the settling behavior of Kırka borax concentrator tailings using different type of polymers. *Journal of Ore Dressing*(3), 1-12.

Sakarya Newspaper G.A.C. (2013, Mart 04). Retrieved Mart 25, 2013, from Sakarya Newspaper: http://www.sakaryagazetesi.info/haberler.php?sayfa=detay&oku=21281&kategori=5

Scheiner, B. J., & Wilemon, G. M. (1987). Applied flocculation efficiency: a comparison of polyethylene oxide and polyacrylamide. Y. A. Attia (Dü.), *Flocculation in Biotechnology and Separation Systems* içinde (s. 175-186). Amsterdam: Elsevier Science Publishers.

Schramm, G. (1998). *A Practical Approach to Rheology and Rheometry.* Karlsruhe: Gebrueder HAAKE.

Schweitzer, G. K., & Pesterfield, L. L. (2009). *The Aqueous Chemistry of the Elements* . Oxford: Oxford University Press.

Sharma, S. K., & Sanghi, R. (2012). *Advances in Water Treatment and Pollution Prevention.* Jaipur: Springer.

Shaw, D. J. (1992). *Introduction to Colloid and Surface Chemistry.* Oxford: Butterworth-Heinemann.

Singh, N. T. (2005). *Irrigation and Soil Salinity in the Indian Subcontinent: Past and Present.* Cranbury: Rosemont Publishing.

Skuse, D. R. (2002). *Specialty Chemicals in Mineral Processing.* Cambridge: Royal Society of Chemistry.

Sönmez, E., & Yorulmaz, S. (1995). Kırka boraks işletmesi artık killerinin tuğla yapımında kullanılabilirliğinin araştırılması. In M. Köse, & H. Kızıl (Ed.), *Endüstriyel Hammaddeler Sempozyumu* (pp. 163-168). İzmir: Dokuz Eylül Üniversitesi Mühendislik Fakültesi Maden Mühendisliği Bölümü.

Steffe, J. F., & Daubert, C. R. (2006). *Bioprocessing Pipelines: Rheology and Analysis*. East Lansing: Freeman Press.

Su, C.-C., & Shen, Y.-H. (2009). Adsorption of polyethylene oxide on smectite: effect of layer charge. *Journal of Collpoid and Interface Science, 332*, 11-15.

Svarovsky, L. (2000). *Solid-Liquid Separation.* Butterworth-Heinemann.

Swaine, D. J., & Goodarzi, F. (1995). *Environmental Aspects of Trace Elements in Coal* (Cilt Energy and Environment-2). Dordrecht: Kluwer Academic Publications.

Swartzen-Allen, S. L., & Matijevic, E. (1976). Colloid and surface properties of clay suspensions. III. Stability of montmorillonite and kaolinite. *Journal of Colloid and Interface Science, 56*(1), 159-167.

Taspinar, Ö., & Çalışan, E. (n.d.). Flocculation and filtration behavior of tincal clays and different minerals in the presence of surfactants and flocculants. *The Bulletin of the İstanbul Technical University, Volume 56*(1), 1-7.

Tripathy, T., & De, B. R. (2006). Flocculation: a new way to treat the waste water. *Journal of Physical Sciences, 10*, 93-127.

Wersin , P. (2003). Geochemical modelling of bentonite porewater in high-level waste repositories. *Journal of Contaminant Hydrology, 61*(1-4), 405-422.

Wersin, P., Curti, E., & Appelo, C. (2004). Modelling bentonite-water interactions at high solid/liquid ratios: swelling and diffuse double layer effects. *Applied Clay Science, 26*(1-4), 249-257.

Williams, R. A. (1992). *Colloid and Surface Engineering : Applications in the Process Industries.* Oxford: Butterworth-Heinemann.

Xu, Y., & Jiang, j.-Q. (2008). Technologies for boron removal. *Industrial and Engineering Chemistry Research, 47*, 16-24.

Yalçın, H., & Baysal , O. (1991). Kırka (Seyitgazi-Eskişehir) borat yataklarının jeolojik konumu, dağılımı ve oluşumu. *MTA Journal*, 93-104.

Yamahira, M., Kikawada, Y., & Oi, T. (2007). Boron isotope fractionation accompanying formation of potassium, sodium and lithium borates from boron-bearing solutions. *Geochemical Journal, Vol. 41*, 149-163.

Yilmaz, A. E., Boncukcuoglu, R., Bayar, S., Fil , B. A., & Kocakerim, M. M. (2012). Boron removal by means of chemical precipitation with calcium hydroxide and calcium borate formation. *Korean Journal of Chemical Engineering, 29*(10), 1382-1387.

Young, R. N., & Thomas , H. R. (1999). *Geoenvironmental Engineering - Ground Contamination: Pollutant Management and Remediation.* Withshire: Thomas Thelford Publishing.

Zhuravlev, L. T. (2000). The surface chemistry of amourphous silica. Zhuravlev model. *Colloids and Surfaces A:Physicochemical and Engineering Aspects, 173*, 1-38.

CURRICULUM VITAE

PERSONAL INFORMATION

Surname, Name: Çırak, Mustafa
Nationality: Turkish (TC)
Date and Place of Birth: 22 May 1983, İzmir
E-mail: mustafa.cirak@gmail.com

EDUCATION

Degree	Institution	Year of Graduation
MS	METU Mining Engineering	2010
BS	METU Mining Engineering	2007
High School	Selma Yiğitalp L.	2002

WORK EXPERIENCE

Year	Place	Enrollment
2008-2014	METU Dept. of Mining Eng.	Research Assistant
2007-2008	Demir Export AŞ	Project Engineer
2006 Summer	Çanakkale Madencilik	Intern Eng. Student
2005 Summer	Dedeman Madencilik	Intern Eng. Student

PUBLICATIONS

1. Çırak, M. (2010). Flocculation behavior of two different clay samples from Kırka tincal deposit (MSc. Thesis). ANKARA: METU

2. Çırak, M., & Hosten, C. (19-22 Eylül 2012). Boraks çözeltisi içerisindeki iki farklı kil süspansiyonunun flokülasyonu ile ilgili ön çalışma. 15. Ulusal Kil Sempozyumu. Niğde.

3. Çırak, M., & Hosten, C. (10-12 Ekim 2012). Using multivariable regression modeling to evaluate the results of a flocculation study. XIII. International Mineral Processing Symposium. Bodrum, Muğla.

4. Hosten, C., & Cirak, M. (2013). Flocculation behavior of clayey dolomites in borax solutions. Powder Technology, 235, 263-270.